ESD-TR-79-41

LEVEL III

12
B.S.

AD A073772

Semiannual Technical Summary

See 1473 in back

Seismic Discrimination

31 March 1979

Prepared for the Defense Advanced Research Projects Agency
under Electronic Systems Division Contract F19628-78-C-0002 by

Lincoln Laboratory

MASSACHUSETTS INSTITUTE OF TECHNOLOGY

LEXINGTON, MASSACHUSETTS

The work reported in this document was performed at Lincoln Laboratory, a center for research operated by Massachusetts Institute of Technology. This research is a part of Project Vela Uniform, which is sponsored by the Defense Advanced Research Projects Agency under Air Force Contract F19628-78-C-0002 (ARPA Order 512).

This technical report has been reviewed and is approved for publication.

FOR THE COMMANDER

Joseph C. Syiek

Joseph C. Syiek
Project Officer
Lincoln Laboratory Project Office

MASSACHUSETTS INSTITUTE OF TECHNOLOGY

LINCOLN LABORATORY

SEISMIC DISCRIMINATION

SEMIANNUAL TECHNICAL SUMMARY REPORT
TO THE
DEFENSE ADVANCED RESEARCH PROJECTS AGENCY

1 OCTOBER 1978 – 31 MARCH 1979

ISSUED 1 AUGUST 1979

LEXINGTON MASSACHUSETTS

ABSTRACT

Lincoln Laboratory has embarked on the task of carrying out the design and specification of a U.S. Data Center which will fulfill U.S. obligations that may be incurred under a possible future Comprehensive Test Ban Treaty. This report includes 17 contributions, relating progress in the Data Center design and associated seismic research. These contributions are grouped as follows: seismic data management system (5 studies), locations and travel times (5 studies), and general seismology (7 studies).

CONTENTS

SUMMARY

This is the thirtieth Semiannual Technical Summary report describing the activities of Lincoln Laboratory funded under Project Vela Uniform. This report covers the period 1 October 1978 to 31 March 1979. Project Vela is a program of research into the discrimination between earthquakes and nuclear explosions by seismic means. A recent new emphasis of the project is in the development of the data-handling and analysis techniques that might be appropriate for the monitoring of a potential Comprehensive Test Ban Treaty, presently under negotiation. The Lincoln Laboratory program during FY 79 has two objectives. The first is to carry out a detailed design study, and produce hardware and software specifications for a Data Center which will fulfill U.S. obligations that may be incurred under the Comprehensive Test Ban Treaty, and under any international agreements that may be associated with this treaty. The second is to carry out seismic research, with particular emphasis on those areas directly related to the operations of the Data Center.

Section I of this report summarizes, in general terms, the functions of the Data Center insofar as they can be formulated at present. Both alphanumeric and waveform data, some in real time, will be transmitted to the Data Center. The main products of the Data Center will be one or more event lists, an archive for all the input data, and a set of event-associated waveform files which will be useful for research and development. The architecture of the Center is being formulated using state-of-the-art computer technology, and will be described in detail in a special report to be issued late in FY 79. For the present, we focus on Center requirements using current estimates of data-flow rates, and we describe some important interface issues that are yet to be completely resolved. Seismicity variations are substantial, and may at times place a severe load on the processing capability of the Center. The average number of events detected per day, including local events, is likely to lie in the range 50 to 100. It is shown that episodes of 2 or 3 times this activity are relatively common. We are also concerned about the process of event detection, and a study compares the computational load generated by a variety of detection algorithms. Research into the effectiveness of these algorithms is continuing.

One of the major tasks of the Data Center will be to locate seismic events. A number of studies related to this task are described in Sec. II. Two investigations apply the master-event technique – one to the improvement in epicenter accuracy that can be obtained using regional data, and the other to the improvement in focal-depth resolution that is possible. A discussion of the information content in arrival-time data is also included. An attempt to improve the regionalization of Rayleigh-wave travel times is described, and an extensive review of station travel-time anomalies is given. Using the ISC Catalog for 1964-75, a new set of travel-time anomalies is given for 751 stations. These anomalies include both first- and second-order terms in azimuth, as well as a zeroth-order term. The tables included constitute the most comprehensive data on station travel-time anomalies currently available.

Section III contains studies in a number of different areas. Amplitude spectra of crustal phases observed from an earthquake in Eastern Canada at a distance of 5° show substantial signal at frequencies as high as 30 Hz. Observed Q values for each of the crustal phases are very high. Another study relates the beginning of investigations into scatter and bias in body-wave magnitude m_b. A development of previous work on the estimation of yields from short-period body-wave amplitudes is described. In another study, the dispersion of mantle Love

waves has been completed. Lateral variations in structure beneath continents and oceans below about 200 km are not required by the data. An analysis of broad-band SRO data is described. Also, some suggested transfer functions for instruments designed for seismic monitoring at regional distances are given in detail.

We continue to develop the capabilities of our in-house PDP-11 computer system. Much of the software used on this system will have application in the Data Center. Some details of recent applications software for the handling of waveforms within the UNIX operating system are given.

M.A. Chinnery

SEISMIC DISCRIMINATION

I. SEISMIC DATA MANAGEMENT SYSTEM

A. SEISMIC DATA MANAGEMENT SYSTEM (SDMS): PROGRESS REPORT

Lincoln Laboratory is engaged in the design and specification of a SDMS which will be documented in detail in a Technical Report scheduled to be issued near the end of FY 1979. This is a brief summary of the requirements and design goals which are guiding the current design effort.

The SDMS is being designed to implement data management, computational, and analysis support functions for large amounts of seismic waveform and parametric data. The principal goal of the design effort is to provide a state-of-the-art seismic data management and computational facility to support the U.S. commitments for International and National Data Centers which may arise from the signing and ratification of a Comprehensive Nuclear Test Ban Treaty (CTBT) presently under negotiation. The requirements stated here derive from the current (incomplete) definition of those functions as they are being negotiated. A principal source of the international requirements is document CCD/558 entitled Report to the Conference of the Committee on Disarmament by an Ad Hoc Group of Scientific Experts to Consider the International Cooperative Measures to Detect and Identify Seismic Events dated 14 March 1978. It is recognized that these recommendations are subject to revision as a result of the treaty negotiations. It is anticipated that the SDMS will implement the data management, computational, and analysis support functions required by both the U.S. national commitments and International Data Center aspects of such a treaty. The SDMS will also serve as an archive for seismic data and a support facility for the use of the archived data in advanced system development and seismic research.

There are two conceptual entities to be supported by the SDMS. They are the International Data Center and the National Data Center. These will be defined in the projected CTBT. The International Data Center, based on the CCD report, is expected to collect seismic data from the participating nations and process the data to provide a daily list of seismic events worldwide. The seismic data are expected to be provided by cooperating nations from stations operated by their seismic analysts. These data are planned to be distributed to the International Centers, now expected to number three, over communication facilities provided through agreement with the World Meteorological Organization (WMO) which currently operates a worldwide teletype communication network for exchange of international meteorological data. The data to be exchanged are expected to be messages containing measurements of seismic parameters describing observed seismic-wave arrivals at the various stations. The International Centers are planned to use these data to locate seismic events worldwide and calculate the seismic parameters of the events, i.e., location, time, magnitude, etc., including seismic parameters which may be useful in discriminating between naturally occurring seismic events and underground explosions. A detailed events list will be produced and distributed with a total delay of three to five days. The International Data Center is expected to serve as a distribution center for the exchange of detailed seismic data used in the monitoring of the treaty obligations. These data are planned to include both waveform and parametric data.

The National Data Center is expected to provide the U.S. input to the International Data Center as well as fulfilling other national goals in the seismic research area. The National Data Center is planned to receive the digitized seismic waveform data from a number of national stations, and probably from other stations as well. The number and exact characteristics of these participating stations are unknown at this time. The identification of the stations and the details of the waveform data from them will not be certain until after the treaty is signed. All of these waveform data are planned to be available for analysis and to be archived for further research as appropriate. The research and analysis users of the system will be provided with state-of-the-art computational facilities by the system, as well as access to the archived data. The data flow into and out of the SDMS is shown schematically in Fig.I-1.

There are two major aspects of the operation of the SDMS which is shown in functional form in Fig.I-2. The SDMS is planned to provide integrated support to the requirements of both the International Data Center and to the U.S. National Data Center. Certain requirements arise from the need to routinely collect, store, and process the incoming waveform data. These requirements come from the National Data Center requirements. The SDMS must provide communication, waveform data handling, display, and computational support. It is most important for the SDMS to capture the real-time waveform data reliably. These waveform data are planned to be processed for the automatic detection of seismic activity. The requirements for the system to capture and store the incoming data for waveform analysis until the event list is issued, up to five days later, places severe demands on the overall system reliability and on the capacity and data rate of the data-storage system. The automatic detection processing places requirements for large amounts of computational capacity in the system.

From the event processing of the seismic data, other activities arise which create requirements associated with the International Data Center commitment. They are archive storage and computational requirements. The International Data Center is planned to archive and make available the parametric and waveform data associated with the published event list. This archive grows steadily during the life of the system, and is planned to be used to supply requests for data to interested participant countries and to analysts and researchers.

The requirement to publish a daily event list and the need to support the analysis of the listed events place a requirement for significant computational power on the system. The automatically detected seismic-wave arrivals are expected to be refined by inspection by expert seismic analysts, who will update the automatically calculated parameters and measure or compute those parameters which are not determined automatically by the detection process. These measurements, along with those supplied by other participants, other participating countries, and possibly other Government agencies, will be processed to associate those arrivals coming from the same event. The associated arrivals will be used to locate the event and to calculate the seismic description of the event. This waveform processing and event list preparation will require significant computer processing. Since the number of stations providing waveform data is as yet undetermined, this further reinforces the requirement for flexibility and expandability in the design of the SDMS.

Another aspect of the design is that the exact level of the requirements cannot be ascertained at this time because the treaty is not final, but the design should be completed prior to completion of the treaty to facilitate implementation when the treaty goes into force. The treaty requirements will place floor under the minimum level of support required. The SDMS must be

easily modified to support the minimum level of treaty-specified requirements, and then grow or shrink to accommodate changes in the level of support arising from changing requirements. The incomplete state of the treaty impacts the National Data Center requirements in that the number and specification of the real-time waveform data sources cannot be determined yet. All these factors force the system design to allow great flexibility and expandability in the system implementation.

The architecture and other design issues of the SDMS are currently being pursued by the Lincoln Laboratory staff in consultation with a wide range of sources from Government agencies, private industry, and academic organizations. This consultation is taking place in the areas of data management, digital-signal processing, display technology, and distributed computer systems technology. The overall goal of the SDMS is to provide a truly efficient, state-of-the-art seismic data management and analysis system. This can only result as a proper synthesis of modern computer technology with the latest in seismological data processing and display techniques. The specifications and design issues of the SDMS will be fully documented in a Technical Report which is expected to be issued near the end of this fiscal year.

A. G. Gann

B. DATA RATES OF WAVEFORM DATA COMING INTO SDMS

The design of SDMS can only proceed with an accurate evaluation of the amount of data it will handle. While the exact makeup of the data has not been completely specified, a reasonable estimate can be made. The current assumption is that the data coming into the SDMS will emanate from 52 stations, each with 9 separate data channels. The breakdown of each station's data by channel is:

(1) 3 channels of long-period (LP) data sampled once per second,

(2) 3 channels of medium-period (MP) data sampled four times per second, and

(3) 3 channels of short-period (SP) data sampled forty times per second.

The total amount of data from each station is given by:

SP = 3 channels * 40 samples/sec * 16 bits/sample = 1920 bps

MP = 3 channels * 4 samples/sec * 16 bits/sample = 192 bps

LP = 3 channels * 1 sample/sec * 16 bits/sample = 48 bps

Station Total = 1920 + 192 + 48 = 2160 bps

Total Data Rate = 52 stations * 2160 bps per station = 112.32 kbps.

To allow for control and status information in the total data-rate estimate, a value of 125 kbps will be used for all SDMS design calculations.

1. Disk Capacities for SDMS

One of the SDMS requirements is the preparation of a 3- to 5-day bulletin. This requirement can only be met if at least 5 days of the incoming waveform data are stored on disk where they can be accessed with a minimum delay. The amount of disk capacity this requires is then:

$$\frac{125000 \text{ bps} * 86400 \text{ sec/day} * 5 \text{ days}}{8 \text{ bits/byte}} = 6750 \text{ Mbytes/day} \quad .$$

The disk to be used in SDMS has an unformatted capacity of 675 Mbytes. Assuming that the formatted capacity is 635 Mbytes, SDMS will require at least 11 of these disks for storing the online waveform data.

2. Disk Throughput

The disk throughput during any I/O operation is controlled by the size of the buffer being written out to the disk. The seek and rotational latency times are much greater than the time it takes to transmit data from memory to the disk. Since each individual I/O operation involves one seek and a half-a-disk rotation time, the larger the amount of data transferred in one I/O operation the greater the data throughput. The seek time on the disks we are discussing is 18 msec. The rotational latency is 8.3 msec. The data transfer rate is 1209 kbytes/sec. The formula for calculating the time needed to transfer one block of data is:

$$36.3 \text{ msec/block (seek + latency)} + 0.0008 \text{ msec/byte} * \text{No. bytes/block} \quad .$$

Table I-1 shows the disk bandwidth for varying buffer sizes.

TABLE I-1

DISK BANDWIDTH AS A FUNCTION OF BUFFER SIZE

Buffer Size (bytes)	Disk Bandwidth (bytes/sec)
512	13942.7
1024	27544.0
2048	53861.0
4096	103127.9
8192	190045.4

3. Tape Storage Requirements

All the waveform data will be archived on tape for at least 6 months. This will require a large number of tapes. The total number of tapes will be minimized by using 9-track 6250-bpi tapes with 8192 byte records. The rate of tape use is found to be:

tape record size = 8192 bytes

inter-record gap = 0.7 in.

$$\text{record + gap} = \frac{8192 \text{ bytes/record}}{6250 \text{ bytes/in.}} + 0.7 \text{ in./gap} = 2.0 \text{ in.}$$

$$\frac{2.0 \text{ in./record}}{8192 \text{ bytes/record}} = 0.000245 \text{ in./byte}$$

$$\frac{2400 \text{ ft/tape} * 12 \text{ in./ft}}{0.000245 \text{ in./byte}} = 117.55 \text{ Mbytes/tape} \quad .$$

The number of tapes per day is calculated with the following equations:

$$\frac{125 \text{ kbps} * 86400 \text{ sec/day}}{8 \text{ bits/byte}} = 1350 \text{ Mbytes/day}$$

$$\frac{1350 \text{ Mbytes/day}}{117.55 \text{ Mbytes/tape}} = 11.5 \text{ tapes/day} \quad .$$

Allowing for a margin of error and for simplicity in handling, the actual rate of tape usage will therefore be about 20 tapes/day.

J. Sax

C. SDMS INTERFACE ISSUES

The SDMS will have a number of interfaces with external organizations. These include participants in the International Data Exchange function, the U.S. National Earthquake Information Service (NEIS), the Department of Energy (DOE), and others. In many cases, the technical interface is simple and is not a consequential system issue. Two of the interfaces with substantial technical impact are discussed here and will be considered in much more detail during the ongoing system design effort. They are the communication interface for alphanumeric data for participants in the International Data Exchange, and the communication interface to the DOE system which will supply near-real-time data from National Seismic Systems.

The current plan for International Data Exchange as outlined in the CCD Working Paper 558 is to use communication services of the World Meteorological Association (WMO) for the exchange of alphanumeric data and event lists prepared by International Data Centers. That network is a low-speed worldwide network currently used for distribution of meteorological data and some small amounts of alphanumeric seismic data. We have accepted the CCD/558 concept and plan to interface to the WMO system. It is not strictly part of our function to evaluate the current WMO network capability or to suggest technical changes. However, since the Data Center services will be influenced by their communication services, we will evaluate available WMO services in the course of our system development and, if appropriate, suggest modifications or improvements.

The DOE communication system interface is technically more complex. It is this interface which will furnish near-real-time seismic signals from up to 45 National Seismic Stations to be designed, installed, and operated by DOE. Each such station generates some 2.4 kbps of data in the form of a 2.4-kbit message once each second. For technical reasons, messages may be delayed from real time by as much as 20 min. The data in a message include 1 sample from each of 3 long-period (LP) sensors, 4 samples from each of 3 medium-period (MP) sensors, and 40 samples from each of 3 short-period (SP) sensors. The message delay, bits per message, messages per second, number and type of channels, and sampling rates are details which are not critical for most issues discussed below, but do represent reasonable specific values which can be used to simplify the discussion.

The DOE interface issues which have been identified and are discussed below are:

(1) Number, type, and capacity of hardware interface,

(2) Reorganization and reformatting of basic data,

(3) Reliability and retransmission capability,

(4) Message formats and interface protocols, and

(5) Seismic quality control.

The number, type, and capacity of communication interfaces must be determined. The waveform data for SDMS could be multiplexed and made available over a single high-speed line. For forty-five 2.4-kbit data sources, this would require a line with at least 108 kbits capacity. Substantially more might be required to allow for catching up for downtime. Another alternative would be a separate medium-speed (say 2.4 or 4.8 kbits to allow for retransmission or catch-up for downtime) line data from each station. Single stations could be split over more than one lower-speed line into the SDMS, but there does not seem any reasonable reason to do this. Also, some number of stations (say 2 to 20) could be multiplexed on a medium- to high-speed line into the SDMS. Our current expectation is that DOE will furnish the data multiplexed onto a single high-speed line or a small number of relatively high-speed lines.

The second issue is reorganization. As mentioned above, the natural unit of data generated by a station is a 2.4-kbit message containing 1 sec of data for all the seismic channels. However, within the SDMS we will generally deal with data which have been organized differently. Using the message contents mentioned above as an example, preferred SDMS basic data units might be as follows. The SDMS will deal with data units which are all samples, in order, from a single seismic channel for a time interval. The desired individual units might contain 4000 data samples (8000 8-bit bytes). Such large units are desirable for efficiency and response considerations. A 4000-sample unit might represent about 100 sec of a SP channel, or about 16 min. of mid-band, or about 66 min. of a LP channel. Time series shorter than nominal length might be used occasionally, such as when there is a known data gap and a unit is terminated short because of it. Also, shorter units (say, 2000 samples) might be used for LP data. We presently plan to perform data reorganization as part of the basic SDMS interface function rather than request that the reorganization be done on the DOE side of the interface. This will result in sizable memory requirements in our interface.

Thirdly, the SDMS need for redundant data-acquisition hardware and buffering by the SDMS interface units depends upon the DOE capability to retransmit data which might be lost due to an interface unit failure. The amount of data lost due to an interface unit failure might range from a few tens of seconds of high-frequency data, to as much as 30 min. of LP data. The maximum possible would depend on the number of samples in a normal demultiplexed unit of any particular kind of channel. It could easily be kept below 15 min. if desired. If the DOE system includes disks and storage of data for at least that length of time, it may be possible to use that capability and avoid unneeded extra hardware and complexity on the SDMS interface. All that would be needed would be the ability to request transmission starting at some point 15 to 30 min. in the past. With a communication line of twice the required average rate, the system would quickly catch up.

Fourthly, there are message format and interface data transfer protocols. DOE has specified a preliminary format for the 2.4-kbit basic message from a station. This is being accepted for now, with the understanding that it may be changed. In addition to the data-format question, there are various levels of communication protocols which must be specified. Such protocols include traditional low-level communication handshaking, ack-nak, retransmission rules. However, they also include much higher-level, task-oriented protocols. These will initiate and accomplish the equivalent of file transfers for large amounts of data from DOE to SDMS and, in the context of monitor functions discussed below, modest or small amounts of data from SDMS to DOE. (Monitor information may go by a separate route, independent of the primary seismic data interfaces and communication lines.)

Finally, seismic quality control is a critical SDMS function. Data must be processed by programs and selectively reviewed by seismic analysts to monitor and maintain its quality in the context of the use to which it is being put. Such monitoring is basically seismic and is distinct from communication issues, correction and detection of communication errors, or algorithmic data authentication. We believe that the SDMS should incorporate the seismic monitoring of the data as part of its functions, and that all other technical monitoring, including error detection and correction, be done within the DOE system. Results of the seismic monitoring, the identification of channels whose seismic content has deteriorated so that maintenance action is indicated, will be passed to the DOE system for action. Closely related is the requirement that DOE operational and maintenance functions be coordinated with SDMS operations so that they do not inadvertently influence seismic capability in an adverse manner.

R.T. Lacoss

D. EARTHQUAKE OCCURRENCE RATES AND SDMS REQUIREMENTS

Storage capacities (disk and tape) and computational capability for the proposed SDMS are predicated by the incoming data rates. The latter depend not only upon the number of contributing seismic stations, but also upon the rate at which seismic events occur. The average numbers of events per day located by the two primary agencies responsible for routine association and location – the USGS Preliminary Determination of Epicenters (PDE) and the International Seismological Center (ISC) – have, during 1964-1977, been ~14 and ~20, respectively. The International Seismic Month (ISM) study, carried out by Lincoln Laboratory, yielded 996 events during a 29-day interval in 1972, or an average of 34 events/day. It seems reasonable to assume that the last rate will be exceeded due to increased operator performance under the stimulus of international seismic monitoring; in addition, the installation of a number of stations specifically designed to monitor local and regional events will substantially increase the number of small events recorded only at short distances. The average number of events located per day may thus reasonably be expected to be within the range of 50 to 100.

We have studied the PDE event list for 1964-1977 in order to determine the nature of fluctuations about the average in the number of events located per day. Figure I-3 shows the histogram of occurrences of a particular number of events/day during this time interval. The histogram is markedly skewed toward higher occurrence rates, and on 4 days more than 100 events have been located. Such a lopsided distribution is not readily amenable to statistical interpretation, and efforts to determine, e.g., given a certain number of events/day, the mean and standard deviation of the time to the next day with activity at least as great, were unsuccessful. The reason for this is that, at least at smaller magnitudes, earthquakes do not occur randomly: a sudden increase in events located often indicates that a large earthquake, with many associated aftershocks, has occurred, and the activity will continue at an enhanced rate for several days or weeks afterward. Earthquake swarms, generally associated with volcanism in regions of subduction or spreading, do not have a mainshock and are usually of short duration.

In estimating the data-storage and computational capacities of the SDMS, we must thus take into account these large variations in activity as well as the average activity, and further recognize that the sudden increases in activity are not strictly random but may continue for days or even weeks. Considerable excess short-term storage and computational capacity are required to deal with these large variations. Daily activity in excess of 100 events/day occurred in 1964 (Alaska), 1965 (Rat Island), and (from SDAC Bulletin) in 1978 (Kuriles). Such activity may

be considered sufficiently rare that the extra capability required to deal with it is economically unfeasible, but the last period of such activity, in the Kuriles, took place in a region which has frequently been discussed in evasion scenarios of the hiding-in-earthquake type.

We have studied the activity during large mainshock-aftershock sequences in the Kuril-Kamchatka region in some detail. This region accounts for over 10 percent of events of $m_b \geqslant 4.5$ reported in the PDE Bulletin during 1964-1977, and is of particular interest for the reasons noted above. Figure I-4 shows the decay of daily activity from the maximum for the 5 occasions on which a mainshock occurred with 25 or more aftershocks occurring within a day of the mainshock. A lower bound to the observed rate of decay of activity from the maximum is shown by the dashed line. It can be seen that in the worst case the activity has decayed to only 40 percent of maximum 7 days after the mainshock. Thus, whatever the maximum daily activity (N_{max}) with which the storage capacity is designed to cope, we are required to be able to deal with $\sim 3.6\ N_{max}$ events during the first 5 days, and $\sim 5.4\ N_{max}$ during the first 10 days of such a mainshock-aftershock series.

We are left with the question of a reasonable upper bound to the number of events the SDMS can be expected to handle. Table I-2 lists the number of occurrences of earthquake sequences generating initial daily activity at 3, 4, 5, and 10 times the average rate for the PDE event list. Sequences of twice the average daily activity occur very frequently (less than monthly), and it seems reasonable to expect the SDMS to handle earthquake sequences involving initial daily rates of 3 to 4 times the average activity. To cope with the slower rate of decay of activity from the initial maximum of such sequences, we therefore require sufficient storage and computational capacity to be able to cope with 10 to 15 times the average activity over the 5-day interval suggested as a suitable delay between data receipt and bulletin publication, or an ability to handle 2 to 3 times average daily event occurrence. The system will, of course, be overloaded by the very active sequences occurring at intervals of a year or more.

It should be noted that the major effect of large increases in activity will be upon analyst manpower and computational requirements. The total volume of real-time data will, of course, remain constant: what will be severely taxed are waveform detection (automatic and manual) and association. It is quite likely that the computer time required for the association scheme will

TABLE I-2

OCCURRENCE RATE OF AFTERSHOCK SEQUENCES OF A GIVEN ACTIVITY

Average Activity x	No. of Event Sequences Exceeding This Activity (1964-1977)	Average Interval
3	34	~5 months
4	16	~10 months
5	9	~1.5 years
10	3	~5 years

increase nonlinearly with the rate of incoming arrival-time data. We propose to examine in detail the relationship between association time and input arrival data rates.

R.G. North

E. COMPUTATIONAL REQUIREMENTS FOR SDMS DETECTION ALGORITHM

Under the current design, the SDMS is required to collect and analyze seismic data from up to 52 nine-channel seismic stations. In order to reduce the amount of data that must be observed by seismic analysts, a detection algorithm will scan the data and identify portions of the data which warrant further investigation by an analyst. The following is an estimate of the computational requirements of several possible detection algorithms.

The requirements of the detection algorithm appear to be:

R2 Although the algorithm need not run in real time, its implementation must be fast enough to catch up if data processing gets behind schedule.

R3 The detector will operate on a single channel of data, or at least on a single station. There will be no array beam forming or using information from other stations at the detector level.

R4 Monitor the data channels and report any that are not operating properly.

R5 The detector must be capable of detecting local, regional, and teleseismic signals at reasonable false-alarm rates.

R6 Report the time of arrival of a signal and possibly several other parameters, such as duration and amplitude. The detector will be primarily a "first pass" over the data, and its description of the detection will be intentionally crude. The arrival time may only be accurate to several seconds. Further automatic processing before the data are viewed by an analyst will not be considered here, but is not ruled out.

The computational requirements of five detection algorithms (referred to as STRAW, POLARIZATION, FRASIER, FFT, and PREDICTION) were investigated and their requirements are summarized in Table I-3.

TABLE I-3

APPROXIMATE NUMBER OF MULTIPLICATIONS AND ADDITIONS REQUIRED PER STATION

Method	Per Point	Per LSTA Point	Per Second
STRAW	13	18	144
POLARIZATION	35	150	1640
FRASIER	128	0	2816
FFT	0	640	600
Prediction	60	0	2640

16

The STRAW detector is similar to the more traditional power-law detectors currently used to detect seismic signals. It was designed to be of minimum complexity in order to set a lower bound on the number of operations required per second. The STRAW algorithm computes a z-statistic of the short-term signal power[1] and whenever this statistic exceeds a threshold value, a trigger is declared. The z-statistic requires estimating the background noise level, and care is taken so that this estimate will not be contaminated by an actual seismic signal. The STRAW detector also monitors the station to make sure that it is operating properly. The other detectors are variations of the STRAW detector, where more sophisticated processing replaces the power-law detector.

The POLARIZATION detector capitalizes on the fact that, in theory, body waves are linearly polarized (rectilinear) and that seismic noise is often elliptically polarized. A polarization filter uses 3 components of data to emphasize those portions of the data which are rectilinear.[2]

The FRASIER and FFT detectors are both multiband detectors for which the input data are filtered into a number of narrow-frequency bands and a detection can occur on any band. The FRASIER detector uses a simple recursive relation to filter the data.[3] The FFT detector uses the fast Fourier transform to filter the data.[1] When a large number of filters are used, the FFT detector is more efficient than the FRASIER detector.

The PREDICTION detector uses a prediction-error filter to predict the noise at a future time, and subtracts the prediction from the data actually present at that time. Since the filter does not predict a seismic signal, a significant prediction error indicates a signal.[4] The prediction-error filter used is an adaptive one used by McCowan.[5]

A summary of the number of multiplications followed by additions required by the different detection algorithms is shown in Table I-3. The computation can be divided into the number of operations required per data point and those required every LSTA point, where LSTA is the length of the short term window (a 3-sec window was assumed). The requirements of the multiband detectors depend on the number of frequency bands. For this many frequency bands, the FFT approach is clearly cheaper than Frasier's. The prediction detector depends on the length of the prediction-error operator, and a length of 20 is assumed.

The more sophisticated detectors require between 4 and 20 times the computer power than the straw detection algorithm. Whether this additional cost is worth it or not will have to be established experimentally.

Although the advanced detectors are attractive, they do bring with them some possible problems. First of all, multidimensional pattern-recognition problems are usually harder than lower-dimensional ones, and they can be hard to optimize to provide the best detection capability. Also, "seismic intuition" can be lost once the data have been extensively transformed.

Both the polarization detector and the prediction-error detector are potentially more powerful than the power-law detector because they use more a priori knowledge about the signals they are trying to detect. On the other hand, their model of the signal is more restrictive than that of the power-law detector. For example, the polarization detector assumes that seismic signals are polarized. In reality, much of the energy of the coda of a seismogram is not obviously polarized and thus the power-law detector may do better than the polarization detector for weak events.

Although the advanced methods have been shown to be quite effective, they have never been used in a completely automatic environment; they seem to require some human guidance to be used effectively. It may be that the most effective use of these techniques is to refine the arrival time once a simple detector has detected it.

K.R. Anderson

REFERENCES

1. M.J. Shensa, "The Deflection Detector – Its Theory and Evaluation on Short-Period Seismic Data," Technical Report ALEX(01)-TR-77-03, Texas Instruments Inc., Dallas (1977).

2. Seismic Discrimination SATS, Lincoln Laboratory, M.I.T. (30 June 1975), DDC AD-A014793/4; (30 June 1976), DDC AD-A032754/4; (31 March 1977), DDC AD-A045453/8; and (30 September 1977), DDC AD-A050584/2.

3. Ibid. (31 December 1973), DDC AD-777151/2; and (31 December 1974), DDC AD-A006194/5.

4. J.F. Claerbout, "Detection of P-waves from Weak Sources at Great Distances," Geophysics 29, 197-211 (1964).

5. Seismic Discrimination SATS, Lincoln Laboratory, M.I.T. (31 December 1975), DDC AD-A025777/4; and (30 June 1976), DDC AD-A032754/4.

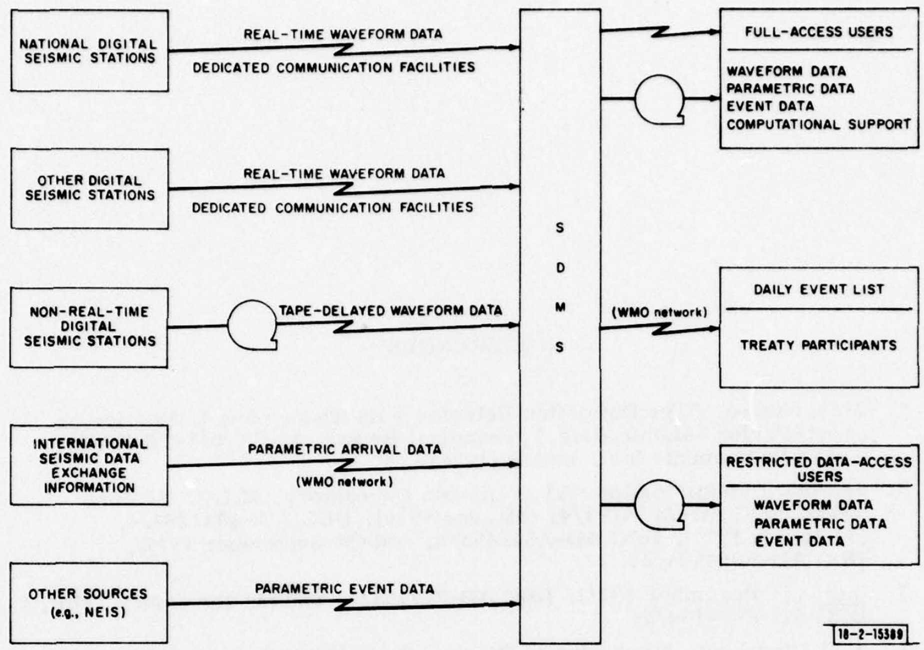

Fig. I-1. SDMS projected external data flow.

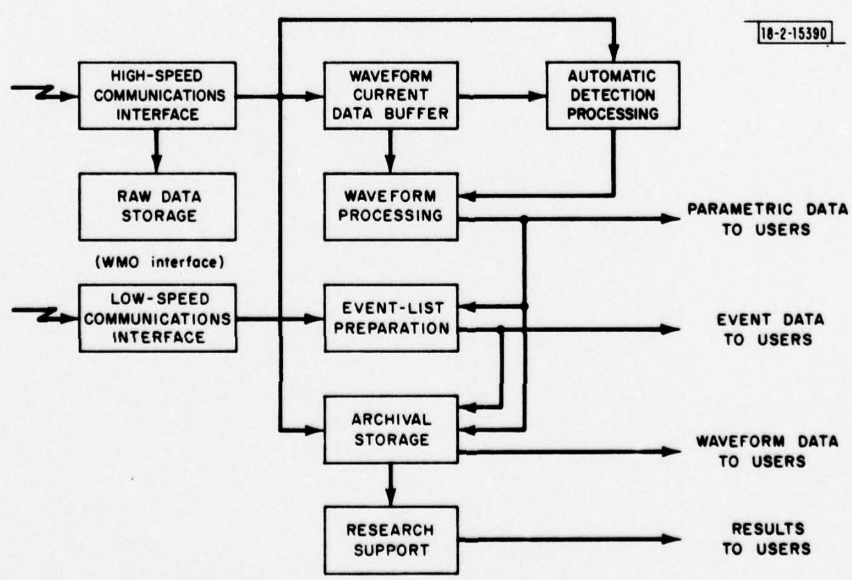

Fig. I-2. Functional organization of SDMS.

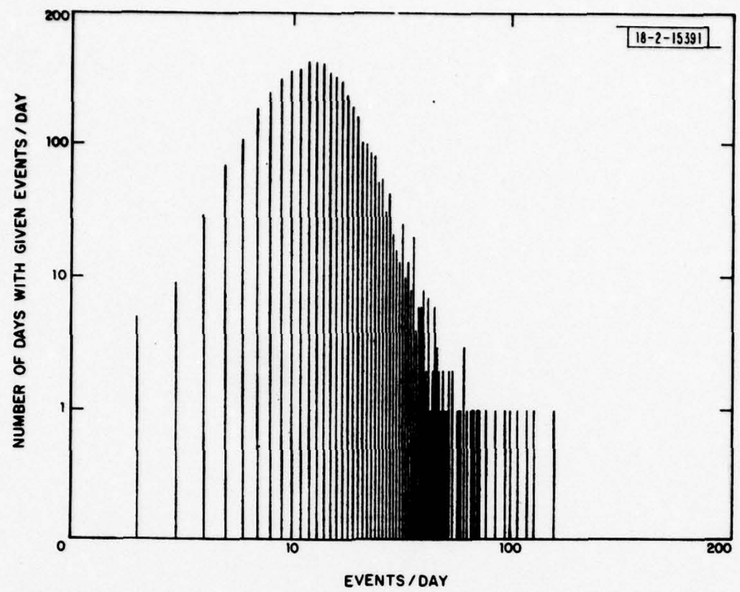

Fig. I-3. Histogram of occurrences of particular numbers of events/day, from PDE Bulletin for 1964–1977. Note logarithmic scales.

Fig. I-4. Number of events/day for first 10 days of 5 sequences in Kuril-Kamchatka region for which activity on first day exceeded 25 events, expressed as ratio of initial activity.

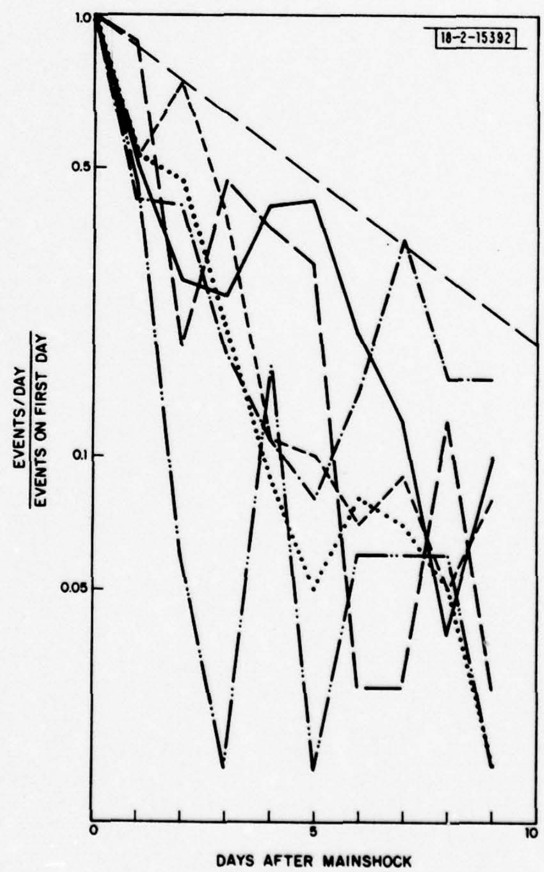

II. LOCATIONS AND TRAVEL TIMES

A. RESULTS OF A MASTER-EVENT LOCATION EXPERIMENT USING A LIMITED NUMBER OF NEAR-REGIONAL STATIONS

An experiment was conducted to determine the improvement of the epicenter locations for three NTS shots by the addition of crustal-phase detections from a limited number of stations less than 10° from the source. In this experiment, the three NTS shots used were REX (m_b 5.0), COMMODORE (m_b 5.8), and BOXCAR (m_b 6.2); and the seven near-regional stations used were Mn-, Kn-, PAS, DUG, MIN, TUC, and BMO.

A master-event method[1] was incorporated in the relocating of these events. Initially, no improvement in the epicenter location of events COMMODORE and BOXCAR was observed after adding the seven stations' crustal phase to the teleseismic detections, but substantial improvement in the epicenter location of REX was observed after these detections were added. This difference was attributed to the large number of teleseismic detections used in the location of COMMODORE and BOXCAR (≈150 each), while only sixteen teleseismic detections were used in locating event REX.

We attempted to simulate the size of event REX for events COMMODORE and BOXCAR by limiting the distance of the teleseismic stations to be less than 30° from the source before using the detections in the relocations. This made a much better comparison between the number of teleseismic detections used in relocating COMMODORE (23), BOXCAR (22), and the number used in relocating REX (16). The fallacy of this method of event size reduction is that the quality of the time picks due to the better signal-to-noise ratio (S/N) is not taken into account.

The results of relocating the epicenters using the master-event method for event REX, and the simulated events COMMODORE and BOXCAR using the additions of crustal phases from one to seven near-regional stations, are listed in Tables II-1, II-2, and II-3.

A general conclusion of this experiment is that location accuracy is enhanced by adding near-regional crustal phases for small events when only a limited number of teleseismic station detectors are available. In particular, the mislocation error for event REX was decreased by adding only one near-regional detection, while this error for event COMMODORE was decreased only when four or more near-regional detections were added to the teleseismic detections. The mislocation errors for event BOXCAR do not show the linear decrease that appears for event REX, but this is probably due to a small timing error (less than ±1.0 sec) for either station Mn-, Kn-, or PAS. If the above assumption is true, improvement in the mislocation error is decreased with the addition of three or more near-regional detections.

R. E. Needham
D. W. McCowan

B. NTS SHOT LOCATIONS RELATIVE TO A MASTER

Nonrandom as well as random errors in computed earthquake and shot locations can be investigated if accurate locations are known _a priori_. Errors in computed focal depths are expected to be greater than the corresponding errors in epicenters, and actual locations generally lie outside the 95-percent confidence limits for the computed locations. For example, Fitch[1] presented evidence for nonrandom errors of 25 km in the focal depths reported in the Bulletins of the International Seismic Center (ISC) for shallow earthquakes in the Kuril region. The corresponding standard errors in focal depth were less than 10 km. These results pertain to the well-recorded earthquakes.

TABLE II-1

RESULTS OF THE REX MASTER-EVENT RELOCATION EXPERIMENT USING LIMITED NUMBER OF NEAR-REGIONAL STATIONS

	Latitude (°N)	Longitude (°W)	Depth (km)	Confidence Ellipse Area (km^2)	Mislocation (km)	Number of Observations
REX Hypocenter	37.27	116.43	0.672	–	–	
Corrected Greeley Common Data $\Delta \geqslant 10.0$ Res $\geqslant -1.0, \leqslant 1.0$	37.18 ± 0.08	116.44 ± 0.1	1.0G	252.48	10.0	16
Corrected Greeley Common Data $\Delta \geqslant 10.0$ Res $\geqslant -1.0, \leqslant 1.0$ +Mn–, Kn–, PAS, DUG, MIN, TUC, BMO	37.22 ± 0.03	116.43 ± 0.05	1.0G	42.89	5.6	24
Corrected Greeley Common Data $\Delta \geqslant 10.0$ Res $\geqslant -1.0, \leqslant 1.0$ +Kn–, PAS, DUG, MIN, TUC, BMO	37.22 ± 0.03	116.42 ± 0.05	1.0G	54.85	5.6	22
Corrected Greeley Common Data $\Delta \geqslant 10.0$ Res $\geqslant -1.0, \leqslant 1.0$ +PAS, DUG, MIN, TUC, BMO	37.22 ± 0.03	116.43 ± 0.05	1.0G	56.34	5.6	21
Corrected Greeley Common Data $\Delta \geqslant 10.0$ Res $\geqslant -1.0, \leqslant 1.0$ +DUG, MIN, TUC, BMO	37.22 ± 0.03	116.46 ± 0.06	1.0G	90.27	6.2	20
Corrected Greeley Common Data $\Delta \geqslant 10.0$ Res $\geqslant -1.0, \leqslant 1.0$ +MIN, TUC, BMO	37.20 ± 0.05	116.45 ± 0.08	1.0G	105.29	8.0	19
Corrected Greeley Common Data $\Delta \geqslant 10.0$ Res $\geqslant -1.0, \leqslant 1.0$ +TUC, BMO	37.21 ± 0.06	116.43 ± 0.1	1.0G	159.67	6.7	18
Corrected Greeley Common Data $\Delta \geqslant 10.0$ Res $\geqslant -1.0, \leqslant 1.0$ +BMO	37.20 ± 0.08	116.43 ± 0.1	1.0G	234.97	7.8	17

TABLE II-2

RESULTS OF THE COMMODORE MASTER-EVENT RELOCATION EXPERIMENT USING LIMITED NUMBER OF NEAR-REGIONAL STATIONS

	Latitude (°N)	Longitude (°W)	Depth (km)	Confidence Ellipse Area (km^2)	Mislocation (km)	Number of Observations
COMMODORE Hypocenter	37.13	116.06	0.746	—	—	—
Corrected Greeley Common Data $\Delta \geqslant 10.0$ Res $\geqslant -1.0, \leqslant 1.0$	37.18 ± 0.05	116.03 ± 0.08	1.0G	87.73	6.2	19
Corrected Greeley Common Data $\Delta \geqslant 10.0$ Res $\geqslant -1.0, \leqslant 1.0$ +Mn-, Kn-, PAS, DUG, MIN, BMO	37.15 ± 0.03	116.10 ± 0.03	1.0G	27.89	4.2	28
Corrected Greeley Common Data $\Delta \geqslant 10.0$ Res $\geqslant -1.0, \leqslant 1.0$ +Kn-, PAS, DUG, MIN, BMO	37.15 ± 0.03	116.10 ± 0.04	1.0G	30.32	4.2	26
Corrected Greeley Common Data $\Delta \geqslant 10.0$ Res $\geqslant -1.0, \leqslant 1.0$ +PAS, DUG, MIN, BMO	37.15 ± 0.03	116.06 ± 0.04	1.0G	36.68	2.2	24
Corrected Greeley Common Data $\Delta \geqslant 10.0$ Res $\geqslant -1.0, \leqslant 1.0$ +DUG, MIN, BMO	37.18 ± 0.04	116.03 ± 0.05	1.0G	55.89	6.2	23

TABLE II-3

RESULTS OF BOXCAR MASTER-EVENT RELOCATION EXPERIMENT
USING LIMITED NUMBER OF NEAR-REGIONAL STATIONS

	Latitude (°N)	Longitude (°W)	Depth (km)	Confidence Depth Area (km^2)	Mislocation (km)	Number of Observations
BOXCAR Hypocenter	37.30	116.46	1.16	–	–	–
Corrected Greeley Common Data $\Delta \geqslant 10.0$ Res $\geqslant -1.0, \leqslant 1.0$	37.30 ± 0.05	116.44 ± 0.07	1.0G	68.78	1.8	22
Corrected Greeley Common Data $\Delta \geqslant 10.0$ Res $\geqslant -1.0, \leqslant 1.0$ +Mn–, Kn–, PAS, DUG, MIN, TUC, BMO	37.27 ± 0.03	116.47 ± 0.04	1.0G	29.01	3.5	31
Corrected Greeley Common Data $\Delta \geqslant 10.0$ Res $\geqslant -1.0, \leqslant 1.0$ +Kn–, PAS, DUG, MIN, TUC, BMO	37.27 ± 0.03	116.47 ± 0.04	1.0G	31.55	3.5	29
Corrected Greeley Common Data $\Delta \geqslant 10.0$ Res $\geqslant -1.0, \leqslant 1.0$ +PAS, DUG, MIN, TUC, BMO	37.27 ± 0.03	116.47 ± 0.04	1.0G	33.02	3.5	27
Corrected Greeley Common Data $\Delta \geqslant 10.0$ Res $\geqslant -1.0, \leqslant 1.0$ +DUG, MIN, TUC, BMO	37.29 ± 0.04	116.46 ± 0.05	1.0G	49.15	1.1	26
Corrected Greeley Common Data $\Delta \geqslant 10.0$ Res $\geqslant -1.0, \leqslant 1.0$ +MIN, TUC, BMO	37.29 ± 0.05	116.45 ± 0.05	1.0G	53.21	1.4	25
Corrected Greeley Common Data $\Delta \geqslant 10.0$ Res $\geqslant -1.0, \leqslant 1.0$ +TUC, BMO	37.29 ± 0.05	116.44 ± 0.07	1.0G	64.67	2.1	24
Corrected Greeley Common Data $\Delta \geqslant 10.0$ Res $\geqslant -1.0, \leqslant 1.0$ +BMO	37.30 ± 0.05	116.44 ± 0.07	1.0G	65.97	1.8	23

Twenty NTS shots and one earthquake were located relative to the shot on 20 November 1975. The relative-location procedure has been described previously by Fitch and Jackson and Jackson and Fitch.[2] Relative locations are more precise than ISC locations because of a diminished dependence on uncalibrated travel times. The shots chosen for relative locations had more than 100 P and PKP times reported to the ISC in the years 1971 to 1973. These data were retrieved from a disk file of all ISC data from the years 1964 through 1975. The formatting of the disk file was done by Adam Dziewonski.

Relative epicenters in Fig. II-1 can be compared with epicenters for the shots and the ISC epicenter for the earthquake in Fig. II-2. Error bars represent one standard deviation. The lack of local ($\Delta < 5°$) and near-regional stations ($5° < \Delta < 25°$) toward the south accounts for the longer N-S error bars. There is general agreement between the computed and actual epicenters for the shots within 95-percent confidence limits given by twice the error bars shown in Fig. II-1. The relative epicenter for the earthquake suggests that its correct location is closer to the cluster of shots near the SE corner of the test site than the ISC location would suggest.

Figure II-3 shows that relative focal depths for shots near the master have an average systematic error of approximately ±2 km. Shots clustered SE of the master show an average systematic error of approximately ±5 km in relative focal depth. Random errors in relative focal depth are about ±5 km at the level of one standard deviation. The corresponding ISC focal depths are approximately 10 ± 5 km. Consequently, relative depths have no more than one-half the systematic error of ISC depths for this activity. It is worth noting that the relative depth of the earthquakes is, with one exception, below the relative depths of the shots in the SE cluster. This suggests that its focal depth is greater than the shots by about 5 km. From the results of this study, it is apparent that, even if the systematic errors are significantly reduced by the use of calibrated travel times, earthquakes within 10 km of the surface will be difficult to distinguish from shots on the basis of computed focal depths.

T. J. Fitch

C. DISTRIBUTION OF LOCATION INFORMATION FROM ARRIVAL TIMES

In a linear problem of the form

$$V^{-1/2}Ax = V^{-1/2}b \qquad \text{(II-1)}$$

the importance of each datum (represented by components of the vector b) in the solution for the model (represented by the vector x) is given by the matrix describing how well the model predicts the data. In Eq. (II-1), V and A are the diagonal matrix of data-variance estimates and the coefficient matrix, respectively. Substitution of the least-squares solution to Eq. (II-1):

$$x = (A^+V^{-1}A)^{-1} A^+V^{-1}b \qquad \text{(II-2)}$$

back into Eq. (II-1) yields the information matrix:

$$V^{1/2}A(A^+V^{-1}A)^{-1} A^+V^{-1/2} \quad . \qquad \text{(II-3)}$$

Importance is defined by the diagonal elements of the information matrix, by Minster et al.[3] A datum that provides independent information for the solution has an importance of one, and the sum of importances equals the number of model parameters. In the case of earthquake locations, there are four model parameters, and Eq. (II-1) represents a linearized form of a nonlinear equation with travel-time residuals as components of the data vector.

The importance of differential travel-time residuals in relative locations of NTS shots (see Sec. B above) is distributed in the following way with respect to epicentral distance: the accumulated importance of local stations, $\Delta < 5°$, is 0.6; that for near-regional stations, $5° < \Delta < 25°$, is 1.4; and the remaining one-half of the total importance of four is distributed among the teleseismic stations. Removing the local stations from the data set raises the accumulated importance of the near-regional stations to 2.0 and does not greatly degrade the relative locations. This is a consequence of the projection of ray paths to the local and near-regional stations onto a narrow band on the focal sphere. In Fig. II-4 these ray paths define the outer ri f data points corresponding to take-off angles close to 38° (measured from the downward vertical). This distribution of ray paths results from the assumption of a 5.0-km/sec compression velocity for the crust beneath the test site. As more stations are removed from the data set, the distribution of importances becomes less uniform with azimuth and distance. Eventually, a small subset of the total data set will provide essentially all the information for the location. In this case, locations might be substantially moved by rereading arrival times from the important stations.

T. J. Fitch

D. A METHOD FOR ESTIMATING RAYLEIGH-WAVE GROUP TRAVEL TIMES

A program has been written based on a method due to Mauk[4] for estimating the Rayleigh-wave group travel time between any two points on the globe. Basically, the method consists of dividing the globe into 5° by 5° latitude-longitude squares which have been marked for their relative content of 20 tectonic structures. This contrasts with the scheme which Filson[5] developed for the ISM, where he used 15° by 15° squares and 3 tectonic structures. Once the tectonic composition of the path between the two points on the globe is known, the group travel time can be expressed as the sum of the group delays in each of the component structures at whatever period is desired. The present version of the program allows nine equally spaced periods between 20 and 100 sec.

As an example of how the program works, we present some calculations on a $\pm 40 \times \pm 40$ latitude-longitude grid centered on the Mashad SRO site. The two plots shown in Figs. II-5 and II-6 are contours of group travel time, at a 20- and 40-sec period respectively, from points on the grid to Mashad. The figures show that, at both periods, there is substantial asymmetry in the contours, with the group travel times increasing most rapidly in the north-south direction. Furthermore, the 20-sec plot (Fig. II-5) shows an anomalously low group-travel-time area about 28° directly south of Mashad. This corresponds to the Arabian Basin part of the Indian Ocean, where one would expect low group velocities.

To show the variation in group velocity that the method allows, a plot of average group velocity at a 100-sec period is shown in Fig. II-7. This plot is on the same grid as were the previous two plots. Here, even at a 100-sec period, the program is able to produce an elaborate group-velocity pattern. This amount of detail, coupled with the ease the Mauk gridwork scheme can be updated or changed, should help us estimate more accurate group travel times to aid in identifying surface wavetrains.

D. W. McCowan
A. M. Dziewonski

E. STATION ANOMALIES FOR P-WAVE TRAVEL TIMES

Lateral heterogeneities in the earth's structure can lead to significant errors in estimation of the parameters of a seismic source. Ideally, one would like to determine the three-dimensional velocity distribution and give a full account of deviations of the ray paths and travel times from those corresponding to a spherically symmetric model. It is clear, however, that this goal is not attainable in the foreseeable future. Another, more pragmatic approach is to calibrate the earth by determining empirically the travel times between each source and each receiver; in essence, this is the philosophy of the "master event" technique. This method, especially well suited for relative location of events within a particular source region, has been successfully used for some time, although on a rather limited scale.

A rather simple partial calibration can be achieved by evaluating the pattern of deviations from the global average at a receiver site. Station corrections have been published by Cleary and Hales,[6] Herrin and Taggart,[7] Lilwall and Douglas,[8] and Sengupta and Julian.[9] The methods used, and the size and quality of the data sets were different in all these studies, yet it is clear that there is very significant correlation between the azimuth-independent terms. These studies have also demonstrated a correspondence between the values of corrections and the tectonic nature of the station sites. Terms dependent on azimuth were also published in Refs. 7 and 8, but Sengupta and Julian[9] found no significant correlation between these two sets of results. It is also rather clear from Fig. 3 of Herrin and Taggart[7] that their azimuthal terms show no significant regional correlation. This negative outcome of the attempt to isolate azimuth-dependent terms has been most likely caused by the lack of a sufficiently large set of observations.

In this study, the data on P-wave arrival times contained in the Bulletin of the International Seismological Center (ISC) for the years 1964-1975 were used to derive an improved set of travel times and to investigate station residuals. Two curves representing deviations from the Jeffreys-Bullen (J-B) tables for surface focus are shown in Fig. II-8. The curve labeled "Direct Average" represents the result of averaging in 1° cells all available data for earthquakes with at least 30 first-arrival readings. One could suspect a bias in this curve due to uneven distribution of stations and receivers. The set labeled "Azimuthal Average" has been obtained by establishing 20 equal-azimuth windows and averaging the travel times for each window separately. The results shown were derived by averaging with equal weight all 20 travel-time curves. Both sets are practically identical up to a distance of 85°; at greater distances, the differences are as large as 0.2 sec. The set obtained by azimuthal averaging may be considered to reflect better the global properties of the Earth and has been applied in the next step of the analysis.

After smoothing by cubic spines, the improved travel-time curve was used to relocate 4536 events with at least 30 arrivals in the distance range from 25° to 100° and at least four stations in each quadrant. The recomputed travel-time curve showed only minor changes — maximum perturbations did not exceed 0.1 sec and it seemed pointless to continue the iterative process.

The residuals for the 4536-event data set with respect to this final travel-time curve were sorted according to stations, and these data have been used to investigate the receiver anomalies. These anomalies clearly represent contributions of the heterogeneities near the source and receiver regions as well as those in the deep mantle;[10] Romanowicz[11] proposed to calibrate the earth by averaging the residuals in properly selected azimuth-distance cells. However, with

very few exceptions, the number of data is inadequate to obtain reliable averages for sufficiently small cells that would reflect the fine effects of subducted slabs, for example. In this study, it appeared more important to investigate the overall spatial coherence of the station residuals. Stations with fewer than 50 residuals were eliminated from further analysis. The full range of azimuth was discretized into 18 windows. An average residual was computed for each window if it contained four or more readings. The azimuthal dependence was assumed to have the following form:

$$\delta t = A_0 + A_1 \cos Az + B_1 \sin Az + A_2 \cos 2Az + B_2 \sin 2Az \quad .$$

The decisions on the number of terms in this expansion to be fitted to the data depended on the azimuthal coverage. Generally, for stations with data for less than 9 windows, only the A_0 term could be determined by simply averaging (with equal weight) the results for the individual windows. For stations with data for more than 13 windows, it was most often possible to obtain a reliable least-squares fit for all five terms. As a rule, terms A_0, A_1, and B_1 could be fitted for stations with the data from 9 to 13 windows. However, the decisions depended on the distribution of the missing windows, and choices were made on an individual basis using an interactive graphics terminal.

The results for 751 stations are listed in Table II-4; most of the entries are self-explanatory. The column RMS0 describes the standard deviation for an individual window after the A_0 term has been removed; RMS1 is the standard deviation after correcting for the azimuthal terms (if any). Comparison of these two numbers allows us to assess the improvement achieved by considering azimuthal dependence. The station correction terms correspond to the following representation:

$$\delta t = A_0 + A_1 \cos(Az-E_1) + A_2 \cos 2\,(Az-E_2) \quad ;$$

thus, the angles E_1 and E_2 represent the "slowest" directions for the appropriate azimuthal terms.

Figure II-9 shows the results for station Kizyl-Arvat in the USSR, which has one of the largest azimuthal terms (A_1 = 1.56 sec) among the stations with good azimuthal coverage. The rms error decreases from 1.08 to 0.21 sec after the azimuth-dependent terms are taken into account.

The question of spatial coherence is examined in Figs. II-10 through II-13. Figure II-10 shows residuals for stations NTI and NEW that are only 40 km apart; clearly, the anomalies are nearly identical at both stations. Nearly equally good correlation exists between stations VIC and LON separated by approximately 250 km (see Fig. II-11). Great similarity can also be observed between residuals at BMO and FHC, shown in Fig. II-12, despite the fact that they are more than 500 km apart. All three figures show substantial similarities, even though they refer to stations between 40.80°N and 48.52°N and from 116.97°W to 123.99°W. For these as well as several other stations in this area, a particular consistency is noted among the phases of the two azimuthal terms. This might lead one to speculate that these two terms may be due to different causes. However, it is possible that in the examples shown so far, the azimuthal variation could be due to the source or lower-mantle effects. Such an explanation is not likely in the case of stations EDM and SES shown in Fig. II-13. Even though those stations are separated by only slightly more than 300 km, the pattern of their residuals is entirely different – while Edmonton has a large (A_1 = 0.7 sec) azimuthal term, there is practically no azimuthal dependence

TABLE II-4

CORRECTIONS TO P-WAVE TRAVEL TIMES FOR 751 STATIONS

[Correction term is to be evaluated according to following formula: $\delta t = A_0 + A_1 \cos(Az - E_1) + A_2 \cos 2(Az - E_2)$. Angles E_1 and E_2 thus indicate the azimuth corresponding to the slowest travel times for a particular term. Further details can be found in the text.]

Station												
Code	Lat.	Long.	Elev.	NOBS	NW	RMS0	RMS1	A_0	A_1	E_1	A_2	E_2
AAB	43.267	77.383	850	2131	18	0.62	0.24	0.26	0.74	89	0.33	119
AAE	9.029	38.766	2442	964	16	0.46	0.43	2.03	0.19	146	0.08	62
AAM	42.300	-83.656	254	274	11	0.41	0.35	-0.02	0.25	29	0.12	113
ABQ	34.943	-106.458	1849	188	11	0.33	0.28	0.37	0.30	344		
ABU	34.859	135.573	200	706	12	0.38	0.34	0.30	0.24	148		
AD-	51.875	-176.679	61	67	5	0.15		0.27				
ADE	-34.967	138.709	655	2328	17	0.46	0.35	0.24	0.37	131	0.21	138
ADK	51.884	-176.685	116	1164	14	0.72	0.50	-0.21	0.41	306	0.62	17
AFI	-13.910	-171.777	706	1036	15	0.50	0.40	0.21	0.24	353	0.43	110
AFR	-17.538	-149.778	50	515	14	0.74	0.61	0.27	0.49	344	0.60	115
AIA	-65.250	-64.267	11	180	7	0.24	0.17	-0.21	0.25	27		
AKU	65.687	-18.107	24	624	17	0.47	0.35	1.50	0.36	133	0.32	138
ALB	49.271	-124.822	25	227	9	0.62		0.60				
ALE	82.483	-62.400	65	2098	18	0.50	0.30	-0.58	0.48	35	0.31	111
ALG	36.772	3.058	59	203	12	0.51	0.50	-0.01	0.18	159		
ALI	38.355	-0.487	35	295	15	0.52	0.46	0.66	0.33	5	0.07	114
ALM	36.853	-2.460	65	279	14	0.63	0.55	0.50	0.50	166		
ALQ	34.942	-106.458	1853	1470	17	0.40	0.35	0.19	0.18	29	0.23	116
ALT	39.055	30.111	1060	124	6	0.63		-0.09				
ANG	17.155	-61.830	23	96	7	0.49	0.28	-0.00	0.68	79		
ANK	39.917	32.817	0	294	8	0.54		0.10				
ANP	25.183	121.517	827	717	15	0.63	0.38	1.36	0.65	300	0.34	121
ANR	40.755	72.360	494	769	17	0.33	0.31	0.53	0.15	16	0.09	146
ANT	-23.699	-70.415	80	198	13	0.66	0.36	-0.13	0.27	149	0.83	94
APA	67.550	33.333	140	1678	18	0.58	0.35	0.09	0.64	229	0.16	71
APP	60.541	13.929	354	89	7	0.48		-0.58				
APT	41.316	-72.064	3	85	7	0.62		0.47				
AQU	42.354	13.403	720	389	13	0.60	0.39	0.02	0.70	28	0.15	78
ARC	40.877	-124.075	59	70	3	0.21		1.14				
ARE	-16.462	-71.491	2452	439	16	0.68	0.36	-0.23	0.78	223	0.35	108
ARG	36.216	28.126	170	421	12	0.45	0.18	-0.37	0.51	131	0.23	61
ARH	45.010	1.312	320	463	15	0.32	0.28	0.37	0.20	63	0.07	44
ART	11.521	42.838	710	79	5	0.39		1.34				
ASH	37.950	58.350	220	1015	16	0.38	0.30	0.68	0.13	352	0.30	95
ASP	-23.683	133.897	600	1573	17	0.37	0.28	-0.75	0.31	305	0.21	55
ASU	33.417	-111.933	354	101	7	0.54		0.68				
ATH	37.972	23.717	95	1062	17	0.67	0.35	-0.12	0.64	209	0.45	142
ATL	33.433	-84.337	272	160	5	0.74		-0.48				
AVE	33.298	-7.413	230	966	17	0.47	0.34	0.15	0.45	200	0.05	35
BAA	-34.592	-58.483	25	72	5	0.69		0.65				
BAB	30.121	-2.186	0	383	15	0.38	0.29	-0.31	0.29	174	0.16	31
BAC	46.567	26.900	168	505	15	0.82	0.47	0.42	0.39	69	0.87	136
BAE	-15.841	-47.820	1200	152	10	0.75	0.53	-0.33	0.80	88		
BAF	47.835	6.995	1025	173	9	0.52		-0.23				
BAG	16.411	120.580	1507	1839	18	0.67	0.36	-0.19	0.71	244	0.38	122
BAK	40.383	49.900	-12	379	10	0.46	0.23	2.59	0.60	173		
BAN	51.172	-115.558	1400	125	7	0.65		-0.48				
BAO	-15.635	-47.991	1211	100	6	0.41		-0.48				
BAS	47.540	7.583	309	365	12	0.51	0.51	0.34	0.11	206		
BCK	37.460	30.589	860	122	6	0.38		-0.30				

TABLE II-4 (Continued)

Station												
Code	Lat.	Long.	Elev.	NOBS	NW	RMS0	RMS1	A_0	A_1	E_1	A_2	E_2
BCN	35.981	-114.834	776	714	16	0.36	0.26	0.65	0.31	14	0.16	6
BCR	7.019	-73.176	750	83	6	0.83		-1.64				
BDB	43.065	0.148	561	221	10	0.25	0.24	-0.15	0.07	295		
BDF	-15.664	-47.903	1260	137	9	0.47	0.41	-0.36	0.35	167		
BEC	32.379	-64.681	41	106	4	1.10		0.31				
BEO	44.821	20.455	129	371	11	0.38	0.30	0.74	0.07	1	0.36	129
BER	60.387	5.326	22	1031	17	0.49	0.35	0.46	0.26	322	0.40	123
BES	47.250	5.987	311	508	14	0.35	0.26	0.24	0.33	200	0.27	0
BFD	-37.176	142.544	235	768	11	0.56	0.13	0.06	0.61	111	0.55	123
BGO	41.378	-83.659	212	158	8	0.46	0.35	-0.33	0.55	77		
BHA	-14.447	28.468	1206	1093	18	0.78	0.50	-0.41	0.66	321	0.53	71
BHK	31.417	76.417	410	205	7	0.20		-0.01				
BHP	8.961	-79.558	36	145	6	0.81	0.49	-0.19	0.93	99		
BIG	59.390	-155.217	562	335	12	0.64	0.17	-0.13	0.90	334	0.15	102
BIZ	45.939	26.104	410	59	4	1.91		-1.16				
BKR	41.733	43.517	1500	1943	17	0.30	0.19	0.72	0.32	63	0.15	148
BKS	37.877	-122.235	276	1525	16	0.30	0.24	0.79	0.21	61	0.10	34
BLA	37.211	-80.421	634	402	15	0.42	0.21	0.19	0.51	93	0.15	11
BLC	64.317	-96.017	16	1686	17	0.36	0.30	-1.01	0.16	343	0.24	82
BLF	-29.109	26.188	1420	238	12	0.49	0.37	0.25	0.40	81		
BLO	39.172	-86.522	230	69	2	0.08		-1.17				
BLR	63.502	-145.845	792	678	14	0.27	0.12	-0.16	0.07	2	0.37	59
BMN	40.431	-117.222	1505	345	13	0.34	0.15	0.51	0.34	359	0.23	166
BMO	44.849	-117.306	1189	2497	16	0.42	0.21	-0.55	0.32	313	0.41	137
BNG	4.367	18.567	378	1031	17	0.74	0.56	-1.25	0.38	180	0.55	84
BNH	44.591	-71.256	472	389	11	0.30	0.17	0.47	0.31	153	0.11	55
BNS	50.964	7.176	200	1274	16	0.28	0.25	0.26	0.13	219	0.12	89
BOD	57.850	114.183	250	2360	18	0.74	0.50	-0.85	0.69	148	0.35	37
BOG	4.623	-74.065	2658	441	15	0.66	0.38	1.21	0.62	247	0.46	43
BOK	23.783	85.883	298	413	11	0.45	0.32	0.53	0.40	115		
BOL	44.487	11.329	80	63	5	1.06		1.01				
BOM	18.900	72.817	0	388	8	0.43		-0.26				
BOU	40.008	-105.271	1654	126	5	0.38		0.83				
BOZ	45.600	-111.633	1575	460	14	0.21	0.19	-0.09	0.13	252	0.02	34
BPT	41.222	-73.242	83	78	7	0.45		0.01				
BRA	48.168	17.105	270	1263	17	0.49	0.32	-0.19	0.44	356	0.26	41
BRG	50.874	13.946	296	836	15	0.26	0.20	-0.08	0.16	357	0.23	101
BRK	37.873	-122.260	81	79	5	0.36		0.35				
BRL	52.464	13.301	50	87	6	0.61		0.97				
BRN	52.419	13.203	45	122	7	0.30		0.93				
BRS	-27.392	152.775	525	2187	17	0.64	0.59	-0.14	0.03	73	0.36	69
BRW	71.303	-156.748	0	954	15	0.52	0.37	0.37	0.46	334	0.41	50
BSF	47.833	6.794	1200	747	15	0.22	0.16	-0.03	0.05	308	0.22	169
BTR	-2.617	29.733	1648	88	7	0.78		0.60				
BUB	47.749	8.603	740	309	11	0.52	0.35	-0.91	0.70	344		
BUC	44.414	26.097	82	770	15	0.51	0.28	0.61	0.55	156	0.14	132
BUD	47.484	19.024	196	693	15	0.48	0.39	0.61	0.17	56	0.33	179
BUH	48.676	8.228	750	1012	16	0.40	0.30	-0.29	0.25	331	0.26	173
BUL	-20.143	28.613	1341	1766	18	0.63	0.53	-0.72	0.36	17	0.32	99
BUT	46.013	-112.563	1758	658	16	0.25	0.24	0.16	0.06	181	0.08	26

TABLE II-4 (Continued)

	Station											
Code	Lat.	Long.	Elev.	NOBS	NW	RMS0	RMS1	A_0	A_1	E_1	A_2	E_2
BY1	-80.005	-119.043	1449	253	7	0.74		0.04				
BYR	-80.017	-119.517	1515	390	11	0.62	0.51	0.25	0.63	187		
CAL	22.535	88.367	6	165	9	0.34	0.32	2.14	0.17	250		
CAN	-35.321	148.999	700	2684	18	0.39	0.37	0.31	0.11	93	0.13	72
CAR	10.507	-66.927	1032	701	16	0.56	0.29	-0.54	0.65	39	0.27	16
CBM	46.932	-68.121	250	175	7	0.44	0.17	0.14	0.62	116		
CBZ	-52.560	169.159	30	65	6	0.33		1.29				
CDF	48.394	7.271	1100	751	15	0.32	0.21	0.17	0.08	305	0.32	166
CDR	43.675	5.767	368	103	7	0.60		0.28				
CED	34.277	-117.334	1067	73	6	0.53		0.45				
CEN	-31.576	-68.754	900	180	13	0.72	0.64	-0.35	0.47	315		
CER	-33.362	19.295	472	84	6	0.63		1.04				
CFF	45.763	3.102	400	144	8	0.46	0.46	0.44	0.04	8		
CHA	26.833	87.167	161	338	10	0.49	0.44	-0.01	0.29	111		
CHC	35.917	-79.050	149	148	6	0.60		0.72				
CHG	18.790	98.977	416	1278	18	0.76	0.49	-0.65	0.76	129	0.29	120
CHI	41.900	-87.633	183	150	6	0.87		-0.58				
CHN	4.967	-75.617	1360	166	9	0.95	0.80	-0.27	0.71	272		
CHT	22.350	91.817	35	476	12	0.61	0.29	1.40	0.79	175	0.39	1
CIN	37.600	28.087	0	977	14	0.15	0.11	-0.47	0.11	66	0.04	43
CIR	-21.013	31.580	430	1220	16	0.49	0.45	-0.07	0.08	266	0.27	8
CIZ	-43.955	-176.566	45	96	5	0.63		1.33				
CLE	41.489	-81.532	328	504	17	0.63	0.26	0.53	0.81	62	0.21	28
CLK	-15.680	34.977	781	1080	16	0.57	0.50	-0.20	0.34	239	0.11	79
CLL	51.310	13.003	230	2101	17	0.21	0.13	-0.16	0.17	166	0.17	146
CLS	38.637	-122.585	457	82	4	0.30		0.41				
CMC	67.833	-115.083	31	775	15	0.48	0.34	-0.46	0.05	263	0.50	41
CMP	45.268	25.038	598	1109	16	0.67	0.37	0.69	0.84	359	0.14	141
CNG	-26.292	32.188	100	863	17	0.39	0.38	0.09	0.06	294	0.15	130
CNH	43.830	125.313	0	94	7	0.28		-0.63				
CNN	39.137	-84.277	203	101	3	0.29		-0.93				
CNT	23.092	113.338	9	77	5	0.57		0.45				
CNU	30.660	104.012	0	91	6	0.55		-0.40				
CNZ	-39.200	175.547	1116	359	8	0.31	0.31	0.23	0.11	230		
COB	-41.088	172.734	213	895	11	0.68	0.52	-0.14	0.68	268		
COI	40.207	-8.418	140	52	4	0.27		0.41				
COL	64.900	-147.793	320	3057	16	0.64	0.30	-0.51	0.81	4	0.16	158
COM	16.253	-92.128	1528	180	7	0.43		0.79				
CON	-36.828	-73.045	15	100	9	0.64		-0.34				
COO	-30.578	151.892	653	220	7	0.39		1.09				
COP	55.683	12.433	13	1129	16	0.36	0.22	0.61	0.21	263	0.33	121
COR	44.586	-123.303	123	290	12	0.52	0.41	0.81	0.52	359		
CPO	35.595	-85.570	574	1226	17	0.66	0.28	-0.68	0.81	112	0.16	96
CPP	-27.354	-70.351	384	67	3	0.36		-0.75				
CRC	37.242	-122.130	607	87	5	0.46		0.87				
CRT	37.190	-3.598	774	243	13	0.63	0.50	1.11	0.49	233		
CRZ	-34.432	172.680	140	278	7	0.58		1.03				
CSC	34.000	-81.033	94	130	5	0.42		-0.26				
CTA	-20.088	146.254	357	2246	16	0.33	0.28	-0.48	0.03	22	0.24	114
CUM	10.465	-64.169	34	169	10	0.43	0.40	0.65	0.26	62		

TABLE II-4 (Continued)

Station Code	Lat.	Long.	Elev.	NOBS	NW	RMS0	RMS1	A_0	A_1	E_1	A_2	E_2
DAC	36.277	-117.594	1433	342	13	0.40	0.28	0.77	0.18	57	0.32	161
DAG	76.770	-18.770	16	654	16	0.44	0.21	-0.59	0.46	165	0.34	165
DAL	32.846	-96.784	187	170	8	0.30	0.24	0.11	0.27	275		
DAR	-12.408	130.818	6	774	11	0.63	0.63	-0.78	0.12	110		
DAV	7.088	125.575	85	1050	14	0.80	0.58	0.20	0.48	300	0.57	108
DBN	52.102	5.177	3	666	15	0.34	0.22	0.79	0.12	295	0.33	139
DBQ	42.507	-90.683	244	194	8	0.59	0.51	-0.65	0.48	97		
DCC	-10.510	25.455	1425	63	5	0.36		0.46				
DDI	30.322	78.056	682	566	12	0.60	0.48	0.31	0.47	316		
DDR	35.998	139.193	800	1695	14	0.42	0.23	0.02	0.41	62	0.51	98
DEV	45.883	22.903	195	450	12	0.27	0.23	0.40	0.20	129		
DIM	42.050	25.583	0	85	6	0.54		0.19				
DJA	-6.183	106.833	8	192	6	0.61		0.67				
DMK	41.822	27.757	280	408	9	0.24	0.19	-0.36	0.30	2		
DNP	-8.650	115.217	15	168	8	0.51		-0.05				
DOM	15.296	-61.391	15	66	7	0.22		-0.16				
DOU	50.096	4.594	225	1419	17	0.42	0.28	0.31	0.33	40	0.26	133
DRB	39.581	28.637	620	242	8	0.25		-0.15				
DRV	-66.665	140.009	40	960	12	0.32	0.29	-0.56	0.04	263	0.15	28
DSH	38.558	68.775	847	2075	18	0.62	0.38	0.49	0.61	272	0.35	75
DUG	40.195	-112.813	1477	1714	17	0.30	0.19	0.31	0.02	217	0.31	159
DUN	-7.409	20.837	709	78	7	0.48		-0.68				
DUR	54.767	-1.583	103	836	16	0.48	0.40	0.63	0.03	306	0.36	126
EAB	56.188	-4.340	250	403	13	0.46	0.40	-0.38	0.38	337		
EAU	55.844	-3.455	350	402	13	0.29	0.25	-0.11	0.20	89		
EBH	56.248	-3.508	375	456	15	0.42	0.33	-0.16	0.15	272	0.33	15
EBL	55.773	-3.044	365	403	14	0.37	0.30	-0.21	0.27	62	0.13	145
EBR	40.821	0.493	50	615	17	0.55	0.51	0.75	0.12	127	0.27	132
EBS	45.000	-101.232	735	50	2	0.09		-0.17				
EDC	40.347	27.864	270	145	6	0.46		0.17				
EDI	55.923	-3.186	125	322	11	0.17	0.16	-0.13	0.09	38		
EDM	53.222	-113.350	730	2395	17	0.52	0.13	-0.50	0.67	328	0.17	61
EDU	56.547	-3.014	275	358	13	0.32	0.29	-0.28	0.24	335		
EGL	55.862	-2.738	245	463	13	0.34	0.31	-0.12	0.20	332		
EIL	29.550	34.950	0	906	16	0.78	0.30	0.03	1.08	183	0.11	133
EKA	55.333	-3.159	300	1348	16	0.24	0.18	0.12	0.10	129	0.21	178
ELL	36.749	29.908	1230	208	7	0.41		0.04				
ELO	56.471	-3.706	495	120	8	0.49		-0.37				
ELT	53.250	86.267	0	1816	18	0.36	0.28	-0.72	0.07	298	0.32	159
ELY	39.131	-114.892	2011	61	6	0.23		0.54				
EMM	44.739	-67.489	20	118	6	0.43		0.11				
ERB	-4.193	152.162	180	80	5	0.63		0.45				
ERE	40.183	44.500	990	171	7	0.52		0.47				
ERZ	39.915	41.277	1850	473	13	0.57	0.32	0.63	0.69	336	0.38	120
ESA	-9.738	150.814	46	953	11	0.18	0.15	-0.14	0.20	244		
ESK	55.317	-3.205	242	991	16	0.33	0.32	0.21	0.07	174	0.08	130
ESM	-4.277	152.686	50	105	6	0.71		-0.40				
ETV	-4.229	151.676	140	114	5	0.88		-0.34				
EUR	39.483	-115.970	2178	2245	17	0.35	0.23	0.51	0.19	55	0.32	168
EWT	-4.115	152.087	30	91	8	0.82		-0.09				

TABLE II-4 (Continued)

Station												
Code	Lat.	Long.	Elev.	NOBS	NW	RMS0	RMS1	A_0	A_1	E_1	A_2	E_2
EZN	39.827	26.322	86	243	9	0.34		-0.70				
FAV	36.121	-94.190	387	630	14	0.49	0.32	-0.76	0.51	190	0.17	17
FAY	36.091	-94.191	404	210	9	0.28	0.26	-0.84	0.15	137		
FBC	63.733	-68.467	45	1018	16	0.64	0.50	-0.60	0.50	169	0.21	59
FCC	58.762	-94.087	39	1141	16	0.27	0.16	-0.49	0.15	37	0.26	65
FDF	14.733	-61.156	510	134	8	0.71	0.36	-0.11	0.97	71		
FEA	39.619	-121.246	1227	63	4	0.29		-0.24				
FEL	47.875	8.017	1485	96	6	0.29		-0.28				
FFC	54.725	-101.978	338	1731	15	0.40	0.30	-0.84	0.32	12	0.18	82
FGU	40.926	-109.386	1982	424	13	0.43	0.37	0.02	0.24	249	0.24	165
FHC	40.802	-123.985	610	682	16	0.34	0.19	0.87	0.26	283	0.28	158
FIR	43.774	11.255	40	208	9	0.67		0.95				
FLG	35.293	-111.702	2445	101	6	0.29		1.34				
FLN	48.762	-0.482	230	1291	16	0.39	0.22	0.01	0.46	296	0.04	17
FLO	38.802	-90.370	160	287	10	0.66	0.43	-0.88	1.01	53		
FOC	45.695	27.183	61	325	9	0.53	0.20	0.64	0.73	110		
FOR	40.863	-73.886	24	61	3	0.39		0.25				
FRB	63.747	-68.547	18	384	13	0.42	0.34	-0.85	0.38	82		
FRE	36.767	-119.797	88	124	8	0.30	0.23	0.49	0.26	310		
FRI	36.992	-119.708	119	794	15	0.44	0.18	-0.16	0.51	340	0.14	11
FRM	37.836	-90.486	161	52	6	0.83		-0.25				
FRR	-18.717	47.599	1554	64	4	0.24		0.06				
FRU	42.833	74.617	655	2238	17	0.33	0.31	0.73	0.14	251	0.07	160
FSJ	54.433	-124.250	772	1675	16	0.37	0.31	0.48	0.14	131	0.26	0
FUQ	5.470	-73.738	2580	106	7	0.67		-0.24				
FUR	48.166	11.276	565	1514	17	0.34	0.28	0.14	0.21	358	0.16	161
FVM	37.983	-90.426	305	127	7	0.29		-0.79				
FYU	66.566	-145.231	137	575	13	0.51	0.18	0.25	0.69	330	0.15	158
GAR	39.000	70.317	1300	1817	17	0.54	0.27	-0.30	0.58	335	0.28	94
GBA	13.604	77.436	25	1858	14	0.39	0.26	-0.16	0.26	98	0.31	112
GCA	36.974	-111.593	1339	522	15	0.71	0.51	0.91	0.37	172	0.52	99
GDH	69.250	-53.533	23	1156	17	0.45	0.24	0.14	0.11	254	0.53	101
GEN	44.418	8.930	53	52	3	0.22		-0.95				
GEO	38.900	-77.067	43	159	7	0.30		0.08				
GIL	64.975	-147.495	350	2342	16	0.64	0.36	-0.58	0.67	14	0.31	162
GIP	50.592	5.974	0	100	7	0.26		0.57				
GLA	33.052	-114.827	627	221	13	0.37	0.32	0.56	0.03	82	0.28	79
GLD	39.751	-105.221	1762	55	3	0.10		0.93				
GLP	40.287	30.310	560	439	12	0.55	0.28	-0.41	0.49	356	0.39	164
GLS	-25.035	128.296	600	121	8	0.42		-0.60				
GMA	65.429	-161.232	858	1524	16	0.32	0.30	0.08	0.15	329	0.14	68
GNZ	-38.644	178.022	30	992	10	0.78	0.25	0.56	0.95	128		
GOA	15.483	73.817	58	143	7	0.87		0.07				
GOL	39.700	-105.371	2359	1241	17	0.35	0.22	0.48	0.28	282	0.26	97
GOT	57.698	11.978	66	253	9	0.41	0.20	-0.38	0.62	253		
GPA	40.287	30.310	560	83	5	0.68		-0.79				
GRC	47.296	3.074	191	562	13	0.15	0.15	-0.07	0.05	297		
GRE	12.047	-61.746	15	158	7	0.40		0.26				
GRF	49.692	11.215	525	1407	16	0.36	0.29	0.18	0.29	6	0.08	6
GRM	-33.313	26.573	610	290	13	0.71	0.54	-0.10	0.65	30	0.12	82

TABLE II-4 (Continued)

Station												
Code	Lat.	Long.	Elev.	NOBS	NW	RMS0	RMS1	A_0	A_1	E_1	A_2	E_2
GRR	48.388	-0.858	220	1297	16	0.38	0.26	0.14	0.30	279	0.22	169
GRS	39.500	46.333	1550	1833	16	0.49	0.41	0.13	0.41	42	0.28	142
GSC	35.302	-116.805	989	116	6	0.38		0.73				
GUA	13.538	144.912	230	541	15	0.87	0.64	-0.49	0.69	182	0.41	110
GWC	55.292	-77.753	8	773	15	0.42	0.31	-0.83	0.43	51	0.12	117
HAL	44.633	-63.600	56	344	13	0.44	0.25	0.07	0.40	250	0.38	44
HAM	53.465	9.925	30	206	10	0.37	0.35	0.92	0.16	134		
HAN	46.603	-119.467	329	53	3	0.50		0.04				
HAU	48.005	6.350	570	762	16	0.33	0.23	-0.04	0.19	302	0.26	178
HBM	39.402	-120.153	1804	66	3	0.40		1.01				
HDM	41.486	-72.523	24	74	6	0.44		0.23				
HEE	50.883	5.983	100	410	12	0.35	0.28	0.35	0.29	145	0.12	118
HEI	49.399	8.726	560	53	6	0.41		-0.12				
HEN	22.000	120.750	22	76	4	0.18		2.65				
HFS	60.134	13.696	265	1404	16	0.47	0.43	-0.51	0.23	271	0.13	85
HHM	48.349	-114.027	1100	1098	16	0.37	0.22	-0.43	0.36	323	0.24	135
HKC	22.304	114.172	27	1376	18	0.64	0.47	0.78	0.60	194	0.10	112
HKT	29.950	-95.833	-122	226	12	0.26	0.18	0.28	0.16	226	0.27	67
HLE	51.500	11.950	92	157	8	0.16		-0.61				
HLG	54.185	7.884	41	114	7	0.51		0.84				
HLW	29.858	31.342	116	865	17	0.66	0.47	0.40	0.50	226	0.41	173
HNR	-9.432	159.947	72	1042	14	0.44	0.35	-0.05	0.20	248	0.33	29
HOF	50.314	11.877	566	149	7	0.34		-0.21				
HON	21.322	-158.008	2	597	12	0.35	0.30	1.05	0.27	228		
HSS	42.965	141.232	215	213	10	0.59	0.35	0.52	0.72	204		
HUA	-12.038	-75.323	3313	475	16	0.64	0.44	0.94	0.64	212	0.14	134
HVD	-30.604	25.496	1378	93	7	0.57		0.41				
HVO	19.423	-155.293	1240	553	12	0.44	0.34	0.78	0.40	232		
HWA	23.967	121.617	18	115	6	0.65		1.66				
HYB	17.417	78.553	510	1954	15	0.34	0.25	-0.55	0.21	106	0.23	113
IAS	47.193	27.562	160	753	14	0.56	0.35	-0.27	0.51	109	0.39	154
IFR	33.517	-5.127	1630	1199	17	0.63	0.26	0.32	0.80	168	0.22	95
ILG	77.947	-39.183	2401	88	6	0.35		-0.60				
ILT	67.900	-178.700	0	1835	16	0.29	0.20	-0.06	0.11	84	0.30	156
IMA	66.068	-153.678	1380	845	15	0.33	0.14	-0.29	0.42	324	0.24	47
INH	-19.547	169.273	110	72	5	0.56		-0.51				
INK	68.292	-133.500	46	1909	17	0.34	0.28	-0.66	0.21	290	0.15	154
IRK	52.272	104.310	467	1961	17	0.48	0.27	0.00	0.57	216	0.10	60
ISK	41.066	29.059	132	1039	16	0.51	0.40	-0.59	0.45	16	0.03	54
ISO	44.183	7.050	876	874	15	0.45	0.38	0.03	0.25	285	0.20	151
IST	41.046	28.996	50	1178	17	0.71	0.52	0.08	0.20	131	0.62	170
ITM	37.180	21.927	400	56	5	1.20		-0.42				
IZM	38.398	27.262	630	340	10	0.60	0.45	-0.22	0.63	153		
JAN	39.657	20.851	540	467	15	0.45	0.33	0.26	0.46	189	0.26	173
JAS	37.947	-120.438	457	2065	17	0.26	0.11	0.14	0.30	31	0.16	152
JAY	-2.500	140.667	400	196	9	0.70		-0.34				
JCT	30.479	-99.802	591	421	13	0.41	0.36	-0.81	0.04	290	0.28	178
JEN	50.952	11.583	193	112	6	0.16		-0.09				
JER	31.772	35.197	770	1428	16	0.46	0.36	0.73	0.28	194	0.29	135
JOS	48.496	20.539	280	681	14	0.45	0.31	-0.16	0.42	16	0.44	77

TABLE II-4 (Continued)

Station												
Code	Lat.	Long.	Elev.	NOBS	NW	RMS0	RMS1	A_0	A_1	E_1	A_2	E_2
KAA	-20.777	116.859	15	182	7	0.63		-0.53				
KAR	24.933	67.143	34	515	12	0.55	0.20	0.94	0.46	189	0.61	162
KAS	41.372	33.767	850	1364	17	0.51	0.38	0.45	0.21	75	0.43	6
KAT	39.200	56.267	90	1412	17	1.08	0.21	1.09	1.46	343	0.26	120
KBL	34.541	69.043	1920	1723	18	0.47	0.25	-0.14	0.51	237	0.26	132
KBS	78.917	11.924	46	1255	17	0.59	0.29	0.88	0.71	251	0.07	156
KDC	57.748	-152.492	0	1745	16	0.35	0.29	-0.17	0.02	335	0.28	16
KDZ	41.641	25.350	329	361	11	0.42	0.41	0.05	0.12	220		
KEB	38.798	38.728	739	115	6	0.40		0.98				
KED	12.926	-12.321	0	67	3	0.37		-1.12				
KER	34.352	47.106	1310	905	16	0.69	0.45	0.05	0.62	236	0.50	49
KES	31.995	-4.455	1124	313	14	0.55	0.39	0.84	0.52	156	0.28	93
KET	-4.333	152.036	17	78	7	0.59		0.27				
KEV	69.755	27.007	80	2201	17	0.32	0.20	0.14	0.33	172	0.13	178
KEW	51.468	-0.313	5	257	9	0.33		0.10				
KHC	49.131	13.579	700	2084	17	0.43	0.27	-0.32	0.46	3	0.12	22
KHE	80.617	58.050	100	1713	18	0.62	0.28	0.69	0.75	253	0.24	0
KHI	34.143	58.642	1600	186	7	0.23		0.18				
KHO	37.483	71.533	1850	1930	18	0.53	0.34	0.61	0.52	310	0.25	109
KIC	6.361	-4.741	175	719	17	0.54	0.46	-0.85	0.23	115	0.33	84
KIM	-28.752	24.780	1321	261	14	0.47	0.44	-0.78	0.13	13	0.20	100
KIP	21.423	-158.015	70	814	13	0.38	0.29	0.78	0.20	256	0.28	93
KIR	67.840	20.417	390	2523	18	0.44	0.34	-0.28	0.37	245	0.14	96
KIS	47.017	28.867	49	1108	16	0.58	0.28	-0.63	0.58	94	0.36	164
KJF	64.199	27.715	160	1378	18	0.42	0.35	-0.29	0.22	281	0.23	60
KJN	64.085	27.712	250	1529	18	0.28	0.17	-0.36	0.29	210	0.15	14
KLG	-30.784	121.458	350	2034	17	0.34	0.30	-0.82	0.25	191	0.02	38
KLS	56.165	15.592	11	259	9	0.47	0.22	-0.50	0.79	225		
KMU	42.237	142.967	180	706	14	0.60	0.37	0.38	0.69	156	0.32	110
KNA	-15.750	128.767	55	901	13	0.50	0.41	-0.72	0.27	40	0.34	70
KOA	-6.224	155.619	65	270	8	0.36		-0.95				
KOD	10.233	77.467	2343	1952	16	0.39	0.23	0.88	0.37	188	0.21	113
KON	59.649	9.598	200	1553	17	0.30	0.17	0.09	0.33	283	0.09	133
KOU	-20.562	164.281	17	1008	13	0.65	0.45	0.16	0.51	10	0.37	55
KPH	21.576	-158.275	0	91	5	0.44		0.42				
KPK	39.583	-121.305	899	54	4	0.35		0.66				
KRA	50.058	19.940	223	1931	17	0.20	0.13	-0.04	0.21	337	0.11	74
KRK	69.724	30.062	0	645	13	0.40	0.26	0.09	0.44	157	0.21	10
KRL	49.011	8.412	114	618	15	0.52	0.45	0.79	0.41	11	0.04	41
KRP	-37.925	175.537	64	2166	15	0.74	0.43	-0.01	0.51	323	0.63	98
KRR	-16.852	29.618	1380	1365	17	0.68	0.57	-0.60	0.41	326	0.38	83
KRT	-4.353	152.052	20	64	5	0.72		0.47				
KRV	40.650	46.333	340	1634	17	0.34	0.27	-0.42	0.20	22	0.23	142
KSA	33.824	35.892	923	1320	16	0.56	0.37	0.71	0.60	183	0.12	108
KSR	-25.850	26.897	1623	123	11	0.96	0.85	0.20	0.73	167		
KTG	70.417	-21.983	6	1510	17	0.54	0.30	0.55	0.64	122	0.13	165
KUG	-10.183	123.667	52	126	8	1.36		0.63				
KUL	37.900	69.750	605	559	11	0.58	0.41	-0.11	0.59	312		
KUN	25.123	102.740	1922	104	5	0.73		0.41				
KUR	45.233	147.867	0	564	11	0.53	0.27	0.15	0.70	202		

TABLE II-4 (Continued)

Station												
Code	Lat.	Long.	Elev.	NOBS	NW	RMS0	RMS1	A_0	A_1	E_1	A_2	E_2
KYS	35.198	140.148	180	598	14	1.02	0.31	0.95	1.54	74	0.19	132
KZN	40.307	21.771	900	253	10	0.47	0.37	0.03	0.41	305		
LAH	31.550	74.333	210	917	17	0.44	0.35	-0.21	0.31	316	0.25	81
LAN	36.050	103.833	1506	116	7	0.68		0.40				
LAO	46.689	-106.222	744	1148	17	0.55	0.30	-0.11	0.51	310	0.40	51
LAR	41.314	-105.583	2400	329	12	0.55	0.55	0.12	0.12	9		
LAT	-6.712	146.990	37	603	11	0.30	0.20	0.09	0.35	190		
LAW	38.959	-95.250	0	262	10	0.42	0.36	-0.95	0.38	39		
LBF	46.987	3.977	660	885	16	0.35	0.17	-0.00	0.30	200	0.37	4
LCG	21.145	-101.725	2200	161	9	0.45	0.28	1.68	0.49	74		
LEE	37.243	-113.377	1067	112	8	0.42	0.29	1.08	0.49	37		
LEM	-6.833	107.617	1252	1469	16	0.83	0.46	0.79	0.94	200	0.51	31
LF4	47.411	-106.944	707	169	5	0.49		-0.19				
LFF	44.937	0.736	160	566	15	0.32	0.28	0.33	0.07	331	0.22	14
LHA	29.637	91.037	3630	127	6	0.21		1.23				
LHC	48.417	-89.267	196	580	15	0.40	0.29	-0.57	0.37	60	0.16	68
LHN	61.049	10.880	505	540	13	0.47	0.26	-0.09	0.49	278	0.18	66
LIC	6.224	-5.028	100	374	14	0.50	0.41	-0.72	0.34	186	0.22	82
LIS	38.716	-9.149	77	309	15	0.55	0.46	0.93	0.38	223	0.21	157
LJU	46.043	14.533	396	1524	16	0.62	0.40	0.07	0.67	162	0.39	162
LMG	-8.908	148.150	1200	216	8	0.61		0.03				
LMP	-16.426	167.800	60	330	7	0.47		-0.06				
LMR	43.333	6.509	200	434	13	0.40	0.33	0.07	0.23	284	0.20	11
LMT	-41.610	146.152	349	90	3	0.18		0.72				
LND	43.040	-81.183	246	138	5	0.43		-0.57				
LNR	-15.852	168.160	8	410	8	0.36		-0.25				
LNS	45.289	6.915	1480	1053	15	0.62	0.25	0.51	0.63	267	0.45	4
LOM	6.122	1.213	5	56	4	0.58		0.50				
LON	46.750	-121.810	854	1290	16	0.47	0.26	0.03	0.40	276	0.34	149
LOR	47.267	3.851	520	1629	17	0.36	0.20	-0.12	0.22	268	0.36	6
LOT	45.448	23.769	1240	61	4	0.36		-0.99				
LPA	-34.909	-57.932	14	221	14	0.69	0.49	-0.12	0.55	69	0.43	36
LPB	-16.533	-68.098	3292	499	17	0.58	0.38	0.06	0.33	206	0.52	61
LPF	48.032	-1.042	170	458	15	0.42	0.29	0.03	0.37	305	0.30	22
LPO	44.683	1.187	330	533	15	0.29	0.18	0.35	0.17	120	0.25	15
LPS	14.292	-89.162	1000	620	13	0.64	0.46	0.36	0.29	238	0.53	54
LRG	43.454	6.361	100	479	13	0.33	0.28	0.28	0.15	248	0.20	9
LSF	46.250	1.534	425	661	15	0.29	0.14	0.14	0.24	184	0.31	1
LSM	36.739	-116.278	1146	290	12	0.42	0.18	0.54	0.40	132	0.35	115
LUB	33.583	-101.867	980	518	16	0.38	0.29	0.01	0.30	320	0.20	13
LUG	-15.518	167.130	150	867	9	0.66	0.28	-0.18	0.84	232		
LUX	49.600	6.133	0	395	13	0.31	0.26	1.44	0.21	50	0.16	99
LVV	49.817	24.033	308	890	15	0.42	0.38	0.12	0.29	22	0.21	119
LWI	-2.238	28.800	1748	903	17	0.54	0.43	0.53	0.30	212	0.36	67
MAG	59.550	150.800	120	1366	16	1.05	0.34	0.20	1.32	186	0.26	52
MAK	43.017	47.433	10	558	14	0.74	0.49	1.03	0.59	215	0.57	11
MAL	36.727	-4.411	60	230	12	0.64	0.24	0.35	0.71	250	0.37	148
MAN	14.662	121.077	70	630	15	0.45	0.39	0.39	0.20	254	0.28	136
MAT	36.542	138.209	440	2641	15	0.40	0.29	-0.54	0.38	42	0.24	78
MAW	-67.603	62.875	6	1767	17	0.46	0.39	-0.11	0.34	330	0.06	128

TABLE II-4 (Continued)

Station Code	Lat.	Long.	Elev.	NOBS	NW	RMS0	RMS1	A_0	A_1	E_1	A_2	E_2
MBC	76.242	-119.358	15	2849	17	0.34	0.26	-0.41	0.14	70	0.26	49
MBO	14.391	-16.955	3	308	13	0.48	0.47	0.59	0.12	294		
MBT	-21.170	119.742	200	489	10	0.38	0.30	-0.72	0.38	358		
MCC	52.052	-118.585	578	367	14	0.53	0.27	0.32	0.52	316	0.27	21
MCQ	-54.499	158.956	14	327	9	0.44		0.92				
MDC	37.882	-121.914	1173	104	6	0.45		1.11				
MDR	13.000	80.183	15	541	12	0.50	0.37	0.40	0.38	99	0.50	157
MDZ	-32.883	-68.850	826	183	11	0.55	0.45	-0.10	0.34	342	0.38	77
MED	3.550	98.683	32	356	10	0.52	0.30	-0.33	0.86	71		
MEK	-26.613	118.545	515	1620	16	0.39	0.38	-0.84	0.08	185	0.08	96
MES	38.199	15.555	45	245	10	1.11	0.71	0.28	1.29	182		
MFF	46.601	-0.143	260	545	15	0.31	0.17	0.26	0.21	266	0.29	179
MFP	3.342	8.661	1338	142	12	0.51	0.45	0.66	0.34	178		
MGL	39.807	-121.557	975	57	3	0.35		-0.09				
MGN	40.925	32.181	750	273	7	0.35		0.73				
MHC	37.342	-121.642	1282	1571	16	0.38	0.29	0.69	0.33	86	0.07	12
MHI	36.300	59.495	1100	57	3	0.20		0.57				
MHK	39.187	-96.579	314	78	6	0.62		-0.18				
MHT	39.200	-96.581	200	206	6	0.69		-0.66				
MID	59.428	-146.339	37	62	6	0.62		1.00				
MIM	45.244	-69.040	140	139	7	0.34		0.17				
MIN	40.345	-121.605	1495	1374	16	0.34	0.21	-0.14	0.37	335	0.05	8
MIR	-66.550	93.000	30	1403	16	0.54	0.33	-0.31	0.65	315	0.21	79
MIZ	39.134	141.136	63	219	10	0.70	[illegible]	1.40	0.21	174		
MJZ	-43.987	170.466	1000	1300	11	0.30	0.29	0.04	0.10	36		
MKS	-5.067	119.633	28	212	9	1.01		1.05				
MLR	45.492	25.944	1360	344	10	0.56	0.51	0.74	0.43	253		
MLS	42.958	1.083	450	88	5	0.46		0.21				
MMA	33.554	-111.958	426	306	12	0.46	0.42	0.76	0.28	342	0.13	83
MNG	-40.619	175.482	396	1680	14	0.79	0.36	-0.46	0.85	119	0.50	96
MNL	33.147	73.750	436	425	8	0.38		0.68				
MNT	45.502	-73.623	112	975	18	0.66	0.34	-0.13	0.76	104	0.27	8
MNV	38.433	-118.153	1507	554	15	0.30	0.20	0.30	0.07	4	0.31	145
MNW	-45.780	167.619	155	877	9	0.32	0.30	0.00	0.17	227		
MNY	44.961	5.691	422	786	15	0.57	0.29	0.19	0.61	234	0.43	8
MOA	47.850	14.266	572	105	6	0.39		-0.04				
MOK	21.456	-157.737	0	86	7	0.55		0.37				
MOM	-2.074	147.411	10	254	10	0.45	0.37	0.38	0.44	203		
MOO	-42.442	147.190	325	565	10	0.34	0.27	0.66	0.34	34		
MOS	55.738	37.625	124	2029	17	0.37	0.29	0.03	0.13	198	0.29	161
MOX	50.646	11.616	454	2089	17	0.23	0.21	-0.13	0.11	59	0.06	118
MOY	51.683	100.983	0	1485	17	0.40	0.22	0.48	0.47	271	0.05	162
MRG	39.633	-79.954	282	493	14	0.66	0.32	0.89	0.81	103	0.14	81
MSH	36.311	59.588	999	1345	16	0.40	0.31	0.90	0.37	341	0.03	57
MSO	46.829	-113.941	1264	371	15	0.34	0.27	0.07	0.10	59	0.32	120
MSZ	-44.671	167.917	38	1166	12	0.70	0.34	0.30	0.58	333	0.62	43
MTD	-16.780	31.583	967	494	11	0.53	0.42	-0.61	0.45	285	0.23	112
MTE	40.403	-7.537	815	62	6	0.39		0.57				
MTN	-12.846	131.130	155	673	13	0.63	0.45	-0.48	0.77	179		
MUN	-31.978	116.208	253	2175	17	0.56	0.45	-0.52	0.33	250	0.35	72

TABLE II-4 (Continued)

Station												
Code	Lat.	Long.	Elev.	NOBS	NW	RMS0	RMS1	A_0	A_1	E_1	A_2	E_2
MWI	16.713	-62.222	46	73	6	0.53		0.72				
NAI	-1.274	36.804	1692	860	15	0.68	0.35	1.56	0.72	268	0.27	147
NAN	32.063	118.783	7	86	6	0.51		0.01				
NAO	60.824	10.832	379	918	16	0.54	0.22	-0.75	0.66	258	0.09	75
NDF	-17.757	177.450	30	228	6	0.57		1.47				
NDI	28.683	77.217	230	2649	18	0.50	0.36	-0.42	0.46	294	0.14	2
NEL	35.712	-114.844	0	90	4	0.32		0.54				
NEM	43.328	145.587	26	149	8	0.74	0.34	-0.77	1.09	200		
NEW	48.263	-117.120	760	2134	16	0.43	0.20	-0.47	0.51	330	0.16	158
NGS	32.732	129.870	27	226	11	0.56	0.37	0.84	0.37	169	0.50	43
NHA	12.210	109.212	5	159	5	0.44		0.17				
NIA	-29.042	167.960	130	103	5	0.50		0.95				
NIE	49.424	20.322	555	1633	17	0.29	0.23	0.28	0.12	343	0.23	74
NIK	52.974	-168.853	207	286	9	0.38	0.26	-1.04	0.42	219		
NIL	33.650	73.252	536	1288	18	0.45	0.24	-0.19	0.24	4	0.48	64
NKM	35.448	-5.410	158	171	10	0.54	0.35	0.46	0.53	255		
NLG	17.067	79.267	220	197	8	0.46		-0.34				
NLM	39.032	-76.981	114	50	4	0.65		-0.12				
NNA	-11.988	-76.842	575	234	12	0.57	0.46	-0.57	0.19	227	0.42	43
NOR	81.600	-16.683	36	1345	17	0.48	0.33	-0.24	0.23	165	0.49	151
NOU	-22.310	166.451	105	966	14	0.60	0.40	0.36	0.23	123	0.53	16
NP-	76.252	-119.372	59	557	14	0.36	0.22	-0.06	0.32	67	0.23	71
NPL	40.847	14.258	7	60	7	0.93		1.06				
NPS	35.262	25.612	370	113	8	0.86		-0.60				
NRN	41.433	76.000	2849	366	11	0.31	0.20	0.15	0.39	8		
NRR	39.572	-119.849	1650	233	12	0.37	0.32	0.16	0.29	30		
NTI	48.630	-116.963	823	1560	16	0.52	0.15	-0.27	0.71	346	0.16	150
NUE	-19.076	-169.928	56	50	3	0.15		0.56				
NUR	60.509	24.651	102	2466	18	0.21	0.11	-0.39	0.05	223	0.24	113
NVL	-70.767	11.833	87	738	16	0.52	0.33	0.06	0.54	14	0.29	99
OBN	55.167	36.600	0	1526	16	0.43	0.22	-0.47	0.37	58	0.40	144
OHR	41.111	20.799	739	360	14	0.70	0.28	-0.09	0.95	242	0.24	62
OIC	34.099	135.317	776	653	13	0.30	0.14	0.12	0.12	1	0.35	75
OIS	34.105	135.327	678	654	13	0.36	0.31	0.10	0.04	196	0.25	56
OPA	21.691	-158.012	150	125	8	0.55		0.87				
ORT	35.942	-84.320	0	472	12	0.59	0.45	0.15	0.39	66	0.32	87
ORV	39.555	-121.500	360	744	14	0.38	0.23	-0.22	0.49	179	0.33	172
OTT	45.394	-75.716	83	1029	18	0.55	0.33	-0.21	0.61	100	0.15	29
OUA	-20.775	167.244	29	293	6	0.48		0.14				
OUL	65.085	25.896	60	1106	18	0.40	0.34	-0.67	0.20	199	0.24	57
OXM	19.297	-99.688	2700	112	7	0.81		0.72				
OYM	35.420	139.243	600	307	13	0.61	0.34	0.03	0.75	67	0.62	87
PAA	-6.301	155.491	699	298	9	0.33	0.23	-0.94	0.43	43		
PAD	45.409	11.886	12	130	8	0.64		2.00				
PAE	-17.662	-149.580	60	549	14	0.64	0.51	0.38	0.24	12	0.64	114
PAL	41.004	-73.909	91	300	10	0.60	0.48	-0.13	0.58	87		
PAO	40.598	110.018	0	105	6	0.71		0.36				
PAS	34.148	-118.172	295	1646	16	0.34	0.25	0.39	0.28	59	0.13	32
PAV	45.183	9.174	77	144	9	1.29		0.39				
PBA	11.667	92.717	79	271	11	0.61	0.53	0.73	0.42	299		

TABLE II-4 (Continued)

Station Code	Lat.	Long.	Elev.	NOBS	NW	RMS0	RMS1	A_0	A_1	E_1	A_2	E_2
PBJ	16.437	-95.407	213	124	7	0.65		-0.12				
PDA	37.743	-25.662	35	115	8	0.26		1.26				
PEK	40.040	116.175	0	514	15	0.53	0.35	-0.10	0.54	244	0.08	68
PEL	-33.144	-70.685	690	242	12	0.58	0.57	-0.54	0.18	132		
PET	53.017	158.650	25	1259	13	0.57	0.31	-0.25	0.24	185	0.61	25
PHC	50.707	-127.432	33	652	13	0.18	0.09	0.66	0.13	333	0.21	75
PIM	18.275	-101.882	81	73	6	0.69		-0.53				
PJD	65.035	-147.508	740	500	13	0.70	0.40	-0.39	1.00	357	0.12	81
PJG	13.588	144.867	138	93	8	1.00		-0.54				
PKR	-30.003	24.742	1267	61	4	0.57		0.74				
PLG	40.374	23.446	580	601	15	0.66	0.34	-0.04	0.82	182	0.43	175
PLV	20.806	106.629	90	350	9	0.57	0.33	1.68	0.76	172		
PMA	55.979	-160.497	314	51	4	0.24		0.30				
PMG	-9.409	147.154	70	1558	14	0.44	0.24	0.02	0.50	180	0.20	170
PMO	-15.004	-147.897	2	679	14	0.61	0.57	0.34	0.30	302		
PMR	61.592	-149.131	0	2520	15	0.38	0.21	-0.57	0.36	50	0.19	20
PNL	59.669	-139.397	579	76	4	0.22		0.35				
PNS	-16.267	-68.473	3986	446	17	0.58	0.48	0.24	0.28	213	0.38	59
PNT	49.317	-119.617	550	1973	16	0.25	0.14	-0.36	0.28	349	0.14	143
POO	18.533	73.850	556	1932	15	0.41	0.33	-0.27	0.35	302	0.12	98
PPN	-17.531	-149.432	100	715	16	0.68	0.56	0.44	0.27	343	0.50	117
PPT	-17.569	-149.576	260	848	16	0.61	0.49	0.49	0.34	345	0.46	113
PRA	50.070	14.433	225	1221	17	0.31	0.23	0.27	0.24	33	0.18	142
PRE	-25.753	28.190	1333	1121	17	0.47	0.27	-0.11	0.46	31	0.29	136
PRI	36.142	-120.665	1187	1581	17	0.44	0.29	0.94	0.18	348	0.42	15
PRK	39.246	26.272	100	724	14	0.40	0.32	0.16	0.23	243	0.23	137
PRS	36.332	-121.370	363	155	6	0.18		0.26				
PRT	43.883	11.092	62	84	6	0.31		0.84				
PRU	49.988	14.542	302	2044	17	0.40	0.22	-0.08	0.44	17	0.23	120
PRY	-26.928	27.473	0	115	11	0.67	0.61	-0.44	0.47	159		
PRZ	42.483	78.400	1599	1108	18	0.41	0.26	1.05	0.25	165	0.36	109
PSO	1.192	-77.325	3010	136	8	0.65		0.69				
PSZ	47.919	19.894	940	491	13	0.37	0.29	-0.13	0.35	9	0.15	119
PTL	38.049	23.865	500	247	9	0.63		-0.43				
PTN	44.572	-74.983	238	50	5	0.42		-0.47				
PTO	41.139	-8.602	88	752	16	0.30	0.25	-0.37	0.17	20	0.18	51
PUL	59.767	30.317	65	1341	17	0.37	0.35	0.01	0.09	237	0.13	115
PVC	-17.740	168.312	80	557	7	0.45		-0.04				
PVL	43.147	25.172	187	495	12	0.27	0.18	0.45	0.15	237	0.28	65
PYA	44.033	43.058	497	744	14	0.37	0.20	0.26	0.33	288	0.22	145
PYR	34.568	-118.741	1247	85	7	0.31		0.77				
QCP	14.637	121.077	58	572	12	0.66	0.63	0.45	0.27	239		
QMB	53.765	-1.858	116	53	4	0.17		0.30				
QUE	30.188	66.950	1721	2594	18	0.43	0.18	0.25	0.46	209	0.31	4
QUI	-0.200	-78.500	2837	261	13	0.65	0.56	1.48	0.40	201	0.22	19
RAB	-4.191	152.170	184	1406	15	0.57	0.39	-0.63	0.39	300	0.42	134
RAC	50.083	18.194	209	145	7	0.40		0.59				
RAL	-4.220	152.202	91	107	8	0.65		-0.28				
RAM	37.766	41.292	1185	115	6	0.65		0.41				
RAO	-29.252	-177.918	110	73	3	0.44		0.15				

TABLE II-4 (Continued)

Station												
Code	Lat.	Long.	Elev.	NOBS	NW	RMS0	RMS1	A_0	A_1	E_1	A_2	E_2
RAR	-21.212	-159.773	28	436	12	0.82	0.56	0.14	1.07	14	0.56	95
RBA	34.009	-6.841	39	321	17	0.70	0.61	0.13	0.32	70	0.39	156
RBZ	33.929	-6.840	116	279	12	0.51	0.46	0.07	0.32	290		
RCD	44.075	-103.208	995	144	7	0.66		-0.20				
RCI	38.106	15.643	29	67	5	0.98		0.39				
RES	74.687	-94.900	15	1775	18	0.46	0.29	-0.46	0.46	34	0.21	100
REY	64.139	-21.906	44	208	11	0.60	0.40	1.61	0.53	60	0.30	99
RHO	36.437	28.224	45	107	7	0.45		1.00				
RIV	-33.829	151.158	25	1523	17	0.76	0.54	0.38	0.71	4	0.21	97
RKT	-23.118	-134.972	100	139	6	0.36		0.04				
RMP	41.811	12.702	380	768	16	0.44	0.39	0.08	0.28	196	0.14	146
ROC	43.125	-77.592	155	178	9	0.45		-0.24				
ROL	37.918	-91.869	200	332	11	0.51	0.42	-0.81	0.47	75		
ROM	41.903	12.513	45	365	11	0.60	0.27	0.82	0.70	214	0.36	8
ROX	-45.476	169.320	106	157	7	0.54		0.26				
RSL	45.688	6.626	1583	874	15	0.52	0.36	-0.05	0.43	304	0.27	32
RUV	-15.189	-147.384	3	415	13	0.79	0.47	-0.10	0.68	344	1.02	110
SAM	39.673	66.990	704	875	16	0.47	0.28	0.51	0.21	260	0.47	178
SAN	-33.453	-70.662	533	166	10	0.42	0.36	-0.23	0.31	138		
SAO	36.765	-121.445	350	425	14	0.37	0.36	0.48	0.12	38		
SAP	43.058	141.332	18	223	10	0.65	0.58	0.21	0.39	168		
SAV	-41.721	147.189	180	1484	15	0.45	0.32	0.75	0.39	11	0.19	117
SBA	-77.850	166.756	38	1776	16	0.76	0.68	0.69	0.41	33	0.31	46
SCB	43.717	-79.233	153	128	5	0.54		0.08				
SCG	16.029	-61.681	646	123	10	0.85	0.51	0.38	1.07	83	0.06	129
SCH	54.817	-66.783	540	1235	17	0.28	0.17	-0.56	0.17	108	0.27	155
SCM	61.833	-147.328	1020	536	12	0.35	0.23	0.07	0.42	324		
SCP	40.795	-77.865	352	170	7	0.28		-0.34				
SDB	-14.926	13.572	1781	751	18	0.69	0.42	0.01	0.66	53	0.41	91
SEA	47.655	-122.308	30	150	7	0.54		1.53				
SEH	23.167	77.083	0	86	4	0.35		0.64				
SEM	50.408	80.250	209	1651	18	0.47	0.16	-0.31	0.60	241	0.19	92
SEO	37.567	126.967	86	237	11	0.56	0.45	-0.02	0.47	123		
SES	50.396	-111.042	770	1832	17	0.18	0.17	-0.48	0.08	45	0.05	59
SET	36.200	5.400	1000	213	11	0.66	0.39	-0.31	0.88	303	0.60	81
SFA	47.123	-70.827	232	784	16	0.63	0.43	-0.32	0.49	126	0.48	13
SFF	-41.337	146.307	213	258	8	0.46		0.87				
SFR	37.787	-122.389	8	58	4	0.29		0.57				
SFS	36.462	-6.205	24	63	6	1.05		1.53				
SGR	47.709	-0.923	90	62	4	0.22		0.38				
SHD	36.433	54.942	1500	114	7	0.44		0.53				
SHE	40.633	48.633	0	274	8	0.52		1.59				
SHF	46.552	-72.763	60	53	3	0.72		-0.62				
SHI	29.644	52.526	1595	2274	18	0.37	0.34	-0.44	0.19	285	0.03	84
SHK	34.530	132.678	285	1589	14	0.45	0.37	-0.21	0.35	123	0.34	78
SHL	25.567	91.883	1600	2393	18	0.50	0.35	-0.54	0.48	156	0.18	16
SIA	34.248	108.920	0	120	6	0.37		0.01				
SIC	50.175	-66.742	283	407	13	0.54	0.45	-0.05	0.34	197	0.29	19
SID	63.786	-18.058	26	182	10	0.42	0.26	1.43	0.55	9		
SIM	44.950	34.117	277	1326	17	0.50	0.36	0.26	0.23	216	0.43	161

TABLE II-4 (Continued)

Code	Station Lat.	Long.	Elev.	NOBS	NW	RMS0	RMS1	A_0	A_1	E_1	A_2	E_2
SIT	57.057	-135.324	19	788	14	0.42	0.20	0.70	0.31	305	0.40	155
SJG	18.112	-66.150	457	521	14	0.75	0.52	-0.93	0.68	43	0.35	35
SKA	63.580	12.280	580	373	11	0.19	0.11	-0.34	0.24	261		
SKI	17.333	-62.739	306	140	8	0.52		0.02				
SKO	41.972	21.440	346	998	18	0.44	0.37	-0.24	0.14	300	0.30	8
SKR	50.667	156.100	250	506	12	0.58	0.39	-0.33	0.61	224		
SLC	40.765	-111.848	1425	698	16	0.36	0.24	0.03	0.16	265	0.33	148
SLD	37.075	-121.221	443	725	14	0.39	0.25	0.96	0.07	38	0.40	17
SLL	60.477	13.323	420	123	7	0.67		-0.54				
SLM	38.636	-90.236	161	196	6	0.30		-0.71				
SMY	52.731	174.103	58	315	11	0.69	0.29	-0.41	1.04	239		
SNA	-70.315	-2.325	57	269	11	0.50	0.36	-0.13	0.61	37	0.02	4
SNG	7.173	100.620	4	392	9	0.66	0.25	-0.31	1.36	61		
SOC	43.583	39.717	192	672	13	0.44	0.37	-0.00	0.19	241	0.28	155
SOD	67.371	26.629	181	2730	18	0.25	0.16	-0.39	0.22	151	0.15	169
SOF	42.685	23.334	546	597	15	0.50	0.47	0.13	0.14	92	0.21	77
SOP	47.683	16.558	260	578	16	0.42	0.15	-0.74	0.49	357	0.23	20
SOR	22.792	-83.008	206	56	3	0.62		0.07				
SPA	-90.000	0.000	2927	1612	16	0.58	0.46	0.02	0.44	292	0.31	139
SPF	43.564	6.696	340	539	13	0.33	0.30	0.19	0.19	230		
SPK	-43.038	146.275	425	68	4	0.74		1.27				
SPO	47.732	-117.344	713	232	9	0.39	0.21	0.55	0.50	355		
SRI	36.758	49.383	243	461	10	0.11		0.77				
SRO	47.813	18.313	150	625	16	0.43	0.39	0.82	0.16	306	0.18	26
SRY	35.608	139.274	254	1140	14	0.56	0.27	-0.22	0.69	42	0.37	97
SSB	45.279	4.542	700	95	7	0.46		0.18				
SSC	48.584	-0.107	300	1300	16	0.33	0.22	0.11	0.30	248	0.18	173
SSF	47.061	3.507	360	1548	17	0.38	0.21	-0.04	0.19	231	0.41	6
SSR	44.531	21.531	0	81	6	0.85		-1.90				
SSS	13.681	-89.198	665	70	4	0.40		0.79				
STC	36.633	-121.233	259	168	8	0.60		1.37				
STG	-42.848	146.207	350	85	6	0.57		0.38				
STJ	47.572	-52.733	62	535	15	0.44	0.38	-0.09	0.24	49	0.20	10
STK	-31.882	141.592	213	509	11	0.40	0.24	-0.09	0.38	150	0.19	104
STR	48.585	7.766	135	1184	17	0.49	0.33	0.38	0.41	4	0.30	145
STU	48.772	9.195	360	956	16	0.58	0.34	-0.41	0.56	349	0.31	158
SUD	46.467	-80.967	267	319	12	0.59	0.45	-0.27	0.63	64		
SUR	-32.380	20.728	0	96	8	0.63		0.78				
SUV	-18.149	178.457	6	57	5	0.46		0.14				
SVE	56.810	60.637	275	2359	18	0.30	0.29	-0.18	0.12	175	0.05	176
SVT	13.168	-61.245	38	114	6	0.57		0.06				
SVW	61.108	-155.622	762	938	15	0.85	0.20	-0.01	1.16	299	0.09	26
SYO	-69.006	39.503	23	591	14	0.86	0.52	-0.26	1.10	338	0.35	129
TAB	38.067	46.327	1430	1622	17	0.53	0.33	0.54	0.53	86	0.30	158
TAC	19.405	-99.194	2297	283	11	0.69	0.36	1.03	0.69	153	0.44	20
TAF	34.814	-2.414	820	310	14	0.53	0.31	0.48	0.58	163	0.20	76
TAM	22.792	5.523	1395	657	17	0.49	0.46	-0.19	0.03	304	0.27	42
TAN	-18.917	47.552	1375	696	10	0.61	0.40	0.44	0.62	259		
TAS	41.325	69.295	470	2187	18	0.30	0.27	0.27	0.14	205	0.11	93
TAU	-42.910	147.320	132	1734	17	0.55	0.34	0.36	0.54	24	0.29	114

TABLE II-4 (Continued)

Station												
Code	Lat.	Long.	Elev.	NOBS	NW	RMS0	RMS1	A_0	A_1	E_1	A_2	E_2
TAV	-4.231	152.220	31	142	8	0.43		-0.30				
TCF	46.288	2.214	640	802	15	0.36	0.16	0.27	0.41	159	0.34	4
TEH	35.738	51.386	1360	1095	17	0.46	0.21	0.47	0.47	11	0.36	171
TEN	28.454	-16.240	1	119	8	0.63		1.54				
TET	-16.146	33.577	153	678	14	0.52	0.44	0.29	0.31	228	0.17	108
TFO	34.268	-111.270	1492	1039	15	0.44	0.35	0.53	0.36	6	0.26	108
TGI	32.963	59.193	1800	94	6	0.24		-0.16				
THO	33.875	-111.874	1134	102	6	0.47		0.71				
THT	-17.569	-149.574	337	126	6	0.38		0.88				
TIF	41.717	44.800	399	1251	17	0.30	0.25	0.63	0.13	27	0.23	135
TIK	71.633	128.867	25	2826	18	0.46	0.26	-0.95	0.33	310	0.42	123
TIM	45.737	21.222	88	116	8	0.46		1.24				
TIO	30.927	-7.262	1335	387	13	0.54	0.31	0.67	0.58	182	0.19	65
TIR	41.347	19.867	197	582	16	0.53	0.35	0.43	0.52	226	0.21	140
TJC	37.217	-104.691	2103	218	6	0.46		1.19				
TLL	-30.167	-70.804	2200	108	10	0.47	0.47	-0.30	0.04	130		
TLS	-5.310	150.045	40	205	8	0.49		0.60				
TMT	41.811	-72.799	290	94	7	0.38		0.49				
TNG	-6.183	106.500	14	233	8	0.66		-0.55				
TNN	65.257	-151.912	504	335	11	0.61	0.38	0.32	0.74	322		
TNP	38.082	-117.218	1932	329	13	0.38	0.14	0.20	0.10	107	0.46	142
TNS	50.224	8.449	815	197	10	0.42	0.42	0.21	0.03	25		
TOA	62.105	-146.172	909	665	12	0.27	0.15	0.34	0.27	353	0.12	7
TOL	39.881	-4.049	480	1121	18	0.23	0.18	0.55	0.17	217	0.10	132
TOO	-37.571	145.491	604	2683	18	0.46	0.34	0.19	0.28	314	0.34	98
TPH	38.075	-117.222	1890	166	8	0.34		0.47				
TPM	18.983	-99.062	1500	98	5	0.38		0.42				
TPT	-14.984	-147.619	3	880	17	0.71	0.46	0.21	0.67	355	0.54	103
TRD	8.483	76.950	0	221	8	0.56		0.55				
TRI	45.709	13.764	126	903	16	0.44	0.32	-0.45	0.31	204	0.35	156
TRN	10.649	-61.403	24	521	13	0.99	0.26	0.04	1.06	106	0.80	46
TRO	69.632	18.928	15	1917	17	0.34	0.18	0.06	0.39	257	0.08	116
TRR	-42.304	146.450	579	1166	14	0.56	0.30	0.59	0.65	17	0.40	114
TSK	36.211	140.110	280	1532	14	0.73	0.32	-0.36	0.97	87	0.38	129
TTA	62.930	-156.022	914	559	14	0.73	0.23	-0.38	0.85	293	0.46	176
TTN	22.750	121.150	9	158	7	0.40		1.91				
TUC	32.310	-110.782	985	1704	17	0.35	0.31	0.04	0.20	335	0.11	113
TUL	35.911	-95.792	256	1202	14	0.40	0.30	-0.52	0.44	250	0.20	74
TUM	47.015	-122.908	20	356	12	0.67	0.24	0.30	0.65	310	0.56	172
TUP	54.433	119.900	0	1075	15	0.38	0.25	-0.02	0.42	236	0.16	98
TVO	-17.782	-149.252	660	562	14	0.62	0.61	0.61	0.11	246		
UAV	8.604	-71.145	1550	240	11	0.79	0.66	-0.33	0.58	342		
UBO	40.322	-109.569	1596	1489	17	0.40	0.30	0.04	0.26	284	0.27	127
UCC	50.798	4.359	105	702	15	0.43	0.31	0.81	0.27	54	0.34	115
UCT	41.832	-72.251	149	79	6	0.23		0.30				
UDD	60.090	13.607	240	255	10	0.39	0.36	-0.80	0.21	233		
UKI	39.137	-123.211	199	222	9	0.37	0.27	1.14	0.33	70		
UME	63.815	20.237	16	2361	18	0.39	0.19	-0.58	0.37	234	0.32	94
UNM	19.329	-99.178	2257	158	8	0.73		0.88				
UPP	59.858	17.627	14	2296	17	0.32	0.25	-0.61	0.27	255	0.05	107

TABLE II-4 (Continued)

Station												
Code	Lat.	Long.	Elev.	NOBS	NW	RMS0	RMS1	A_0	A_1	E_1	A_2	E_2
URS	33.538	133.489	25	72	5	0.36		0.48				
UZH	48.633	22.300	159	1867	17	0.30	0.25	0.26	0.17	221	0.18	86
VAH	-15.237	-147.636	3	694	15	0.68	0.42	-0.04	0.41	342	0.79	109
VAL	51.939	-10.244	14	751	15	0.65	0.63	0.58	0.19	216	0.13	105
VAM	35.407	24.200	225	658	15	0.60	0.37	0.57	0.62	205	0.19	125
VAN	37.950	58.100	250	1072	17	0.42	0.32	-0.33	0.36	65	0.22	122
VAR	25.300	83.017	88	297	9	0.58	0.33	-0.53	0.87	185		
VAY	41.321	22.570	168	431	15	0.56	0.46	-0.07	0.50	214	0.37	14
VHM	17.177	-96.745	1829	237	11	0.48	0.43	1.02	0.28	258	0.04	89
VIC	48.519	-123.415	197	1049	15	0.50	0.28	-0.09	0.52	272	0.32	172
VIE	48.248	16.362	198	995	17	0.55	0.38	-0.16	0.49	76	0.21	36
VIS	17.717	83.300	41	186	7	0.61		0.54				
VKA	48.265	16.318	400	1144	17	0.45	0.36	-0.14	0.31	44	0.20	37
VLA	43.120	131.893	75	1724	13	0.58	0.33	-0.04	0.65	187	0.08	152
VLS	38.177	20.590	375	683	13	0.50	0.35	-0.21	0.51	243		
VLV	-39.790	-73.276	12	58	6	0.78		0.08				
VOU	46.399	5.651	495	590	14	0.28	0.18	0.04	0.22	300	0.22	21
VRI	45.870	26.725	400	1144	16	0.59	0.47	0.19	0.51	34	0.35	122
VUL	-4.283	152.146	332	128	8	0.53		-0.23				
VUN	-18.043	178.464	160	209	6	0.41		0.03				
VYB	60.717	28.800	0	92	7	0.68		-0.90				
WAB	-5.495	143.728	2032	646	12	0.62	0.25	1.01	0.65	213	0.34	104
WAN	-4.194	152.176	25	94	8	0.65		-0.21				
WAR	52.242	21.024	110	66	6	0.45		0.46				
WCB	-19.935	134.357	366	78	8	0.56		-1.14				
WDC	40.580	-122.540	300	522	14	0.91	0.41	-0.48	1.05	293	0.25	155
WEL	-41.286	174.768	122	853	14	0.72	0.59	-0.31	0.55	107	0.22	95
WES	42.385	-71.322	60	482	17	0.41	0.27	0.35	0.42	163	0.22	72
WIL	-66.259	110.527	10	236	9	0.43	0.25	0.01	0.74	278		
WIN	-22.567	17.100	1728	820	18	0.82	0.53	0.30	0.61	12	0.65	80
WIT	52.813	6.668	17	1101	15	0.39	0.25	1.16	0.23	310	0.32	151
WKU	34.188	135.173	10	167	10	0.58	0.56	0.09	0.20	197		
WLS	48.413	7.354	775	1179	15	0.36	0.29	0.17	0.13	293	0.27	166
WMO	34.718	-98.589	505	544	14	0.46	0.21	-0.89	0.56	326	0.13	17
WRA	-19.948	134.351	245	1662	17	0.37	0.32	-1.06	0.23	217	0.11	74
WRM	49.833	5.381	242	279	10	0.31	0.30	1.70	0.11	95		
WRS	34.150	71.408	343	1695	17	0.63	0.40	-0.34	0.65	255	0.40	74
WSC	39.050	-77.124	120	344	11	0.46	0.39	-0.31	0.32	143		
WTZ	-37.985	176.988	43	116	5	1.17		-0.25				
WUC	30.543	114.350	26	56	5	0.51		0.32				
YAK	62.017	129.717	125	2225	16	0.35	0.23	-0.89	0.25	186	0.26	25
YER	37.135	28.283	730	156	7	0.22		-0.02				
YKC	62.478	-114.478	198	2122	17	0.41	0.24	-0.76	0.44	309	0.11	54
YKT	59.369	-138.877	336	62	5	0.36		0.05				
YOU	-34.278	148.382	503	268	8	0.53		0.33				
YSS	47.017	142.717	75	1912	15	0.28	0.21	0.44	0.20	1	0.14	118
ZAG	45.817	15.983	155	576	15	0.51	0.35	0.42	0.30	39	0.47	115
ZAK	50.383	103.283	0	1847	18	0.34	0.23	0.16	0.33	261	0.15	116
ZSC	31.097	121.187	100	96	5	0.50		-0.01				
ZUL	47.481	8.390	740	250	10	0.48	0.43	-0.83	0.40	331		
ZUR	47.369	8.580	604	117	7	0.42		-0.77				

observed at Suffield; both are excellent stations, with RMS1 values of 0.13 and 0.17 sec, respectively. It is difficult to escape the conclusion that the source of the anomaly observed at Edmonton must be relatively shallow under that station.

In summary, the azimuthal terms are important (with the A_1 term generally much more significant) and, in general, their application should lead to reduction in the rms error commensurate with that resulting from usage of the A_0 term alone. The azimuthal terms show substantial correlations over very large areas, but occasionally a dramatic, well-established change may take place over a short distance.

TABLE II-5
COMPARISON OF SEVERAL SETS OF STATION CORRECTIONS

(a) Cross-Correlation Coefficients

	TR	S&J	H&T	L&D	C&H
TR	–	0.675	0.764	0.800	0.683
S&J	0.675	–	0.649	0.744	0.612
H&T	0.764	0.649	–	0.727	0.661
L&D	0.800	0.744	0.727	–	0.623
C&H	0.683	0.612	0.661	0.623	–

(b) Regression Coefficients

	Dependent Variable				
	TR	S&J	H&T	L&D	C&H
TR	–	0.882	0.825	1.070	0.931
S&J	0.517	–	0.508	0.766	0.611
H&T	0.708	0.830	–	0.919	0.861
L&D	0.598	0.723	0.575	–	0.626
C&H	0.501	0.613	0.507	0.619	–

Legend:
TR This Report
S&J Sengupta and Julian[9]
H&T Herrin and Taggart[7]
L&D Lilwall and Douglas[8]
C&H Cleary and Hales[6]

Table II-5(a) shows cross-correlation coefficients between the A_0 terms determined here and on four other studies. The relatively high level of correlation between the present results and those of others indicates that this set of correlations is less noisy. Higher correlations have been obtained with the sets of corrections from studies in which azimuthal terms were considered[7,8] than when only A_0 terms were evaluated by simple averaging.[6,9]

Table II-5(b) serves to reinforce the conclusion that the present set of A_0 coefficients contains the least amount of noise. If the results published here are treated as independent

variables, the slope of the straight line that relates any two sets of corrections is very close to one, the expected result. For other sets of data, the slope is significantly less than one, indicating greater contamination by noise.

A. M. Dziewonski

REFERENCES

1. Seismic Discrimination SATS, Lincoln Laboratory, M.I.T. (30 September 1978), DDC AD-A065574.
2. Ibid. (30 September 1977), DDC AD-A050584/2.
3. J. B. Minster, T. H. Jordan, P. Molnar, and E. Haines, "Numerical Modelling of Instantaneous Plate Tectonics," Geophys. J. R. Astr. Soc. 36, 541-576 (1974).
4. F. J. Mauk, "A Tectonic-Based Rayleigh Wave Group Velocity Model for Prediction of Dispersion Character through Ocean Basins," PhD Thesis, Geology Department, University of Michigan (1977).
5. J. R. Filson, "Long Period Results from the International Seismic Month," Technical Note 1974-15, Lincoln Laboratory, M.I.T. (4 March 1974), DDC AD-776089/5.
6. J. R. Cleary and A. L. Hales, "An Analysis of the Travel Times of P Waves to North American Stations in the Distance Range of 32° to 100°," Bull. Seismol. Soc. Am. 56, 467-489 (1966).
7. E. Herrin and J. N. Taggart, "Regional Variation in P Travel Times," Bull. Seismol. Soc. Am. 58, 1325-1337 (1968).
8. R. Lilwall and A. Douglas, "Estimation of P Wave Travel Times Using Joint Epicenter Method," Geophys. J. R. Astr. Soc. 19, 165-181 (1970).
9. M. K. Sengupta and B. R. Julian, "P-Wave Travel Times from Deep Earthquakes," Bull. Seismol. Soc. Am. 66, 1555-1579 (1976), DDC AD-A042240/2.
10. A. M. Dziewonski, B. H. Hager, and R. J. O'Connell, "Large-Scale Heterogeneities in the Lower Mantle," J. Geophys. Res. 82, 239-255 (1977), DDC AD-A046030/3.
11. Seismic Discrimination SATS, Lincoln Laboratory, M.I.T. (31 March 1977), DDC AD-A045453/8.

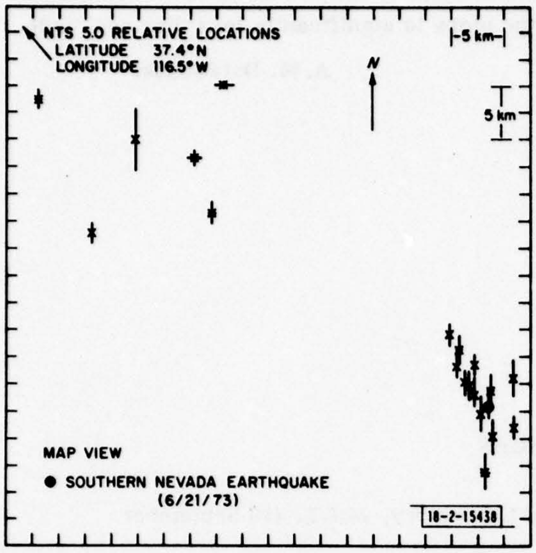

Fig. II-1. Relative epicenters of larger NTS shots, and one earthquake.

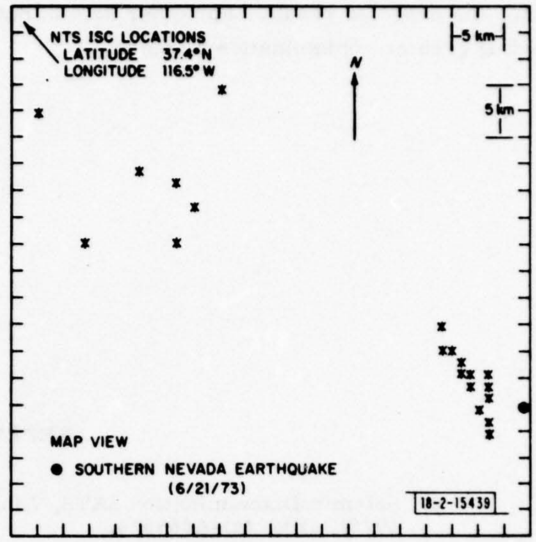

Fig. II-2. Known short epicenters and ISC epicenter for earthquake used in Fig. II-1.

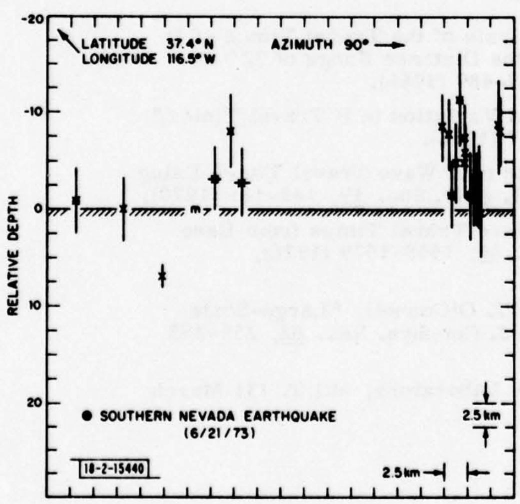

Fig. II-3. Relative depth of NTS shots and earthquake used in Figs. II-1 and II-2.

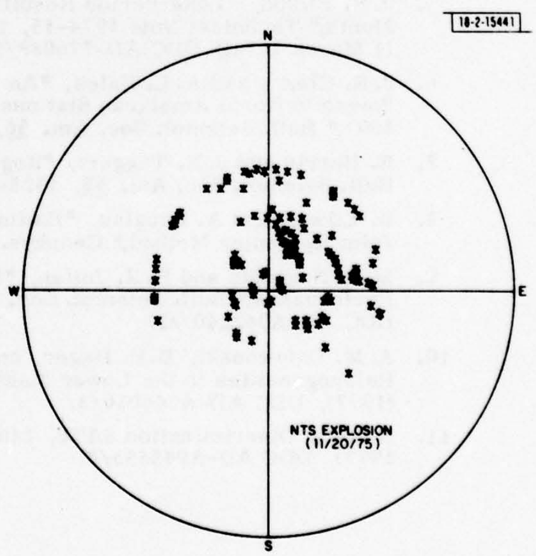

Fig. II-4. Equal-area projection on lower hemisphere of focal sphere. Ray paths computed for a Herrin earth model.

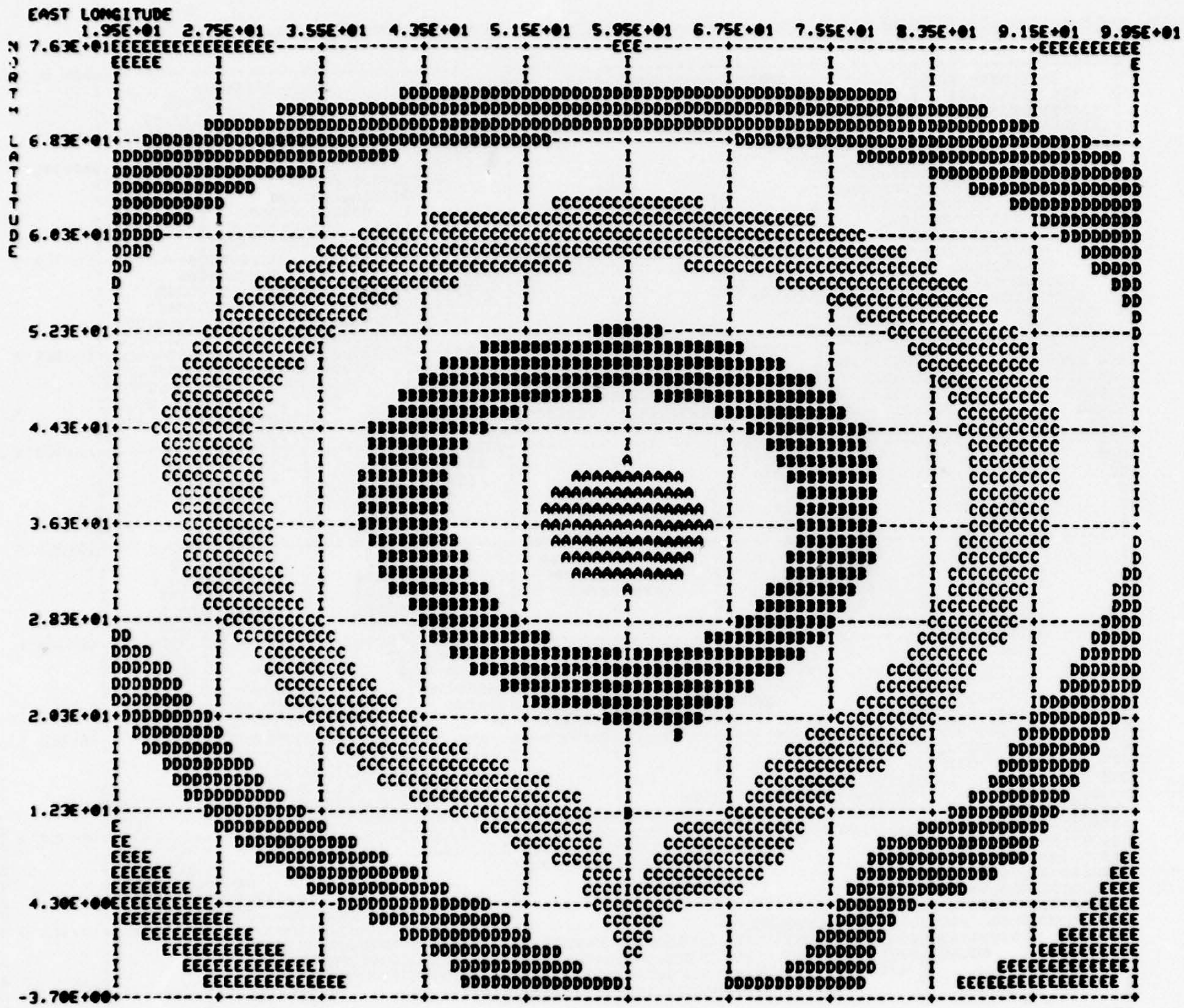

A: 0 to 198 sec

B: 396 to 594 sec

C: 792 to 990 sec

D: 888 to 1086 sec

E: 1584 to 1980 sec

Fig. II-5. Rayleigh group travel times at 20-sec period for locations around Mashad SRO.

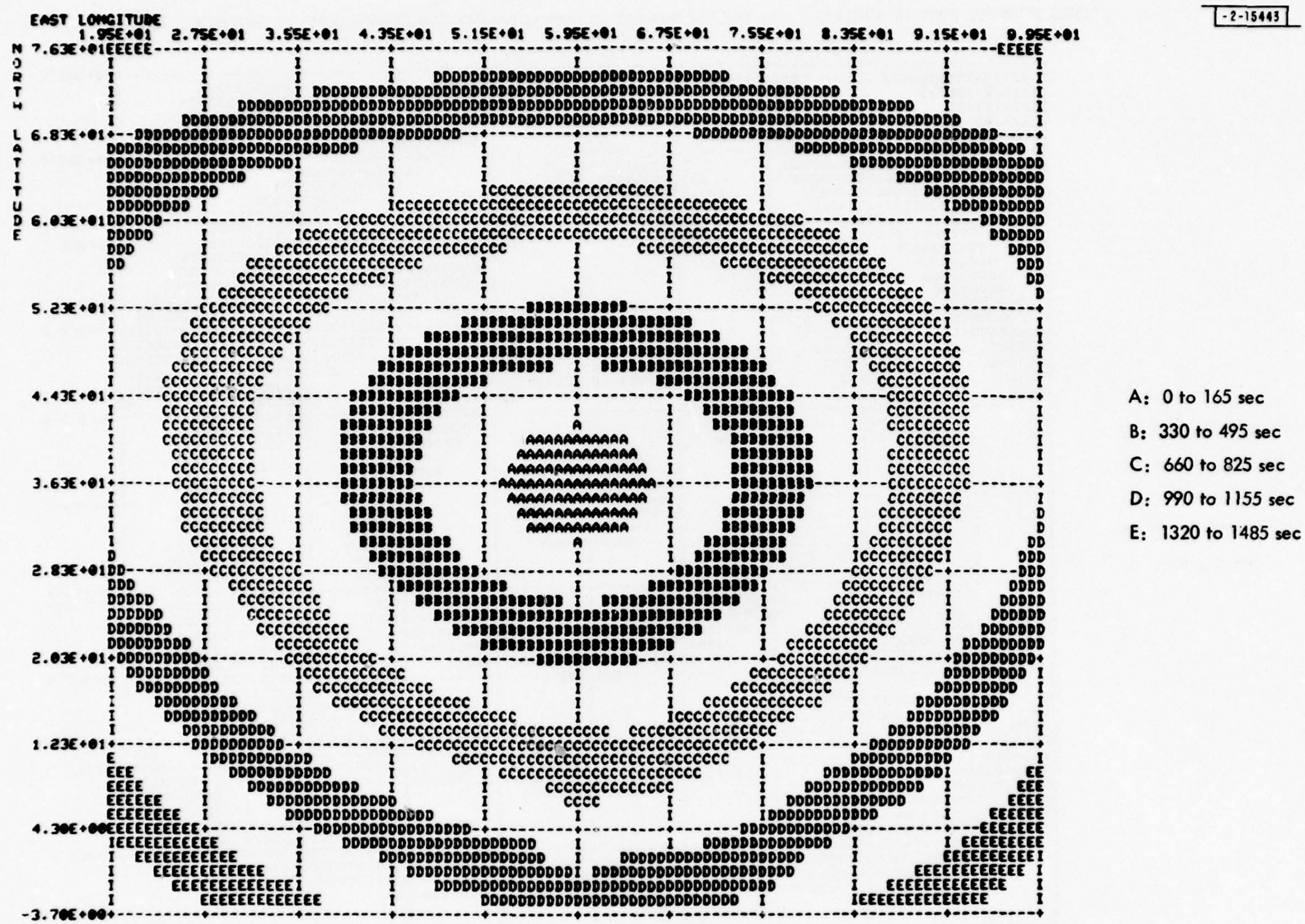

Fig. II-6. Rayleigh group travel times at 40-sec period for locations around Mashad SRO.

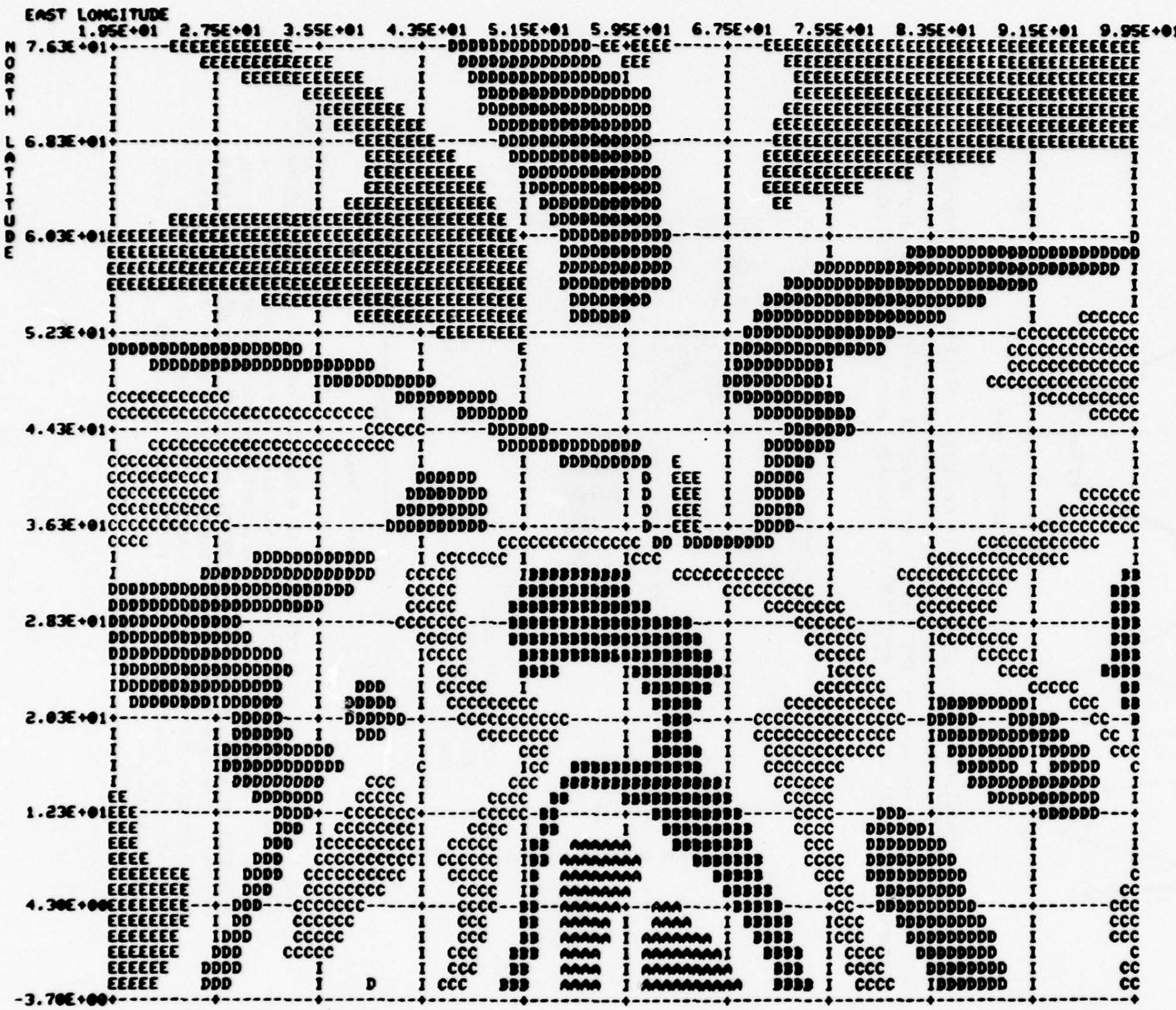

-2-15444

A: 3.76 to 3.78 km/sec

B: 3.80 to 3.82 km/sec

C: 3.84 to 3.87 km/sec

D: 3.89 to 3.91 km/sec

E: 3.93 to 3.95 km/sec

Fig. II-7. Average Rayleigh group velocities at 100-sec period for locations around Mashad SRO.

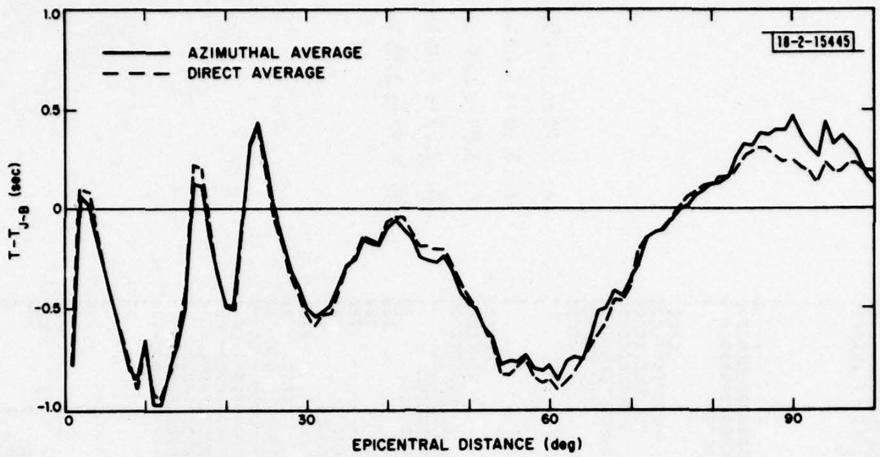

Fig. II-8. Deviations of P-wave travel times from J-B tables for surface focus. Total of 1,657,156 travel times for 24,142 events with depth of focus between 0 and 100 km as located by ISC have been used to derive values shown here. Terms "Azimuthal Average" and "Direct Average" are explained in text.

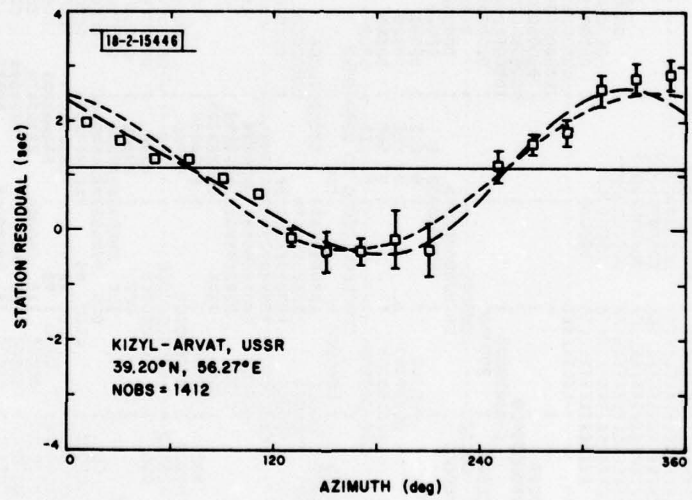

Fig. II-9. Travel-time residuals as a function of azimuth for station Kizyl-Arvat in USSR. Squares represent average residuals for a given azimuth window; error bars indicate standard error of mean, absence of bars indicates that error was less than dimension of a square. Straight line indicates mean residual; short-dashed line is least-squares fit considering average and a term that varies as cos $(Az-E_1)$; long-dashed line is fit that considers also a term cos 2 $(Az-E_2)$.

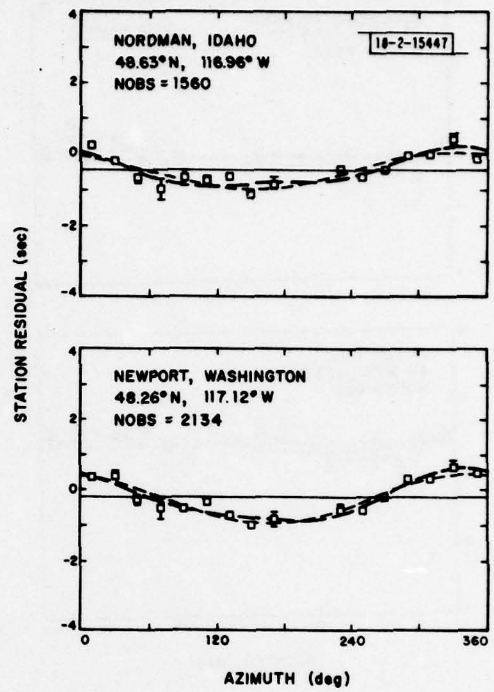

Fig. II-10. Same as Fig. II-9 but for stations Nordman, Idaho and Newport, Washington. Distance between stations is approximately 40 km. Note similarity between residual patterns at both stations.

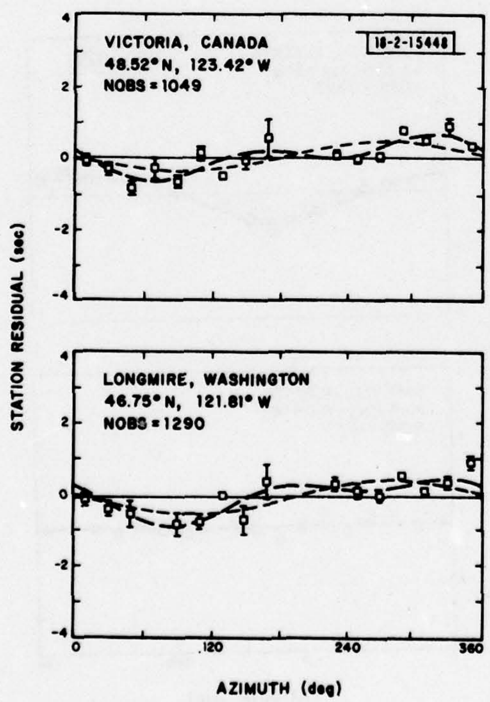

Fig. II-11. Same as Fig. II-9 but for stations Victoria, British Columbia and Longmire, Washington. Distance between stations is approximately 250 km.

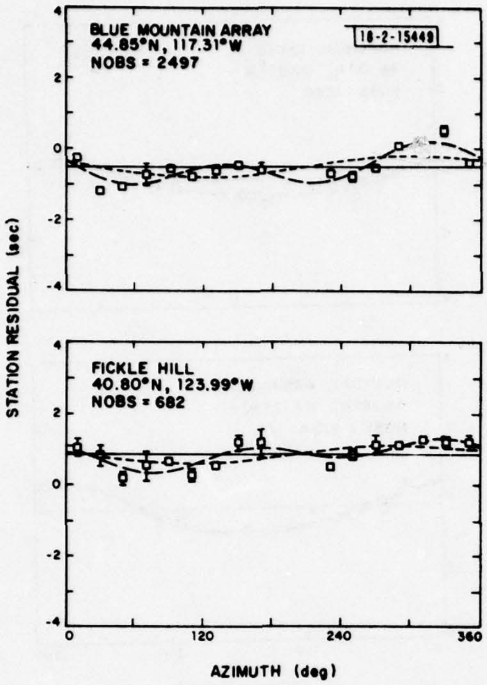

Fig. II-12. Same as Fig. II-9 but for stations Blue Mountain Array, Oregon and Fickle Hill, California. Distance between stations is over 500 km.

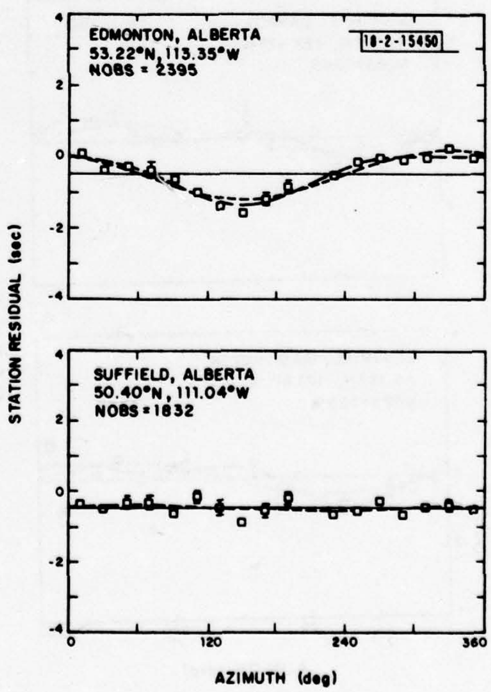

Fig. II-13. Same as Fig. II-9 but for stations Edmonton, Alberta and Suffield, Alberta. Distance between stations is 320 km. Note that pattern of residuals is entirely different at both stations. This should be compared with coherent pattern of residuals in Figs. II-10 through II-12. Inference is that source of anomaly observed at Edmonton must be rather shallow.

III. GENERAL SEISMOLOGY

A. AMPLITUDE SPECTRA OF CRUSTAL PHASES FROM A CANADIAN EARTHQUAKE

Amplitude spectra show that earthquake signals originating and recorded in eastern Canada can have signal-to-noise ratios significantly greater than 1 at frequencies as high as 30 Hz. Apparent Q's of crustal phases are in the range of 1000 to 4000. Similarly high Q values have been reported for Lg waves by Ruzaikin et al.[1] for paths crossing central Asia.

Bill Shannon of the Dominion Observatory of Canada provided us with digital SP records of a southern Quebec earthquake of 23 February 1978 (Fig. III-1). The signals were sampled at 60 Hz. The velocity sensitivity of the recording system is flat between 2 and 15 Hz, and drops by a factor-of-10 between 15 Hz and the Nyquist frequency of 30 Hz. The amplitude spectra are from 10-sec samples of P, S, and Lg wavetrains recorded at MNQ (Fig. III-2) which is the most-distant station from the source, an arc distance of 5°.

A comparison of the noise amplitude spectrum in Fig. III-3(a) with the signal amplitude spectra [Figs. III-3(b) through (d)] shows that signal strength in the pass band from 1 to 25 to 30 Hz is significantly above the noise level. Upper bounds on attenuation or equivalently lower bounds on Q were estimated from the slopes of displacement amplitude spectra. Single-station estimates of absolute Q are not possible without knowing a priori the source spectrum. The spectral slopes are given by

$$\frac{\log I(f_2) - \log I(f_1)}{\log (f_2) - \log (f_2)} \qquad \text{(III-1)}$$

where I(f) is the displacement amplitude spectrum which is equated to $I_o\, e^{-\pi f/QU}$ for an estimate of Q. The velocity of energy propagation U is assumed to be 8.13, 4.72, and 3.60 km/sec for compressional, shear, and Lg propagation, respectively.[2] Slopes were measured in the band of the flat velocity response and the high-frequency band. The results are given in Table III-1. If the slopes are entirely the result of signal diminution from attenuation, the corresponding Q's are given in Table III-2. The highest Q's are estimated for the crustal-phase Lg which suggests that this phase propagates with a mechanism that is distinct from that for the crustal body waves P and S. A wave guide effect could account for anomalously high Q values if, for example, longer-period energy was preferentially leaked out of the guide. Such a mechanism

TABLE III-1
OBSERVED SLOPE

	Band 1 (2 to 15 Hz)	Band 2 (15 to 30 Hz)
P	−1.00	−3.35
S	−1.30	−3.00
Lg	−1.00	−3.00

TABLE III-2
Q

	Band 1 (2 to 15 Hz)	Band 2 (15 to 30 Hz)
P	2500	1400
S	2000	2940
Lg	3430	3620

could account for extremely high Q values reported by Walker et al.[3] for Sn propagating through the oceanic lithosphere in the western Pacific (Sean Solomon, personal communication).

T. J. Fitch
M. W. Shields

B. SCATTER IN OBSERVED m_b VALUES

The scatter of individual station m_b values about the network mean $\overline{m}$ is well known. However, the details of the physical processes which lead to this scatter are much less well known. In particular, it is very difficult to assess how much improvement in both amount of scatter and bias in the network mean can be obtained by a process of path calibration.

For simplicity, let us write the magnitude observed at the i^{th} station in a network as

$$m_i = \log (A/T)_i + Q_i(\Delta, L) + \phi_i \quad . \tag{III-2}$$

Here, A_i and T_i are the observed amplitude and period, Q_i is the standard Gutenberg-Richter distance-depth correction, and ϕ_i summarizes all those effects which lead to a departure of m_i from the true event magnitude m.

The various components of ϕ can be listed as follows:

(1) Departures of the Gutenberg-Richter Q correction from the true global mean correction corresponding to a particular attenuation t*.

(2) Regional variations from the global mean correction, including regional variations in t*.

(3) Near-receiver effects (i.e., station amplitude corrections).

(4) Near-source effects.

(5) Radiation pattern.

(6) Quasi-random scattering by inhomogeneities.

(7) Measurement errors.

Of these, the first five are essentially deterministic and could, at least in principle, be removed by a process of network calibration. The last two are stochastic quantities. Measurement errors are in most cases very small. Scattering appears to occur mainly in the vicinity of the receiver, but there have been suggestions[4] that scattering near the source may sometimes be significant.

Before the application of corrections, ϕ seems to be normally distributed,[5] with standard deviation, averaged over many events, typically in the range 0.3 to 0.4 (see Refs. 3 through 5). North[6] found that the application of corrections for station amplitude biases leads to a reduction in this standard deviation of about 15 percent. Figure III-4 shows the distribution of standard deviations observed at North's[6] 72-station network for those events in the ISC Catalog with m_b less than 6.0, and at least 15 stations reporting. The distribution of standard deviations is skewed, as would be expected, since the distribution of sample variances for a normal parent population is a chi-square distribution. The reduction in mean standard deviation, from 0.356 to 0.311, is about 12 percent.

The reduction in the standard deviation that can be obtained by using a better global mean amplitude-distance correction appears to be somewhat less than 10 percent. Veith and Clawson[7]

were able to reduce the mean standard deviation of USCGS data file earthquakes from 0.381 to 0.350 by this means. Evernden and Clark[8] also revised the amplitude-distance curve for stations in the U.S., and Evernden and Kohler[9] report a reduction of standard deviation to 0.26 from data in the earlier study, though they give no information about how this number was obtained. It appears that the distributions of both stations and events were limited in extent, and they may have succeeded in removing some regional variations in t*.

Scattering from inhomogeneities near the receiver appears to be very sensitive to source location,[4,10] and may set a practical limit to the reduction in scatter achievable for a global network. Evidence from studies of LASA[11] and NORSAR[10] suggests that this scatter has a standard deviation of about 0.25 over distances of tens of kilometers. Frasier[10] considered the amplitude variations at NORSAR for 1-Hz signals observed from 11 events at various azimuths to the array. Standard deviations of individual subarray center sensors relative to the array beam were found to lie in the range 0.13 to 0.30. The average standard deviation for these 11 events was 0.24.

Two conclusions can be made immediately. The process of path calibration is likely to reduce the standard deviation of m_b values from about 0.30 to about 0.25, unless incredibly detailed calibrations are attempted. Also, the statement of Evernden and Kohler[9] that this standard deviation can be reduced to 0.21, or even 0.15 for a high-quality network, seems completely unjustified. This agrees with the conclusion of Ringdal,[4] who used a very different approach.

M. A. Chinnery

C. ON ESTIMATING YIELDS FROM BODY-WAVE OBSERVATIONS

In a previous SATS,[12] we gave expressions for the body waves radiated by a moment-tensor point source. If a pressure is applied to the walls of a small cavity with a time history given by

$$P(t) = P_o(1 - e^{-t/\tau}) \tag{III-3}$$

where P_o is the asymptotic limit and τ is a time constant, then the far-field radial displacement will be

$$\vec{s}_r(t, r) = \frac{M}{\rho\alpha^3 r\tau} \exp\left[-\frac{t - r/\alpha}{\tau}\right] \quad . \tag{III-4}$$

Here, M is the isotopic moment defined as P_o times the volume of the cavity, and ρ and α are the density and P-wave velocity in the source region. This result allows us to calculate the radiated seismic energy.

The energy flux is

$$\vec{S} = -\frac{\partial \vec{s}}{\partial t} \cdot T \tag{III-5}$$

where T is the propagating stress tensor. If Eq. (III-4) is substituted into Eq. (III-5) and the result is integrated over a surface surrounding the source, the total radiated energy is

$$E = \frac{2\pi M^2}{(\lambda + 2\mu)(\alpha\tau)^3} \quad . \tag{III-6}$$

Here, λ and μ are the Lamé parameters in the source region. Incidentally, Eqs. (III-4) and (III-6) are inconsistent with cube-root scaling. This is not surprising since cube-root scaling is based on near-field observations where $1/r^2$ terms are important.

Equation (III-6), although simple in form, shows the inherent difficulty in yield estimation. To begin with, the energy or yield is proportional to the amplitude squared of the observed P waves, since they will be proportional to the moment M. This is reasonable since the energy in mechanical systems is generally proportional to the amplitude squared of the observed vibrations. The real problem is in the denominator, where the energy is proportional to the inverse cube of the P-wave velocity times the time constant. It is also inversely proportional to the Lamé parameters. If we define a characteristic length

$$L = \alpha\tau \tag{III-7}$$

then the fractional change in yield due to a fractional error in estimating (or measuring!) L is

$$\frac{dE}{E} = -3\frac{dL}{L} \quad . \tag{III-8}$$

In other words, a 30-percent error in estimating L produces an order-of-magnitude error in the calculated yield. Similarly, a 50-percent error in estimating M also produces an order-of-magnitude error in E. The former effect should dominate, if only because measuring the width of a seismic pulse is difficult in practice.

What makes this state of affairs even more depressing is the implied assumption in Eq. (III-4) that the seismic amplitudes have been accurately reduced to the focal sphere in order to calculate the moment. This means correcting for: the effects of the free surface at the stations, geometrical spreading, and earth attenuation. In addition, because the source is within a P wavelength of the free surface, separating the primary and depth phases will not be straightforward. The inescapable conclusion of Eq. (III-6) is that there are many significant linear elastic questions to be settled before embarking on a nonlinear hydrodynamic approach to yield estimation.

D. W. McCowan

D. LATERAL VARIATIONS IN MANTLE LOVE-WAVE DISPERSION FROM SRO DATA

In a recent SATS,[13] preliminary results of a study of mantle wave (100- to 500-sec period) dispersion have been given. The high sensitivity and broad dynamic range of the SRO instruments permit detection and analysis of signals at such long periods from events as small as $M_s = 6.5$. Enough data have now been collected for a preliminary regionalization of mantle Love-wave dispersion. In all, 207 paths from the SRO stations to the 34 events shown in Fig. III-5 have been used. Phase velocity has been measured from pairs (G2, G4) and (G3, G5) on each seismogram. This double measurement for each path provides a valuable check on the accuracy of the results obtained. Phase velocities from (G2, G4) and (G3, G5) differed by less than 0.005 km/sec for 53 paths, and by less than 0.010 km/sec for 109 paths. Paths for which the two measurements differed by more than 0.010 km/sec were rejected.

The average dispersion curve differed by, at most, 0.025 km/sec (~0.5 percent) from that given by the (interpolated) normal-mode eigenfrequencies ${}_0T_\ell$ for model PEM-A.[14] Among its other features, this model has been designed to fit the observed normal-mode eigenperiods to an overall rms error of 0.183 percent.[14] This fit to an average earth model is much better than that given by previous data[15] and is presumably due not only to the better data quality, but also to the greater number of paths sampled, giving a closer measurement of average earth properties.

Following previous studies,[15,16] we have regionalized the earth into structural provinces of oceanic, stable continental, and tectonic, and inverted the data obtained to determine average

dispersion for these three regions. The variations in regional dispersion obtained in this manner were significantly less (by a factor of 3) than that of a previous mantle Love-wave study.[15] However, using Rayleigh waves, other workers[16,17] have also found less variation than that given in the same study.

Following the demonstration from shorter-period (<100-sec) Rayleigh-wave studies[18,19] of substantial variations in oceanic dispersion with age, a regionalization taking this into account has been carried out by Ocal.[17] However, Ocal had insufficient data to invert for oceanic variations and assumed dispersion for age-dependent oceanic models[19] to invert only for 3 continental regions.

The present data base is adequate to invert simultaneously for several oceanic regions as well as these 3 continental structures. The oceans were divided into 3 age zones (0 to 30, 30 to 60, and 60+ million Year Age) and the rest of the world into stable shield, foldbelt, and tectonic. The last two divisions correspond to regions of active shallow and deep (subduction zone) seismicity, respectively. Since these non-oceanic divisions differ somewhat from those of Ocal,[17] they are shown in Fig. III-6. An attempt was made to resolve more than 3 oceanic regions, but when this was done, resolution was degraded because the width of the resulting smaller areas was comparable to the wavelength used.

The results of an inversion to determine regional dispersion in the 3 oceanic regions and the shield, foldbelt, and tectonic zones are shown in Fig. III-7. For purposes of clarity, the oceanic zones are shown separately from the others, but at any given period the six points shown are the result of an independent inversion. The bars denote plus-or-minus one standard deviation about the mean. The dispersion in each case is shown as deviations from the mean of all observations. The 3 oceanic regions exhibit dispersion very close to that predicted by models of the oceanic lithosphere as a function of age,[19] and the slower dispersion in youngest (<30 M.Y.) zones is particularly marked. The two older age zones are not as well separated as predicted by the appropriate models.

The "continental" dispersion curves exhibit expected behavior in that shield is fastest and foldbelt is slowest. Note that the dispersion for the latter is slower at shorter periods, gradually merging with the other two. The tectonic region has dispersion characteristics surprisingly close to the mean, in view of the low velocities known to occur above the descending lithosphere slabs in these areas. A similar result has been obtained by Ocal[17] who suggested that the descending high-velocity slab outweighs the effect of the uppermost low-velocity areas.

In all cases, the dispersion at periods in excess of the 400-sec period is statistically almost indistinguishable. To what extent this is real, and not dictated by the somewhat higher variance of the data input to the inversion, is unclear. Preliminary calculations of dispersion for various types of models of upper-mantle structure indicate, however, that the dispersion differences observed do not require any velocity variations below 200 km depth. Although the resolution of higher modes at greater depths is substantially better than that of the fundamental mode dispersion studied here, the present data do provide fairly good resolution down to ~500 km depth.

R. G. North

E. ANALYSIS OF BROAD-BAND ANMO RECORDINGS OF DEEP EVENTS

In the latter half of 1977, the backup SRO installation at Albuquerque, New Mexico was operated in a broad-band mode during the off hours. This was accomplished by removing the SP

shaping filter and feeding the output of the seismometer directly to the digitizer. Since the anti-alias filter had been removed previously, the resulting instrument response was just that given for the Geotech 36000 seismometer by McCowan and Lacoss.[20] In the period of time when broadband data were recorded, we retrieved and analyzed five Fiji-Tonga events all occurring at depths greater than 600 km. These were selected because of the likelihood that they had small source volumes and, consequently, impulsive waveforms. Figures III-8 and III-9 show the results of this analysis on one event, an $m_b = 5.4$ shock occurring on 25 September 1977 at a depth of 606 km.

The second trace in both figures is the impulse response of the seismometer convolved with constant Q operators with attenuation times of 0.5 and 0.7, respectively. The third traces are the least-squares shaping filters which convert the second traces into the first, which is the recorded data. These are interpreted as the actual earth input to the seismometer. The fourth traces are the result of convolving the second and third traces, and can be seen to be accurate copies of the data. Because inverse filtering introduces substantial numerical noise, the fifth traces are the third traces lowpass-filtered.

The results show that the lowpass-filtered earth motion, after the effects of the instrument and earth attenuation have been removed, is more impulsive for the case where $t^* = 0.7$ than it is for $t^* = 0.5$. If the original assumption about the sharp source time function is correct, then this result contrasts with the lower values of t^* reported by Frasier and Filson[21] for explosions. The other impulse occurring approximately 2 sec after the P wave is PcP which, at this distance, is superimposed on P. This phase is unresolvable on the original recording.

Since this result is based on the assumption that the source is impulsive, it produces the largest value of t^* consistent with the data. Conservation of energy, however, requires that the stress loading in the source region be relieved in a nonzero time interval, which would tend to lower the observed t^*.

In principle, this method is a way of measuring Q using only a single station. To be practical, however, considerable data should be available for many deep shocks at the same hypocentral location, and more realistic source time functions should be used as they become available.

D. W. McCowan

F. TRANSFER FUNCTIONS FOR SEISMIC STATIONS USED FOR MONITORING AT REGIONAL DISTANCES

Selecting response characteristics for seismic stations whose primary purpose is to collect data in the "regional" distance range, $0 \leq \Delta \leq 20°$, involves a compromise between providing adequate data bandwidth and introducing complexity into the time-domain impulse response. On the one hand, if the passband of the instrument extends close to the Nyquist frequency, typical anti-alias filters have such steep skirts that the respective time-domain effects dominate the impulse response. On the other hand, if the Nyquist frequency is chosen to be substantially higher than the instrument passband, then the resulting data rates for SP responses are excessive. With this trade-off in mind, we have selected LP and SP responses which provide a reasonable balance between good bandwidth and simplicity in the time domain.

The LP frequency and time-domain displacement responses are shown in Figs. III-10 and III-11. The sampling rate is 1 Hz. This is the same as the present SRO configuration, except that the 6-sec notch filter has been removed. As can be seen, the amplitude response is down 40 and 80 dB at the microseism and Nyquist frequencies, respectively, from its peak at the

25-sec period. The corresponding time-domain impulse response shown in Fig. III-11 is similar in shape to other LP systems, e.g., the WWSSN. Removal of the notch filter should facilitate recovery signals in the microseism band when their S/N are high enough to warrant it. The poles and zeros of the LP Laplace transform are given in Table III-3.

TABLE III-3

LAPLACE TRANSFORM COEFFICIENTS FOR THE PROPOSED SYSTEM RESPONSES

LP System	
Poles	**Zeros**
$s + 4.648 \pm 3.463j$	s^5
$s + 0.1179$	$s + 50.07$
$s + 40.73$	$s + 0.1256$
$s + 0.1500$	
$s + 100.0$	
$s + 264.0$	
$s + 0.2010 \pm 0.2410j$	
$s + 0.1337 \pm 0.1001j$	
$s + 0.0251$	
$s + 0.00924$	
$s + 0.8547 \pm 0.2555j$	
$s + 0.5415 \pm 0.6834j$	
SP System	
Poles	**Zeros**
$s + 4.648 \pm 3.463j$	s^4
$s + 0.1179$	$s + 0.1256$
$s + 40.73$	$s + 50.10$
$s + 0.1500$	
$s + 100.0$	
$s + 264.0$	
$s + 16.73 \pm 3.397j$	
$s + 63.29$	
$s + 63.29$	
$s + 100.0$	

Note: Values supplied by Jon Peterson of the Albuquerque Seismological Center.

The SP amplitude response is shown in Fig. III-12. It peaks at 3 Hz and drops off 24 dB at the Nyquist frequency. This is the same as the present configuration of the SRO except that the sampling rate has been increased to 40 Hz. As previously noted,[20] sampling this response at 20 Hz provided only marginal alias rejection. Increasing the sampling rate by an octave doubles this rejection. It also enhances the action of "natural" anti-alias filtering through earth attenuation. In this frequency range, the effect of attenuation is nonlinear with frequency: doubling the system bandwidth more than doubles the effect of Q.

Time-domain displacement impulse responses are shown in Figs. III-13 and III-14 for two values of the attenuation parameter t*. The first, t* = 0.1 in Fig. III-13, is a value characteristic of crustal-phase propagation in the regional distance range. The other, t* = 0.5 in

Fig. III-14, is characteristic of teleseismic P-wave propagation. As can be seen in Fig. III-14, attenuation in this frequency band introduces a substantial group delay. This is an unavoidable consequence of the mechanism of attenuation, and will have to be accounted for when using high-frequency arrival times to locate regional events. The poles and zeros of the SP Laplace transform are also given in Table III-3.

D. W. McCowan

G. SEISMIC APPLICATIONS SOFTWARE

In previous Semiannual Technical Summaries, we mentioned our waveform database format – a standardized, general format for seismic data in the UNIX system. We also described the programs developed to generate data in this format (by reading magnetic tapes or retrieving data from the Datacomputer), and to interactively display it on the Tektronix scope. Now we have added to these facilities by providing a set of general routines in both C and Fortran that perform the basic functions necessary for working with a waveform database. Using these general routines, we have started to provide a package of basic seismic processing programs similar to those which comprised our PDP-7 Seismic Data Analysis Console.

1. The Waveform Database Format

A waveform database is a group of UNIX files that contain seismic waveform data and descriptive information in a specified format. A database name may be up to 6 characters long, and the file names are created by adding appropriate suffixes to the database name. The essential parts of a waveform database are the gram index file and the gram files. The other component files may or may not exist, but certain processing programs will expect certain files to be present. Figure III-15 shows the relationship between files in a waveform database, and Table III-4 lists the components of the alphanumeric waveform database files.

The gram index file ("dbname. gi")

The gram index file is an alphanumeric file, each line of which describes a seismogram. The seismograms themselves are found in the gram files described below. Each entry in the gram index file may also refer to an event described in the database event file. In this case, the gram index file may contain arrival information relating to that event. Every waveform database must contain one (and only one) gram index file.

The gram files ("dbname. # . g")

For each entry in the gram index file, there must be a gram file, which is a binary file that contains the actual data points of the seismogram. Each gram file has a header that specifies the number of points to follow and the data type, which may be either integer or floating point.

The event file ("dbname. ev")

The event file is an alphanumeric file, each line of which describes a seismic event that may be associated with some of the seismograms in the database. An event file is created by the programs that set up Datacomputer retrieval requests from seismic bulletins, and is used by programs such as mkphases and rotate (described below).

TABLE III-4

COMPONENTS OF THE WAVEFORM DATABASE FILES

Gram Index File

- Name of seismogram file
- Station name
- Start date and time of data
- Number of data points
- Sampling interval between data points
- Calibration
- Instrument code
  - LP or SP
  - Orientation
  - Filtered or unfiltered
  - Beam or single sensor
  - Type of instrument
- Arrival information
  - Event number
  - Distance of event from station
  - Azimuth of event from station
  - Phase code
  - Arrival date and time
- Comment

Event File

- Event number
- Origin date and time
- Latitude
- Longitude
- Depth
- m_b
- m_s
- Geographic region code
- Seismic region code
- Geographic region name

(The following items are taken from the Datacomputer event summary file and are present only for data originally obtained from the Datacomputer)

- Datacomputer event number
- Number of waveforms in waveform file
- Number of SP waveforms in waveform file
- Number of LP waveforms in waveform file
- Source of location information
- Method of calculating depth
- Number of stations used in computing location
- Number of stations used in computing m_b
- Number of stations used in computing m_s

Marker File

- Gram file name
- Sample number marked
- Marker name

The marker file ("dbname.mk")

Each entry in the alphanumeric marker file describes a named "flag" that has been associated with a particular data point in a particular seismogram. Markers can be created by using the display program cursor, the mkphases program, or by using the editor. They can be displayed by the display program, and are used by programs such as measure and window.

The transform files ("dbname.#.t")

These files are similar in name and format to the gram files, but each contains the complex Fourier transform of the associated gram file. They are created by the transform program and used by the ampspect and phaspect programs.

The display files ("dbname.#.d")

Each display file contains a description of a particular display view of the database. They are usually created and used by the display program, but may also be modified by user programs.

2. Dbsubs

Dbsubs is a set of subroutines designed to make it easier for applications programmers to work with waveform databases. They perform all the basic functions and take care of such details as formatting, error-checking, constructing filenames, and other sorts of housekeeping tasks.

The subroutines are oriented around two basic scenarios. The first allows the user to sequentially read an input database and modify its marker file, create transform files, or produce any output that does not fall under the database system. The second scenario allows the user to read sequentially from one input database and produce a modified output database. Nearly all the waveform operations that have been suggested to us so far fall under these two basic scenarios.

The dbsubs package includes the following subroutines.

setup

Gets the database arguments from the command line and performs initialization. If an output database is being created, setup copies the input event and marker files to the output database.

getgil

Reads the next sequential line from the input gram index file, unpacks the parameters, and returns them in a structure (in C) or a labeled common area (in Fortran). Sets a flag if the end of the gram index file is reached.

putgil

Takes the gram index parameters from a structure (in C) or a labeled common area (in Fortran), formats them, and writes a line to the output gram index file. It will properly insert the output database name into the output gram file name.

opgin

Given a gram number, opgin opens the corresponding input gram file and reads the header, leaving the pointer positioned to read the first data point. It will return the number of samples

and the data type found in the header. Once opgin has been called, the user may utilize the standard binary read routines on the gram file.

Opgout

Given a gram number, number of samples to be output, and data type, opgout creates a corresponding output gram file and writes out the header, leaving the pointer positioned to write the first data point. Once opgout has been called, the user may utilize the standard binary write routines on the gram file.

optin

Given a gram number, optin opens the corresponding input transform file and reads the header, leaving the pointer positioned to read the first data point. It will return the number of samples found in the header. Once optin has been called, the user may utilize the standard binary read routines on the transform file.

optout

Given a gram number and number of samples to be output, optout creates a corresponding output transform file and writes out the header, leaving the pointer positioned to write the first data point. Once optout has been called, the user may utilize the standard binary write routines on the transform file.

getev

Given the event number from the gram index line, getev locates the corresponding line in the input database event file and reformats it into a structure (in C) or a labeled common area (in Fortran).

apndcm

Opens the comment file, adds the current date and time to the end of the file, and returns to the calling program, leaving the file open and the pointer positioned for further writing. If the output database does not contain a comment file, one will be created.

marker routines

There are several routines provided to read and write marker files. They have been designed to handle three basic situations, or any combination thereof:

(a) Markers are being created by the program. In this case, "apndmk" can be used to add new markers to the output marker file.

(b) Marker values are used as input to the program. In this case, "getmk" can be used to look for specific named markers in the input database.

(c) All markers in the input database must be modified before being written to the output database. In this case, use "clrmk" to clear the output marker file, "grammk" and "nextmk" to get all the input markers for a given gram, and "apndmk" to write the modified markers to the output database.

3. Seismic Processing Programs

Before starting to work on these programs, a survey was taken asking the group members to rate a list of suggested programs in terms of their usefulness. Then we proceeded to implement the programs roughly in the order of priority, adjusted slightly to favor the programs that could be completed most quickly. The following programs (listed in order of priority) have been completed and released.

dec

Shortens the gram files by decimating, that is retaining only every n^{th} point. As with all generally written waveform database programs, this involves modifying the gram index file to change the "sampling interval" and "number of samples" parameters, and modifying the marker file to reflect the change in sample numbers caused by the decimation.

measure

Types out the exact time and amplitude at a specified marker. This would usually be used in conjunction with the interactive display program.

mkphases

For a database containing event information, mkphases computes theoretical phase arrival times and creates labeled markers to flag each of the resulting data points.

window

Shortens the gram files by retaining the segment lying between preset "start" and "end" markers.

markpeak

Adjusts a marker to fall on the nearest peak. This is useful if the marker was originally set by using the Tektronix cursor, which cannot resolve adjacent points unless the waveform is blown up on the screen.

wdup

Makes a copy of a waveform database.

wmv

Moves or renames a waveform database.

floatgram

Converts the grams of a database to floating point.

intgram

Converts the grams of a database to integer, scaling if necessary.

gramdump

Dumps a (binary) gram file in alphanumeric format.

wfix

Deletes gram files not referred to in the gram index file. (This would usually be due to purposeful editing of the gram index file by the database owner.)

wrm

Deletes a waveform database.

The following programs are currently in progress.

filter

Applies a 3-pole Butterworth filter to all the gram files in the input database, and creates an output database containing the filtered gram files. Has options to specify phase-free filtering, the order of the desired filter, a decimation factor, the filtering of only certain grams, and the filtering of only the first n points in each gram processed.

transform

Computes the Fourier transform of each gram in a database and creates transform files to contain the results.

ampspect

Plots an amplitude spectrum from a waveform database transform file.

phaspect

Plots a phase spectrum from a waveform database transform file.

The following programs are on the list to be implemented.

rotate

Given a database containing 3-component data and event information, create a new database replacing the east and west components with computed radial and transverse components.

getphase

Shorten the gram files by computing a theoretical phase arrival and selecting the data that fall in that window.

concatenate

Combine two or more waveform databases.

L. J. Turek
D. A. Bach

REFERENCES

1. A. I. Ruzaikin, I. L. Nersesor, V. I. Khalturin, and P. Molnar, "Propagation of Lg and Lateral Variations in Crustal Structure in Asia," J. Geophys. Res. 82, 307-316 (1977).
2. R. P. Massé, "Compressional Velocity Distribution Beneath Central and Eastern North America," Bull. Seismol. Soc. Am. 63, 911-935 (1973).
3. D. A. Walker, C. S. McCreery, G. H. Sutton, and F. K. Duennebier, "Spectral Analyses of High-Frequency Pn and Sn Phase Observed at Great Distances in the Western Pacific," Science 199, 1333-1335 (1978).
4. F. Ringdal, "P-Wave Amplitudes and Sources of Scattering in m_b-Observations," J. Geophys. Res. 43, 611-622 (1977).
5. D. Von Seggern, "Joint Magnitude Determination and Analysis of Variance for Explosion Magnitude Estimates," Bull. Seismol. Soc. Am. 63, 827-845 (1973).
6. R. G. North, "Station Magnitude Bias – Its Determination, Causes, and Effects," Technical Note 1977-24, Lincoln Laboratory, M.I.T. (29 April 1977), DDC AD-A041643/8.
7. K. F. Veith and G. E. Clawson, "Magnitude from Short-Period P-Wave Data," Bull. Seismol. Soc. Am. 62, 435-452 (1972).
8. J. F. Evernden and D. M. Clark, "Study of Teleseismic P: II-Amplitude Data," Phys. Earth Plan. Int. 4, 24-31 (1970).
9. J. F. Evernden and W. M. Kohler, "Bias in Estimates of m_b at Small Magnitudes," Bull. Seismol. Soc. Am. 66, 1887-1904 (1976).
10. Seismic Discrimination SATS, Lincoln Laboratory, M.I.T. (31 December 1973), DDC AD-777151.
11. Ibid. (31 December 1970), DDC AD-718971.
12. Ibid. (31 March 1977), DDC AD-A045453.
13. Ibid. (30 September 1978), DDC AD-A065574.
14. A. M. Dziewonski, "Parametrically Simple Earth Models Consistent with Gross Earth Data," Phys. Earth. Planet. Int. 10, 12-48 (1975).
15. M. Kanamori, "Velocity and Q of Mantle Waves," Phys. Earth. Planet. Int. 2, 259-275 (1970).
16. A. M. Dziewonski, "On Regional Differences in Dispersion of Mantle Rayleigh Waves," Geophys. J. R. Astr. Soc. 22, 289-325 (1970).
17. E. A. Ocal, "The Effect of Intrinsic Oceanic Upper-Mantle Heterogeneity on Regionalisation of Long-Period Rayleigh-Wave Phase Velocities," Geophys. J. R. Astr. Soc. 49, 357-370 (1977).
18. D. W. Forsyth, "The Early Structural Evolution and Anisotropy of the Oceanic Upper Mantle," Geophys. J. R. Astr. Soc. 43, 103-162 (1975).
19. A. R. Leeds, L. Knopoff, and E. G. Kausel, "Variations of Upper Mantle Structure under the Pacific Ocean," Science 186, 141-143 (1974).
20. D. W. McCowan and R. T. Lacoss, "Transfer Functions for the Seismic Research Observatory Seismograph System," Bull. Seismol. Soc. Am. 68, 510-512 (1978), DDC AD-A060931.
21. C. W. Frasier and J. R. Filson, "A Direct Measurement of the Earth's Short-Period Attenuation Along a Teleseismic Ray Path," J. Geophys. Res. 77, 3782-3787 (1972).

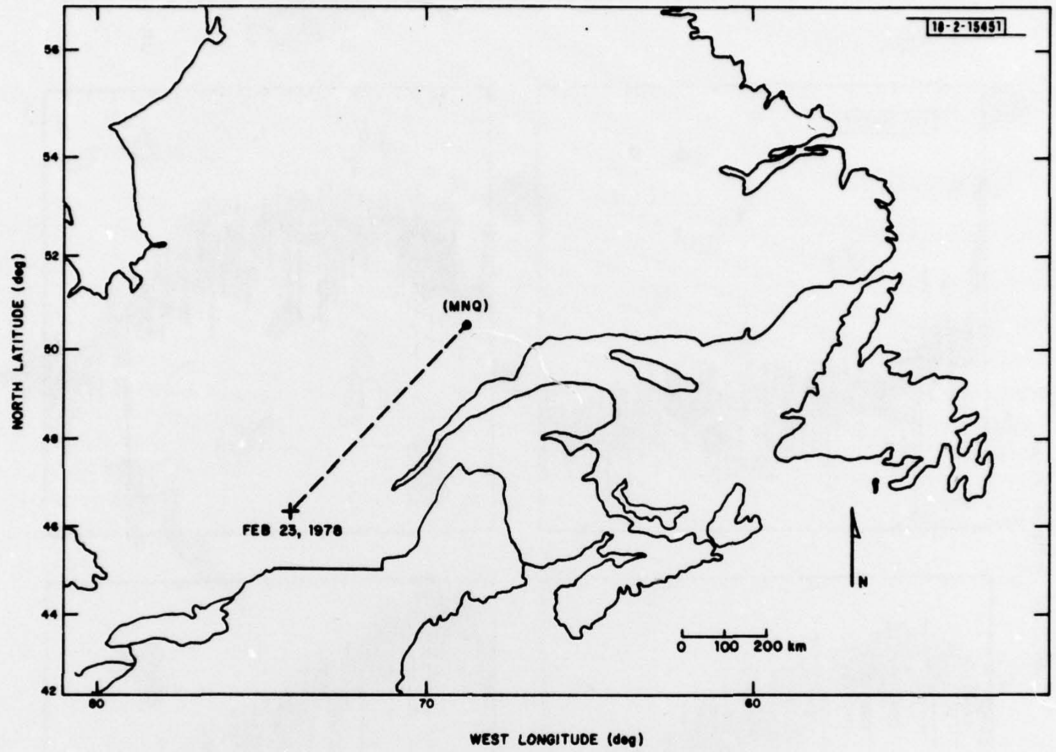

Fig. III-1. Map of northeastern North America, showing location of 23 February 1978 earthquake relative to station MNQ.

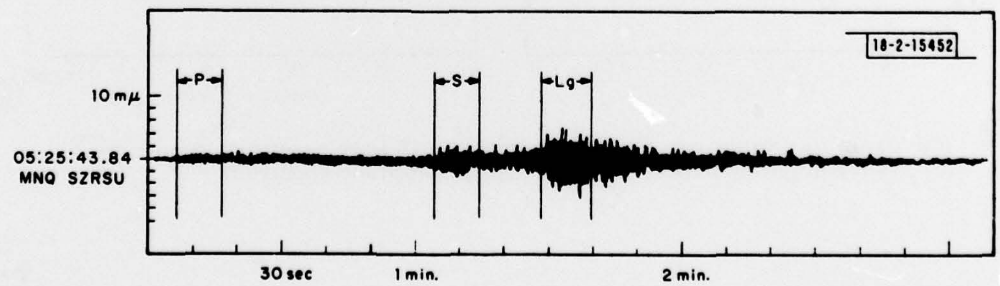

Fig. III-2. 10-sec samples of P, S, and Lg wavetrains recorded at MNQ.

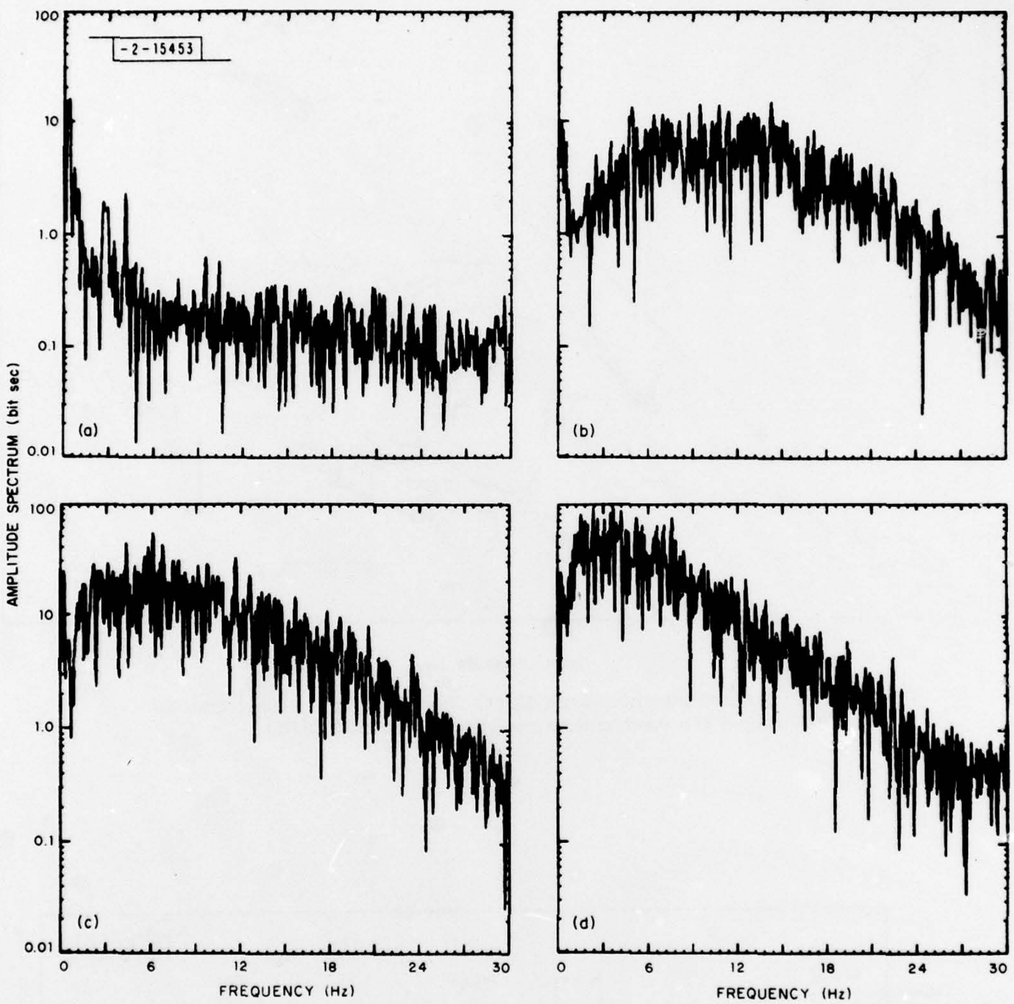

Fig. III-3. (a) Noise amplitude spectrum, (b) P-wave amplitude spectrum, (c) S-wave amplitude spectrum, and (d) Lg amplitude spectrum.

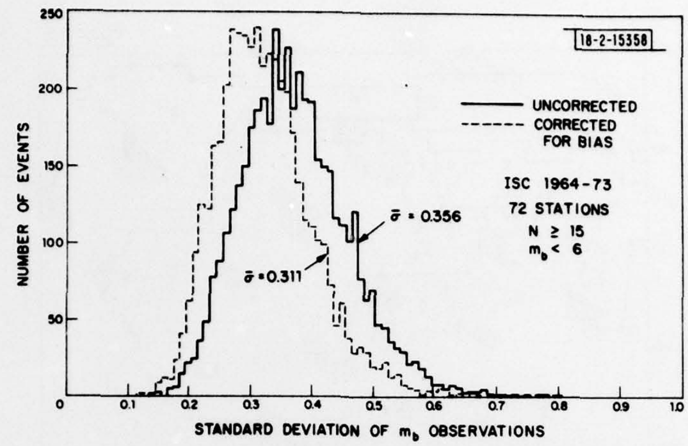

Fig. III-4. Distribution of observed m_b standard deviations before and after application of station amplitude corrections. Data are taken from ISC Catalog 1964-73, for events with $m_b < 6.0$ and at least 15 stations reporting.

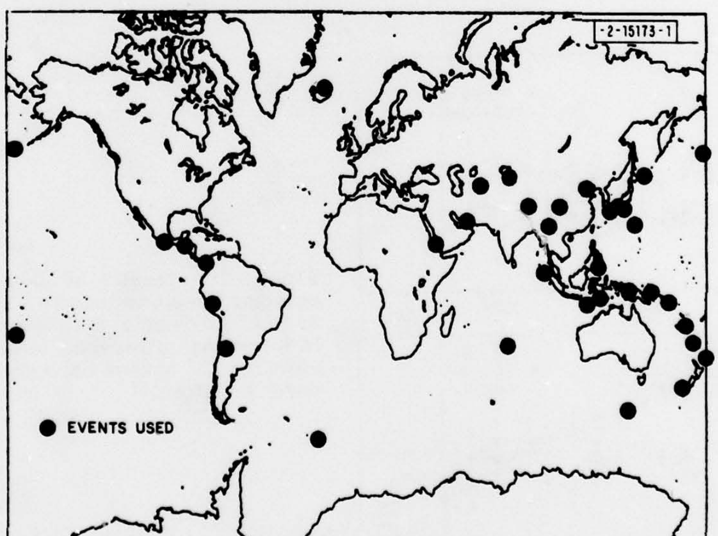

Fig. III-5. Events of $M_s \geqslant 6.5$ during 1976-78 used to provide data for mantle Love-wave study.

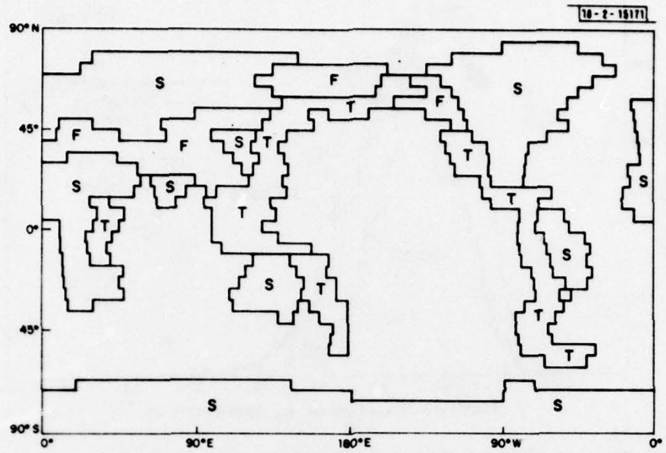

Fig. III-6. Continental division of earth into shield (S), foldbelt (F), and tectonic (T) regions.

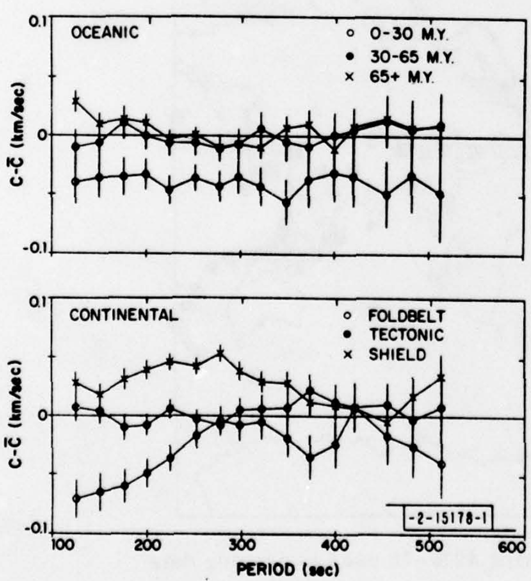

Fig. III-7. Results of Love-wave phase velocity regionalization into 3 oceanic and 3 continental regions. Dispersion is shown as difference from mean phase velocity $\overline{C}$. Error bars denote one standard deviation.

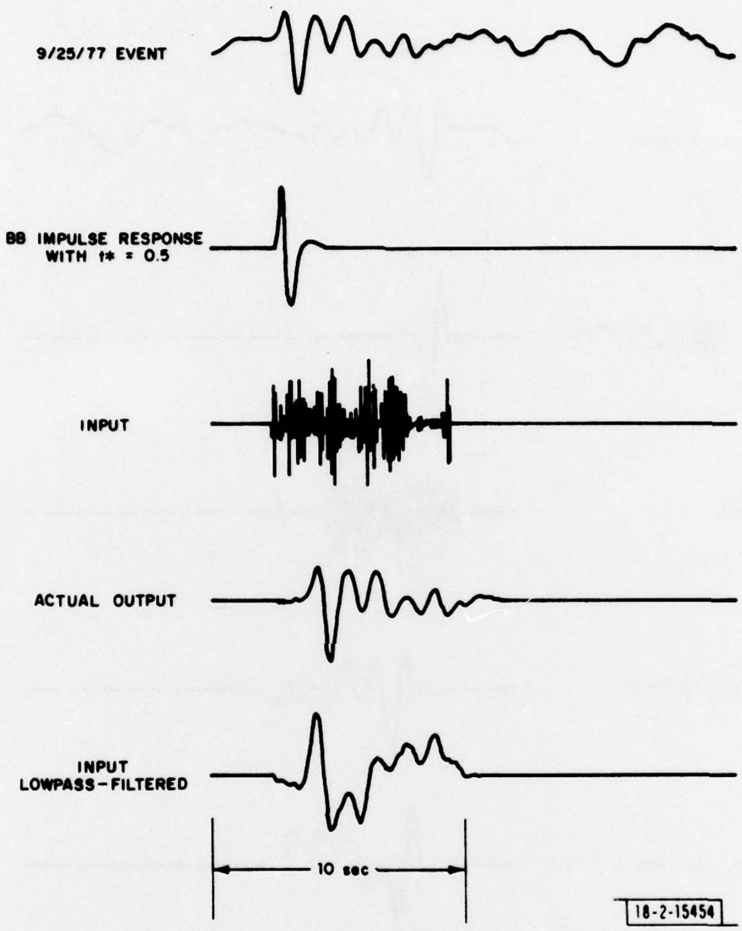

Fig. III-8. Broad-band processing results for a deep Fiji-Tonga event with attenuation time t* = 0.5.

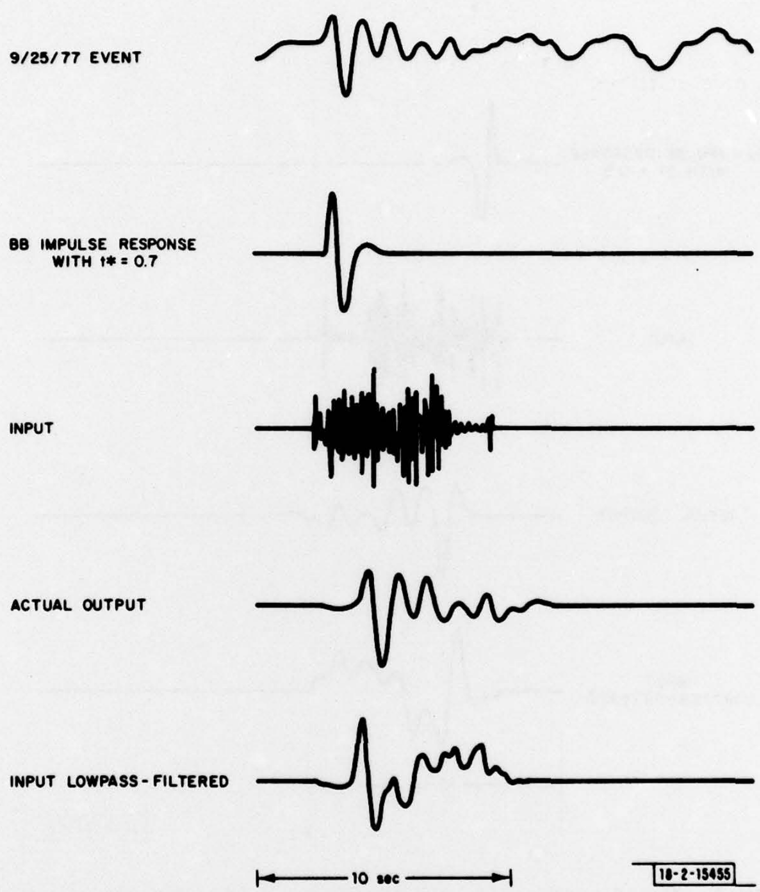

Fig. III-9. Broad-band processing results for a deep Fiji-Tonga event with attenuation time t* = 0.7.

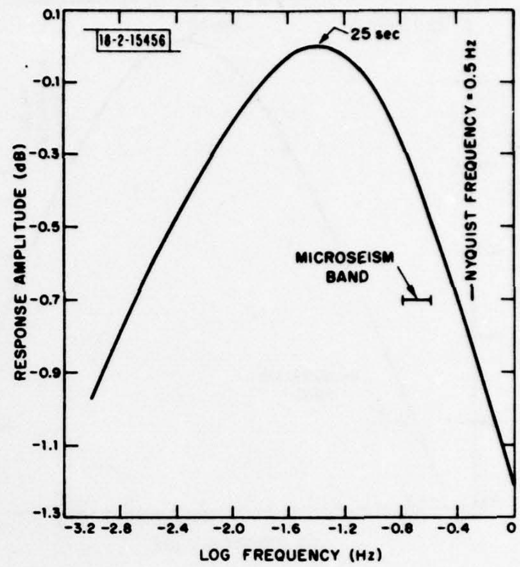

Fig. III-10. SRO LP displacement response without 6-sec notch filter.

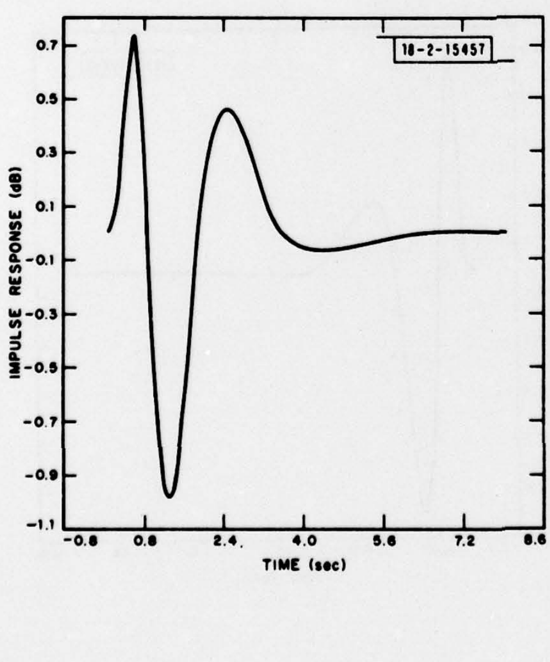

Fig. III-11. SRO LP impulse response without 6-sec notch filter. Sampling rate = 1 Hz.

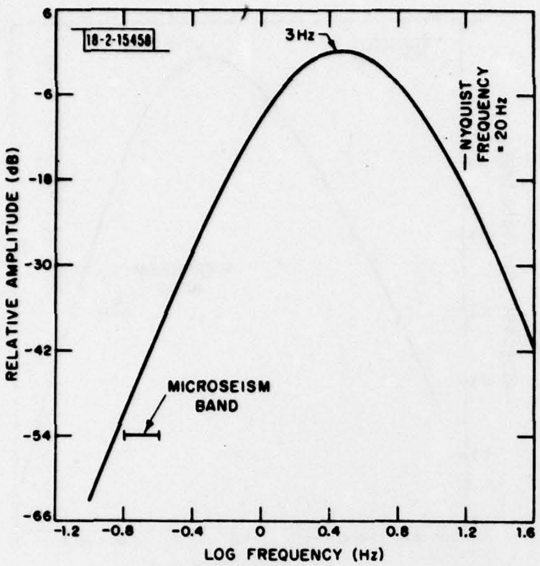

Fig. III-12. SRO SP displacement response.

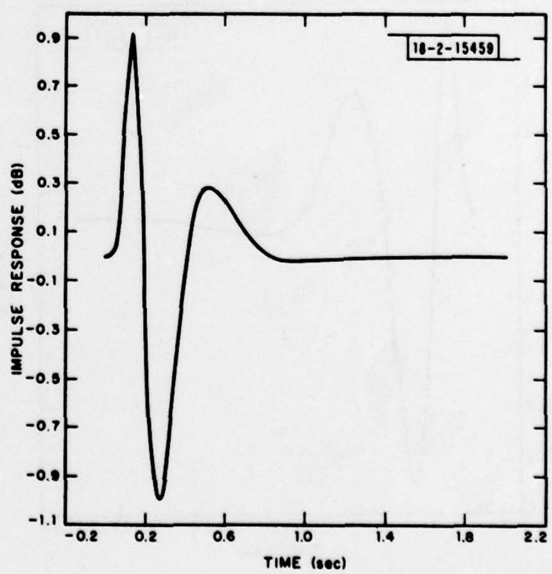

Fig. III-13. SRO SP impulse response. Sampling rate = 40 Hz; attenuation time t* = 0.1.

Fig. III-14. SRO SP impulse response. Sampling rate = 40 Hz; attenuation time t* = 0.5.

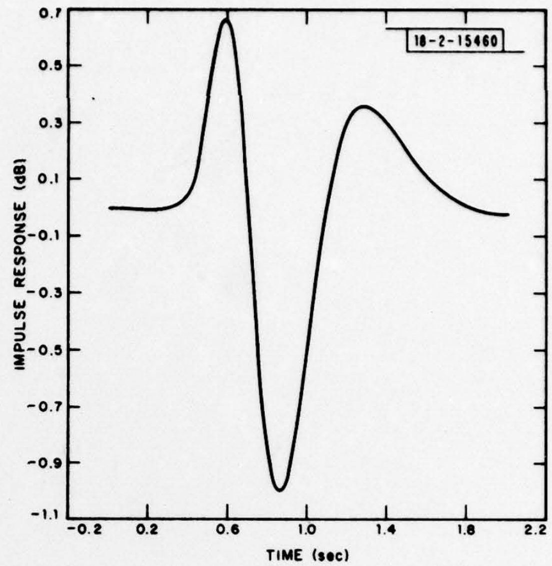

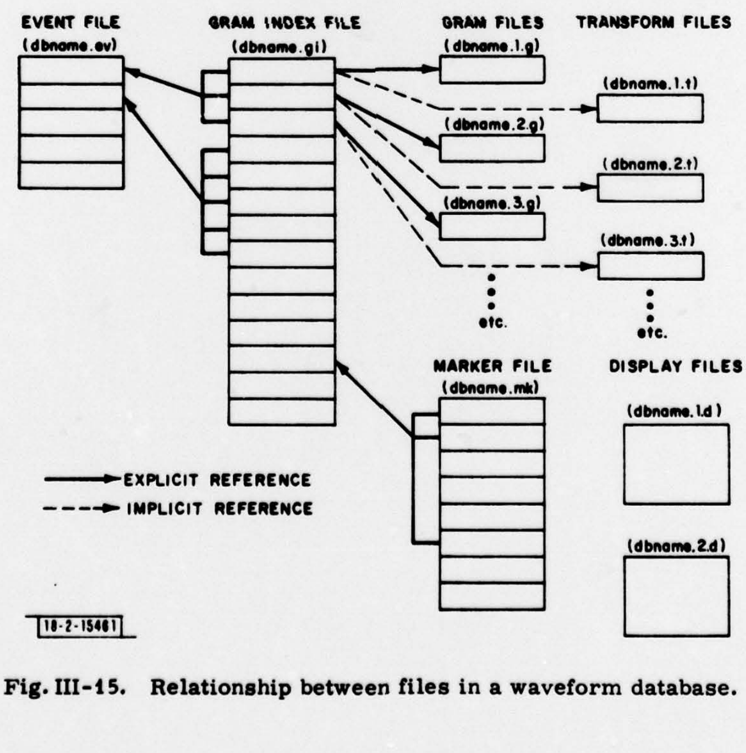

Fig. III-15. Relationship between files in a waveform database.

GLOSSARY

bpi	Bits per Inch
CCD	Conference of the Committee on Disarmament
CPU	Control and Processing Unit
CTBT	Comprehensive Nuclear Test Ban Treaty
DOE	U.S. Department of Energy
FFT	Fast Fourier Transform
ISC	International Seismological Center
ISM	International Seismic Month
J-B	Jeffreys-Bullen Tables
LP	Long Period
MP	Medium Period
NEIS	National Earthquake Information Service
NTS	Nevada Test Site
PDE	Preliminary Determination of Epicenter
SATS	Semiannual Technical Summary
SDAC	Seismic Data Analysis Center
SDMS	Seismic Data Management System
S/N	Signal-to-Noise Ratio
SP	Short Period
SRO	Seismic Research Observatory
USGS	U.S. Geological Survey
WMO	World Meteorological Organization
WWSSN	World-Wide Standard Seismograph Network

UNCLASSIFIED

SECURITY CLASSIFICATION OF THIS PAGE (When Data Entered)

(19) REPORT DOCUMENTATION PAGE

READ INSTRUCTIONS BEFORE COMPLETING FORM

1. REPORT NUMBER
(18) ESD-TR-79-41 ✓

2. GOVT ACCESSION NO.

3. RECIPIENT'S CATALOG NUMBER

4. TITLE (and Subtitle)
(6) Seismic Discrimination

A065574

5. TYPE OF REPORT & PERIOD COVERED
(9) Semiannual Technical Summary rept.
1 Oct[redacted]78 – 31 Mar[redacted]79

6. PERFORMING ORG. REPORT NUMBER

7. AUTHOR(s)
(10) Michael A. Chinnery

8. CONTRACT OR GRANT NUMBER(s)
(15) F19628-78-C-0002, ARPA Order-512

9. PERFORMING ORGANIZATION NAME AND ADDRESS
Lincoln Laboratory, M.I.T. ✓
P.O. Box 73
Lexington, MA 02173

207 650

10. PROGRAM ELEMENT, PROJECT, TASK AREA & WORK UNIT NUMBERS
ARPA Order 512
Program Element No. 62701E
Project No. 9F10

11. CONTROLLING OFFICE NAME AND ADDRESS
Defense Advanced Research Projects Agency
1400 Wilson Boulevard
Arlington, VA 22209

12. REPORT DATE
(11) 31 March 1979

13. NUMBER OF PAGES
80

14. MONITORING AGENCY NAME & ADDRESS (if different from Controlling Office)
Electronic Systems Division
Hanscom AFB
Bedford, MA 01731

(12) 76p.

15. SECURITY CLASS. (of this report)
Unclassified

15a. DECLASSIFICATION DOWNGRADING SCHEDULE

16. DISTRIBUTION STATEMENT (of this Report)

Approved for public release; distribution unlimited.

17. DISTRIBUTION STATEMENT (of the abstract entered in Block 20, if different from Report)

18. SUPPLEMENTARY NOTES

None

19. KEY WORDS (Continue on reverse side if necessary and identify by block number)

seismic discrimination	surface waves	NORSAR
seismic array	body waves	ARPANET
seismology	LASA	

20. ABSTRACT (Continue on reverse side if necessary and identify by block number)

Lincoln Laboratory has embarked on the task of carrying out the design and specification of a U.S. Data Center which will fulfill U.S. obligations that may be incurred under a possible future Comprehensive Test Ban Treaty. This report includes 17 contributions, relating progress in the Data Center design and associated seismic research. These contributions are grouped as follows: seismic data management system (5 studies), locations and travel times (5 studies), and general seismology (7 studies).

DD FORM 1 JAN 73 1473 EDITION OF 1 NOV 65 IS OBSOLETE

UNCLASSIFIED

SECURITY CLASSIFICATION OF THIS PAGE (When Data Entered)

207 650

alk